CANMET

Canada Centre for Mineral and Energy Technology

Centre canadien de la technologie des minéraux et de l'énergie

Mining Research Laboratories

Laboratoires de recherche minière

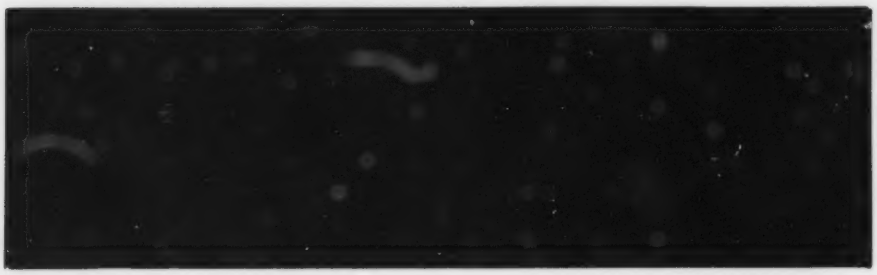

Energy, Mines and Resources Canada

Énergie, Mines et Ressources Canada

Canada

THE ENERGY OF OUR RESOURCES · THE POWER OF OUR IDEAS

L'ENERGIE DE NOS RESSOURCES · NOTRE FORCE CREATRICE

Anisotropic Properties Study of Lac du Bonnet Granite Specimens: Report #7

R. Jackson

MRL 92-060(TR) March 1992

This document is an account [illegible] for Mines and Energy Technology (CANMET)

Ce document est un rapport [illegible] de la technologie des mines et de l'énergie (CANMET)

81 pp

92-06676/

Anisotropic Properties Study of Lac du Bonnet Granite Specimens: Report #7

by

Rand Jackson[1]

Abstract

Compressive and shear wave velocity measurements, as well as uniaxial compression testing, was conducted on samples obtained from borehole 406-010-S2 located in the Lac du Bonnet batholith near Pinawa, Manitoba. The purpose of the study is to ascertain if any anisotropy in terms of the uniaxial mechanical properties exists in the Lac du Bonnet samples and, if so, to what extent.

The uniaxial, dilational and yield compressive strengths, 25 MPa, 40% and 50% tangent moduli and 40% and 50% Poisson's ratios exhibited maximum anisotropies of 1.34, 1.41, 1.53, 1.51, 1.59, 1.33, 1.38 and 1.22 respectively. Deformation anisotropies are related largely to the existence of micro-cracks in the samples. Four hundred and twenty (420) level results indicated a higher degree of anisotropy in terms of the 50% tangent modulus of elasticity (1.51) than was indicated by a similar test series conducted on samples obtained from the 240 level (1.18). Samples from the higher in situ stress field of the 420 level appear to be more profoundly effected by drilling, stress relaxation and the attendant crack formation and propagation.

---

[1]Research Officer, Canadian Mine Technology Laboratory, Mining Research Laboratories, CANMET, Energy, Mines and Resources Canada, Ontario.

Keywords:
Anisotropy, Rock Properties, Mechanical, Young's Modulus, Poisson's Ratio, Uniaxial Compressive Strength, Compressive Wave Velocity, Shear Wave Velocity, Lac du Bonnet

MV.4432358

Étude des propriétés d'anisotropie des échantillons de granite provenant de Lac du Bonnet: rapport #7

par

Rand Jackson[1]

Résumé

On a réalisé des mesures de résistance à la compression et des mesures de la vitesse des ondes de cisaillement, ainsi que des essais de compression uniaxiale, sur des échantillons obtenus dans le trou de sondage 406-010-S2 effectué dans le batholite de Lac du Bonnet près de Pinawa au Manitoba. Dans cette étude, il s'agit de déterminer si les échantillons provenant de Lac du Bonnet présentent une anisotropie quelconque du point de vue de leurs propriétés mécaniques uniaxiales, et si tel est le cas, de déterminer l'importance de cette anisotropie,

La résistance à la dilatation uniaxiale et à la compression uniaxiale à la limite d'écoulement, 25 MPa, les modules tangents de 40 % et 50 %, et les coefficients de Poisson, ont montré des valeurs maximales d'anisotropie de 1,34, 1,41, 1,53, 1,51, 1,59, 1,33, 1,38 et 1,22 respectivement. Les anisotropies de déformation sont largement associées à l'existence de microfissures dans les échantillons. Des résultats obtenus au niveau quatre-cent vingt

(420) ont indiqué un plus fort degré d'anisotropie (1,51) du point de vue du module tangent d'élasticité de 50 % que les résultats d'une série d'essais similaires conduits sur des échantillons obtenus au niveau 240 (1,18). Des échantillons obtenus dans le champ de contraintes in situ plus élevées, au niveau 420, semblent avoir été plus profondément affectés par le forage, la relaxation des contraintes, et la formation et la propagation concomitantes des fissures.

---

[1] Agent de recherche, Laboratoire de technologie minière, Laboratoires de recherche minière, CANMET, Énergie, Mines et Ressources Canada, Ontario.

Mots-clés:
Anisotropie, propriétés des roches, mécanique, module de Young, coefficient de Poisson, résistance uniaxiale à la compression, vitesse des ondes de compression, vitesse des ondes de cisaillement, Lac du Bonnet

Contents

ABSTRACT i

RESUME ii

INTRODUCTION 1

IDENTIFICATION OF SPECIMENS AND TESTS 1

DESCRIPTION OF TEST MEASUREMENTS 3

DATA TREATMENT 4

DATA SUMMARY 6

FAILURE CHARACTERISTICS 7

OBSERVATIONS 7

ACKNOWLEDGEMENTS 9

REFERENCES 9

APPENDIX A 27

Tables

1. Summary of sample depth, dimensions, density and orientation 10

2. Summary of ultrasonic velocity properties 12

3. Summary of uniaxial compression properties 16

4. Ellipsoidal fit & rotation into standard form: uniaxial compressive strength 18

5. Ellipsoidal fit & rotation into standard form: dilational stress 19

6. Ellipsoidal fit & rotation into standard form: yield stress 20

7. Ellipsoidal fit & rotation into standard form: 40% tangent modulus 21

6. Ellipsoidal fit & rotation into standard form: yield stress 20

7. Ellipsoidal fit & rotation into standard form: 40% tangent modulus 21

8. Ellipsoidal fit & rotation into standard form: 50% tangent modulus 22

9. Ellipsoidal fit & rotation into standard form: 25MPa tangent modulus 23

10. Ellipsoidal fit & rotation into standard form: 40% Poisson's ratio 24

11. Ellipsoidal fit & rotation into standard form: 50% Poisson's ratio 25

12. Mean maximum anisotropies of uniaxial mechanical properties 26

Figures

1. Core orientation for anisotropy specimens 2

Introduction

As part of the Canadian Nuclear Fuel Waste Management Project, Atomic Energy of Canada Limited is characterizing various rock formations to determine their suitability for long term disposal of high level wastes. The program also includes the construction of an underground research laboratory (URL) near Pinawa, Manitoba to provide an opportunity for extensive in situ investigations.

Biaxial testing conducted on core obtained during the construction and operating phases of the URL has indicated that the rock may be anisotropic in terms of modulus of elasticity (Lang, 1985). It was felt that further study in the form of acoustic velocity and uniaxial compression testing could provide additional insight into this behaviour.

Testing of sample suites from the 240 level has indicated that there is indeed some anisotropy in the mechanical properties of the Lac du Bonnet granite on that level largely related to the prevailing orientation of microcracks (Jackson, 1988). This report presents results from a similar test program conducted on samples obtained from the 420 level.

Identification of Specimens and Tests

Four sections of 200 mm diameter core labelled A through D were obtained from borehole 406-010-S2 (trend = 66.91°, plunge = -2.10°). The rock can be described as a massive, grey, medium to coarse grained granite, composed of quartz, k-feldspar (oligoclase), plagioclase feldspar and biotite.

Each 200 mm diameter section was recored according to the configuration illustrated in Figure 1. The resulting 45 mm diameter specimens were then identified according to their location and orientation as follows;

A: depth of the collar of the 45 mm hole from the collar of the 200 mm hole,

B: angle β gives the location of the collar of the 45 mm hole around the circumference of the 200 mm core. The angle is measured clock-wise (looking down hole) from the orientation mark on the top of the core,

C: angle α is the angle between the core axis of the 45 mm core and the 200 mm core. The angle is measured clockwise (ie. dip) from the down hole direction of the 200 mm core.

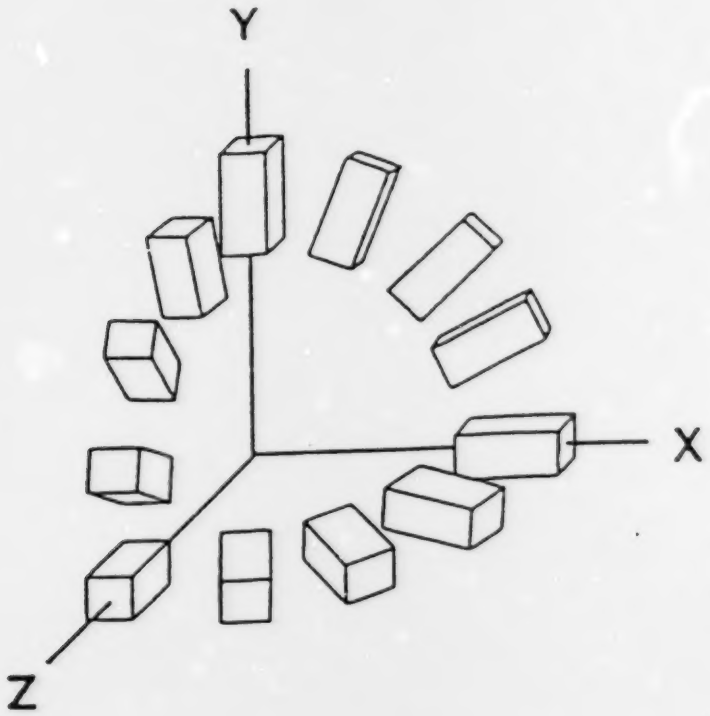

Figure 1: Core Orientation for Anisotropy Specimens(after Peres-Rodrigues, 1967)

Table 1 provides a summary of the specimen identification number and its depth, dimensions, density and orientation. The following properties were determined for the samples listed;

1) compressive wave velocity (@ σ_1 = 0 and 30 MPa), V_{p0}, V_{p30}
2) shear wave velocity (@ σ_1 = 0 and 30 MPa), V_{s0}, V_{s30}
3) dynamic shear modulus (@ σ_1 = 0 and 30 MPa), G_{d0}, G_{d30}
4) dynamic Young's modulus (@ σ_1 = 0 and 30 MPa), E_{d0}, E_{d30}
5) dynamic Poisson's ratio (@ σ_1 = 0 and 30 MPa), ν_{d0}, ν_{d30}
6) uniaxial compressive strength
7) dilational compressive strength
8) yield compressive strength
9) Poisson's ratio (@ 40% and 50% of σ_1), ν_{40}, ν_{50}
10) tangent modulus of elasticity (@ 40% and 50% of σ_1), E_{t40}, E_{t50}
11) 25 MPa tangent modulus of elasticity, E_{t25MPa}

Description of Test Measurements

Compressive and shear wave velocity measurements were carried out on samples prior to being gauged for elastic deformation measurement. The testing equipment consisted of: transmitting and receiving platens utilizing piezoelectric transducers, a high voltage pulse generator, a signal amplifier and a Tektronix 2230 100 MHz digital storage oscilloscope equipped with delay sweep and a time base resolution of 0.01 micro-seconds. Measurements were taken with no axial load and at a stress level of 30 MPa in order to investigate the effects of crack closure on the transverse and longitudinal velocities of the samples.

For an outline of the uniaxial compression procedure, the reader is referred to Technical Data 303410-M01/78 (Annor and Geller, 1978). The two Phillips PR 9302 strain bridges and the Mosely Autograph 2FRA X-Y recorder referred to in that document were replaced, in the present study, by a Sciemetric Model 321 Electronic Measurement System equipped with a Model 84B

Strain Gauge Adapter and a Hewlett Packard 7046B X-Y recorder. These equipment were used to measure and record the axial and transverse strains as a function of axial load.

Data Treatment

The compressive and shear wave velocities were determined by dividing the specimen length by the wave travel time through the specimen. The dynamic properties were, then, calculated using the following equations (3);

Dynamic Young's Modulus

$$E_d = \frac{\rho V^2 (3 V_p^2 - 4 V_s^2)}{(V_p^2 - V_s^2)} \qquad (1)$$

where; E_d = dynamic Young's modulus
V_s = shear wave velocity
V_p = compressive wave velocity
ρ = density

Dynamic Shear Modulus

$$G_d = \rho V_s^2 \qquad (2)$$

where; G_d = dynamic shear modulus

Dynamic Poisson's Ratio

$$\mu_d = \frac{V_p^2 - 2 V_s^2}{2 (V_p^2 - V_s^2)} \qquad (3)$$

where; μ_d = dynamic Poisson's ratio

The Young's modulus values were determined using actual stress/strain data to perform a cubic fit of the form;

$$\sigma = a_0 + a_1\varepsilon + a_2\varepsilon^2 + a_3\varepsilon^3 \qquad (4)$$

where; σ = stress (MPa)
ε = strain
and a_0, a_1, a_2 and a_3 are coefficients

Strains corresponding to stress levels of 25 MPa and 40% and 50% of the peak deviator stress are then substituted into the first derivative of the best fit equation to determine its instantaneous slope and, therefore, its tangent modulus. Poisson's ratios were determined from the ratio of the axial to the circumferential tangent moduli.

Stress versus axial strain, circumferential strain and volumetric strain curves for all tests are presented in Appendix A. The point at which the stress vs. volumetric strain curve reverses direction indicates the onset of unstable crack growth and, for the purposes of this study, has been termed the 'yield strength' of the sample.

Also included in the figures is a curve which illustrates the deviation between the volumetric stress/strain actually exhibited by the samples and that which would be anticipated from purely elastic considerations. The elastic component of the volumetric strain was predicted using the 40% Young's modulus and Poisson's ratio determined for each specimen (presumably when the specimen is behaving in a linear elastic fashion). It is then subtracted from the observed volumetric strain and the incremental deviation between the two is plotted against stress.

Generally, a large deviation from linear elastic behaviour is observed during initial loading as a result of crack closure. This is followed by a region exhibiting little or no difference from linear elastic behaviour. Finally, the deviation begins to, again, increase indicating crack formation and propagation. The stress at which the deviation begins to increase has been dubbed the 'dilational' stress by investigators at the URL.

As stated earlier, the samples were cored from 200 mm diameter sections along three orthogonal axes and at 22.5° intervals between those axes. This configuration made it possible to resolve the mechanical properties of interest into x, y and z coordinates according to the cartesian system defined by the orthogonal axes. The points thus derived are then fitted to an ellipsoid-type quadratic equation which can be described as;

$$[x \;\; y \;\; z] \begin{bmatrix} \alpha_1 & \alpha_2 & \alpha_3 \\ \alpha_2 & \alpha_4 & \alpha_5 \\ \alpha_3 & \alpha_5 & \alpha_6 \end{bmatrix} \begin{bmatrix} x \\ y \\ z \end{bmatrix} = 10^5 \qquad (5)$$

The most probable values of the α_i coefficients were calculated using the method of least squares from the results determined for each specimen set. The standard form of each ellipsoid was subsequently obtained using a suitable rotation of the coordinate axes. The maximum degree of anisotropy could then be calculated by determining the ratio of the major to minor semi-axes (Peres-Rodrigues, 1966). Because the samples were recored from the same borehole and were, therefore, oriented according to the same coordinate system, it was also possible to obtain an aggregate fit using the results from all 48 specimens.

Data Summary

Table 2 contains the results of the ultrasonic velocity measurements for each sample including the calculated values of the dynamic shear modulus, dynamic Young's modulus as well as Poisson's ratio estimated on the basis of velocity data. Table 3 summarizes the uniaxial mechanical properties for each sample including its uniaxial, dilational and yield compressive strength. As mentioned earlier, the tangent moduli of elasticity and Poisson's ratios were also determined for each sample at stress levels of 25 MPa and at 40% and 50% of the sample's failure load. Tables 4 through 11 list the most probable ellipsoids, rotation matrices and normal equations for the uniaxial, dilational and yield compressive strengths, 40% tangent modulus, 50% tangent modulus, 25 MPa tangent modulus, 40% Poisson's ratio and 50% Poisson's ratio,

respectively for each core section as well as the aggregate results. Table 12 provides a summary of the maximum anisotropies determined for the properties listed above.

Individual stress/strain curves for the specimens are contained in Appendix A.

Failure Characteristics

The predominant mode of failure was that of axial splitting and slabbing. Partially formed single diagonal failure planes were also apparent in some samples although the explosive nature of the failures made it impossible to measure failure angles.

Observations

As an earlier report in this test series mentioned (Jackson, 1988), anisotropies determined by performing an ellipsoidal fit on a limited amount of data often leads to misleading results due to the existence of one or more anomalous specimens within the sample set. This is indicated by the large differences between the mean anisotropies calculated for the individual core sections and that determined using the aggregate sample population for the ellipsoidal fit. As is indicated in Table 12, anisotropies determined using the complete sample set (n=48) for the fitting process are consistently lower than those of each section (n=12) for all mechanical properties.

Interestingly, the smallest difference between mean and aggregate anisotropies was observed for the dilational strength or that stress level which results in the initiation of new crack growth (1.44 vs 1.41). This implies that the dilational strength is the least varying parameter of the rock determined for this investigation and could possibly be a limiting condition for strength regardless of initial crack density or orientation.

The largest strength anisotropy was observed for the yield strength results or that stress level associated with the onset of unstable crack growth. If one can assume that the anisotropy observed in the Lac du Bonnet granite is a result of a prevailing micro-crack orientation (Lama

et. al., 1978), it becomes apparent that that prevailing orientation relative to the axis of loading has its greatest influence on the initiation of unstable crack growth and, by implication, the long term strength of the rock.

It is interesting to note that, for 3 of the 4 sections, the highest uniaxial compressive strength was exhibited by the sample with the α=0°, β=0° orientation. This corresponds to the sample re-cored along the central axis of the original 200 mm core. Review of previous test results in this series indicate, however, that this behaviour is peculiar to this data set.

There appears to be little to choose between the maximum anisotropies of 1.59 and 1.51 for the 40% and 50% tangent moduli. The corresponding values of 1.22 and 1.32 for Poisson's ratio, however, would seem to indicate that the samples are behaving more isotropically at 40% of the failure load than at 50%. The consistently higher values of the 50% Poisson's ratio also serve to indicate that crack initiation and growth is well advanced even at stresses as low as 50% of the failure load.

Previous test programs in this series have included estimates of the elastic modulus at a stress level of 25 MPa under the supposition that deformation of a sample is most profoundly effected by pre-existing cracks during initial loading. The 25 MPa modulus values, however, exhibited the lowest anisotropy (1.33) of the three deformation moduli determined as part of this program.

In this type of analysis, the major semi-axis of the standard form will represent the largest predicted deformation modulus to be found at that stress level. If this is the case, the direction associated with the major semi-axis should coincide directly with the prevailing orientation of the microcracks if indeed one exists. Since the rotation matrices given in Tables 4 through 8 are comprised of direction cosines which transform the coordinate system defined by the trend and plunge of the borehole into ones containing the standard form, their orientation in space should be readily obtainable. This analysis is left to investigators at the URL.

Acknowledgements

The author would like to acknowledge the valuable assistance of Ms. Irene Muller during this test program.

References

Annor, A. and Geller, L.; Dilatational velocity, Young's modulus, Poisson's ratio, uniaxial compressive strength and Brazilian tensile strength for WN1 and WN2 samples; CANMET/MRL Technical Data 303410-M01/78, 1978.

Jackson, R.; Anisotropic properties study of Lac du Bonnet granite specimens: report #5; CANMET/MRL Technical Report 88-39(TR), 1988.

Lama, R.D., Vutukuri, V.S.; Handbook on mechanical properties of rocks; Volume II, Chapter 6, Trans Tech Publications, 1978.

Lang, P.; Personal communication; 1985.

Peres-Rodrigues, F.; Anisotropy of granites. Modulus of elasticity and ultimate strength ellipsoids, joint systems, slope attitudes and their correlations; Proc. 1st Cong. ISRM, Lisbon, Spain, 1966.

Table 1: Summary of sample depth, dimensions, density and orientation

Core Section	Sample Number	Sample Depth (m)	Length (mm)	Diameter (mm)	Density (Mg/m^3)	Orientation	
						α	β
A	A1	1.304	101.32	44.58	2.65	0.0	0.0
	A2	1.912	102.12	44.52	2.63	22.5	0.0
	A3	1.774	100.47	44.47	2.62	45.0	0.0
	A4	1.681	102.84	44.47	2.68	67.5	0.0
	A5	1.599	102.95	44.59	2.63	90.0	0.0
	A6	1.394	102.25	44.64	2.62	90.0	22.5
	A7	1.442	101.35	44.61	2.62	90.0	45.0
	A8	1.485	102.15	44.15	2.63	90.0	67.5
	A9	1.537	100.45	44.20	2.63	90.0	90.0
	A10	1.882	101.42	44.52	2.63	22.5	90.0
	A11	2.105	100.75	44.53	2.63	45.0	90.0
	A12	2.164	102.86	44.57	2.63	67.5	90.0
B	B1	2.314	101.82	44.41	2.63	0.0	0.0
	B2	2.908	101.02	44.45	2.64	22.5	0.0
	B3	2.784	101.85	44.47	2.64	45.0	0.0
	B4	2.709	100.42	44.43	2.63	67.5	0.0
	B5	2.358	102.00	44.24	2.64	90.0	0.0
	B6	2.408	101.68	44.26	2.64	90.0	22.5
	B7	2.462	101.73	44.27	2.64	90.0	45.0
	B8	2.627	101.55	44.60	2.64	90.0	67.5
	B9	2.566	103.19	44.60	2.63	90.0	90.0
	B10	2.861	101.42	44.45	2.64	22.5	90.0
	B11	3.110	100.65	44.53	2.64	45.0	90.0
	B12	3.170	99.36	44.56	2.68	67.5	90.0

Table 1: cont'd

Core Section	Sample Number	Sample Depth (m)	Length (mm)	Diameter (mm)	Density (Mg/m^3)	Orientation	
						α	β
C	C1	5.066	100.95	44.47	2.64	0.0	0.0
	C2	5.682	101.85	44.45	2.64	22.5	0.0
	C3	5.516	102.18	44.43	2.63	45.0	0.0
	C4	5.436	101.20	44.40	2.63	67.5	0.0
	C5	5.109	99.30	44.60	2.63	90.0	0.0
	C6	5.165	101.27	44.62	2.63	90.0	22.5
	C7	5.361	103.61	44.60	2.62	90.0	45.0
	C8	5.260	100.12	44.72	2.62	90.0	67.5
	C9	5.298	102.28	44.68	2.63	90.0	90.0
	C10	5.651	101.31	44.50	2.62	22.5	90.0
	C11	5.882	101.63	44.51	2.64	45.0	90.0
	C12	5.927	103.50	44.55	2.63	67.5	90.0
D	D1	6.080	98.62	44.66	2.63	0.0	0.0
	D2	6.700	101.70	44.46	2.63	22.5	0.0
	D3	6.572	102.52	44.47	2.63	45.0	0.0
	D4	6.477	103.00	44.39	2.63	67.5	0.0
	D5	6.125	101.14	44.31	2.63	90.0	0.0
	D6	6.174	102.96	44.31	2.63	90.0	22.5
	D7	6.221	103.14	44.36	2.63	90.0	45.0
	D8	6.380	102.67	44.35	2.63	90.0	67.5
	D9	6.320	102.86	44.34	2.63	90.0	90.0
	D10	6.659	101.45	44.49	2.63	22.5	90.0
	D11	6.895	100.51	44.53	2.63	45.0	90.0
	D12	7.020	100.88	44.55	2.63	67.5	90.0

Table 2: Summary of ultrasonic velocity properties

Sample Number	Pressure (MPa)	P-Wave (km/s)	S-Wave (km/s)	Dynamic Shear Modulus (GPa)	Dynamic Young's Modulus (GPa)	Poisson's Ratio
A1	0.1	2.54	1.73	7.91	16.89	0.07
	30.0	4.04	2.13	11.99	31.35	0.31
A2	0.1	2.63	1.72	7.76	17.52	0.13
	30.0	4.05	2.04	10.91	29.05	0.33
A3	0.1	2.92	1.65	7.10	18.00	0.27
	30.0	4.20	2.06	11.15	29.90	0.34
A4	0.1	3.13	1.73	8.01	20.49	0.28
	30.0	4.27	2.20	13.00	34.27	0.32
A5	0.1	3.13	1.72	7.83	20.07	0.28
	30.0	4.31	2.11	11.67	31.34	0.34
A6	0.1	3.08	1.76	8.14	20.46	0.26
	30.0	4.31	2.02	10.66	28.99	0.36
A7	0.1	3.10	1.77	8.24	20.71	0.26
	30.0	4.22	2.05	11.04	29.72	0.35
A8	0.1	3.07	1.71	7.71	19.64	0.27
	30.0	4.10	2.12	11.79	31.09	0.32
A9	0.1	2.92	1.69	7.51	18.75	0.25
	30.0	4.08	2.11	11.65	30.73	0.32
A10	0.1	2.63	NA	NA	NA	NA
	30.0	4.07	2.08	11.39	30.15	0.32
A11	0.1	2.81	NA	NA	NA	NA
	30.0	4.03	2.06	11.12	29.44	0.32
A12	0.1	2.96	1.70	7.58	19.02	0.25
	30.0	3.93	2.07	11.23	29.39	0.31

Table 2: cont'd

Sample Number	Pressure (MPa)	P-Wave (km/s)	S-Wave (km/s)	Dynamic Shear Modulus (GPa)	Dynamic Young's Modulus (GPa)	Poisson's Ratio
B1	0.1	2.61	1.69	7.52	17.12	0.14
	30.0	4.01	2.15	12.13	31.49	0.30
B2	0.1	2.60	1.65	7.20	16.72	0.16
	30.0	3.98	2.05	11.09	29.27	0.32
B3	0.1	2.93	1.68	7.42	18.62	0.26
	30.0	4.11	2.03	10.89	29.14	0.34
B4	0.1	3.07	1.71	7.70	19.63	0.28
	30.0	4.26	2.05	11.09	29.91	0.35
B5	0.1	3.12	1.74	7.98	20.34	0.27
	30.0	4.38	2.08	11.42	30.92	0.35
B6	0.1	3.13	1.72	7.83	20.08	0.28
	30.0	4.33	2.08	11.40	30.78	0.35
B7	0.1	3.04	1.70	7.67	19.47	0.27
	30.0	4.12	2.10	11.66	30.88	0.32
B8	0.1	2.98	1.72	7.81	19.51	0.25
	30.0	4.01	2.07	11.32	29.85	0.32
B9	0.1	2.92	1.71	7.69	19.08	0.24
	30.0	3.98	2.04	11.00	29.07	0.32
B10	0.1	2.57	1.67	7.34	16.66	0.13
	30.0	4.04	2.08	11.44	30.18	0.32
B11	0.1	2.81	1.66	7.23	17.86	0.23
	30.0	3.98	2.10	11.61	30.36	0.31
B12	0.1	2.97	1.73	8.02	19.92	0.24
	30.0	3.87	2.01	10.79	28.38	0.32

Table 2: cont'd

Sample Number	Pressure (MPa)	P-Wave (km/s)	S-Wave (km/s)	Dynamic Shear Modulus (GPa)	Dynamic Young's Modulus (GPa)	Poisson's Ratio
C1	0.1	2.49	1.67	7.32	16.06	0.10
	30.0	4.02	2.12	11.82	30.93	0.31
C2	0.1	2.77	1.72	7.76	18.44	0.19
	30.0	4.16	2.16	12.34	32.43	0.31
C3	0.1	2.94	1.73	7.88	19.43	0.23
	30.0	4.15	2.06	11.15	29.81	0.34
C4	0.1	3.06	1.69	7.52	19.23	0.28
	30.0	4.27	2.03	10.80	29.25	0.35
C5	0.1	3.04	1.64	7.11	18.38	0.29
	30.0	4.34	2.01	10.63	28.97	0.36
C6	0.1	3.06	1.67	7.36	18.94	0.29
	30.0	4.33	2.05	11.04	29.93	0.36
C7	0.1	3.03	1.72	7.77	19.61	0.26
	30.0	4.20	2.06	11.09	29.76	0.34
C8	0.1	3.03	1.65	7.11	18.34	0.29
	30.0	4.09	2.08	11.31	30.00	0.33
C9	0.1	3.01	1.70	7.59	19.22	0.27
	30.0	4.06	2.04	10.92	29.07	0.33
C10	0.1	2.70	1.67	7.33	17.45	0.19
	30.0	4.02	2.10	11.59	30.42	0.31
C11	0.1	2.94	1.72	7.80	19.33	0.24
	30.0	4.02	2.13	11.98	31.24	0.30
C12	0.1	3.12	1.77	8.22	20.77	0.26
	30.0	4.09	2.10	11.56	30.58	0.32

Table 2: cont'd

Sample Number	Pressure (MPa)	P-Wave (km/s)	S-Wave (km/s)	Dynamic Shear Modulus (GPa)	Dynamic Young's Modulus (GPa)	Poisson's Ratio
D1	0.1	2.56	1.74	7.98	17.06	0.07
	30.0	4.11	2.10	11.57	30.62	0.32
D2	0.1	2.66	1.89	9.38	18.57	-0.01
	30.0	3.91	2.06	11.21	29.31	0.31
D3	0.1	2.82	1.92	9.68	20.72	0.07
	30.0	4.04	2.33	14.19	35.53	0.25
D4	0.1	2.87	2.00	10.48	21.61	0.03
	30.0	3.96	2.18	12.53	32.13	0.28
D5	0.1	3.00	1.88	9.28	21.86	0.18
	30.0	4.18	2.06	11.15	29.86	0.34
D6	0.1	3.01	1.81	8.64	21.00	0.22
	30.0	4.26	2.08	11.42	30.65	0.34
D7	0.1	3.07	1.74	7.91	20.02	0.26
	30.0	4.13	2.10	11.58	30.70	0.33
D8	0.1	2.99	1.76	8.18	20.19	0.23
	30.0	4.07	2.11	11.68	30.78	0.32
D9	0.1	3.09	1.77	8.27	20.74	0.25
	30.0	4.10	2.04	10.95	29.24	0.34
D10	0.1	2.56	1.79	8.45	17.25	0.02
	30.0	3.76	2.28	13.67	33.06	0.21
D11	0.1	2.65	1.90	9.45	18.47	-0.02
	30.0	3.82	2.01	10.62	27.81	0.31
D12	0.1	2.91	1.92	9.68	21.58	0.11
	30.0	3.90	2.47	16.08	37.40	0.16

Table 3: Summary of uniaxial compression properties

Sample Number	Compressive Strength (MPa)			Tangent Modulus of Elasticity (GPa)			Poisson's Ratio	
	Uniaxial	Dilational	Yield	50 %	40 %	@ 25 MPa	50 %	40 %
A1	161	56	95	56.85	54.06	34.51	0.34	0.28
A2	149	56	92	46.83	44.42	31.06	0.33	0.33
A3	140	58	78	52.08	49.01	35.46	0.42	0.33
A4	132	52	59	52.40	49.26	39.72	0.61	0.46
A5	142	62	63	64.59	62.78	42.04	0.52	0.42
A6	149	59	78	51.39	48.66	37.59	0.50	0.37
A7	141	57	59	57.80	54.58	37.04	0.68	0.49
A8	151	58	75	57.50	54.19	39.31	0.53	0.39
A9	156	65	65	57.39	53.96	35.13	0.58	0.45
A10	150	56	81	52.23	49.67	33.22	0.45	0.32
A11	134	49	84	45.90	44.57	31.28	0.37	0.29
A12	140	57	75	48.12	44.76	32.10	0.46	0.36
B1	169	68	109	56.54	53.53	34.26	0.33	0.25
B2	155	61	90	54.42	52.37	33.68	0.37	0.41
B3	135	54	73	48.73	45.80	33.52	0.47	0.34
B4	147	60	63	63.26	58.72	43.32	0.63	0.45
B5	154	57	89	67.88	65.25	45.70	0.38	0.27
B6	160	64	89	56.25	54.88	41.41	0.45	0.34
B7	155	61	83	53.31	51.00	35.77	0.44	0.33
B8	151	59	88	52.88	49.37	32.97	0.39	0.30
B9	150	64	72	51.45	47.61	31.13	0.52	0.38
B10	163	64	80	54.24	51.36	34.01	0.49	0.37
B11	141	55	73	48.40	45.06	32.25	0.50	0.37
B12	146	59	77	49.44	46.25	31.75	0.49	0.37

Table 3: cont'd

Sample Number	Compressive Strength (MPa)			Tangent Modulus of Elasticity (GPa)			Poisson's Ratio	
	Uniaxial	Dilational	Yield	50 %	40 %	@ 25 MPa	50 %	40 %
C1	153	61	108	46.43	43.57	28.46	0.26	0.20
C2	166	68	90	56.22	52.38	33.43	0.47	0.37
C3	142	52	91	48.38	45.67	34.93	0.34	0.27
C4	149	63	72	54.63	51.12	38.59	0.50	0.39
C5	146	59	73	50.98	48.81	38.96	0.51	0.38
C6	155	68	76	56.16	53.99	40.24	0.62	0.49
C7	151	60	82	55.72	52.96	38.56	0.45	0.35
C8	143	55	60	48.02	45.00	32.03	0.77	0.52
C9	154	60	86	48.97	45.98	30.63	0.39	0.30
C10	156	59	70	51.62	49.39	34.00	0.58	0.42
C11	155	60	86	50.68	48.23	32.86	0.41	0.33
C12	140	57	90	47.51	44.62	32.54	0.35	0.27
D1	163	63	90	54.79	51.61	33.14	0.46	0.35
D2	152	57	101	52.72	49.39	32.78	0.35	0.28
D3	137	56	79	50.08	47.40	36.42	0.40	0.31
D4	151	60	90	50.21	48.25	36.45	0.38	0.27
D5	163	68	70	57.44	55.46	43.17	0.62	0.45
D6	160	61	83	56.05	54.30	41.89	0.47	0.38
D7	150	61	85	48.59	46.34	33.37	0.43	0.34
D8	151	62	93	53.42	50.01	33.48	0.37	0.29
D9	149	60	78	56.83	52.53	33.58	0.51	0.40
D10	155	59	81	50.50	47.59	31.90	0.48	0.37
D11	140	58	58	50.31	45.89	32.85	0.76	0.49
D12	133	52	73	48.98	45.32	33.67	0.44	0.33

Table 4: Ellipsoidal fit & rotation into standard form: uniaxial compressive strength

	MOST PROBABLE ELLIPSOID	ROTATION MATRIX	NORMAL EQUATION
CORE A:	$(x\ y\ z)\begin{pmatrix}+4.2187 & +0.1299 & +1.3259\\ +0.1299 & +4.8825 & +0.9603\\ +1.3259 & +0.9603 & +3.7022\end{pmatrix}\begin{pmatrix}x\\y\\z\end{pmatrix} = 10^5$	$\begin{pmatrix}+0.6519 & -0.7295 & +0.2069\\ +0.5142 & +0.6258 & +0.5865\\ +0.5573 & +0.2760 & -0.7831\end{pmatrix}$	$\frac{X^2}{149^2}+\frac{Y^2}{130^2}+\frac{Z^2}{203^2}=1$
CORE B:	$(x\ y\ z)\begin{pmatrix}+4.5177 & -0.1853 & +0.6703\\ -0.1853 & +4.0826 & +1.2664\\ +0.6703 & +1.2664 & +3.3669\end{pmatrix}\begin{pmatrix}x\\y\\z\end{pmatrix} = 10^5$	$\begin{pmatrix}+0.8489 & -0.5228 & -0.0773\\ -0.4521 & -0.6425 & -0.6187\\ -0.2738 & -0.5602 & +0.7818\end{pmatrix}$	$\frac{X^2}{148^2}+\frac{Y^2}{139^2}+\frac{Z^2}{212^2}=1$
CORE C:	$(x\ y\ z)\begin{pmatrix}+4.4622 & -0.3446 & +0.2257\\ -0.3446 & +4.6537 & +0.0593\\ +0.2257 & +0.0593 & +3.8971\end{pmatrix}\begin{pmatrix}x\\y\\z\end{pmatrix} = 10^5$	$\begin{pmatrix}+0.6242 & -0.7758 & +0.0924\\ -0.6685 & -0.5915 & -0.4509\\ -0.4045 & -0.2197 & +0.8878\end{pmatrix}$	$\frac{X^2}{143^2}+\frac{Y^2}{152^2}+\frac{Z^2}{163^2}=1$
CORE D:	$(x\ y\ z)\begin{pmatrix}+4.9258 & -0.1047 & +0.7789\\ -0.1047 & +3.7869 & +1.2053\\ +0.7789 & +1.2053 & +3.6198\end{pmatrix}\begin{pmatrix}x\\y\\z\end{pmatrix} = 10^5$	$\begin{pmatrix}-0.6096 & +0.6923 & +0.3861\\ +0.7533 & +0.3542 & +0.5541\\ -0.2468 & -0.6286 & +0.7375\end{pmatrix}$	$\frac{X^2}{148^2}+\frac{Y^2}{135^2}+\frac{Z^2}{207^2}=1$
AGGREGATE RESULTS:	$(x\ y\ z)\begin{pmatrix}+4.4784 & -0.1371 & +0.7061\\ -0.1371 & +4.3868 & +0.8183\\ +0.7061 & +0.8183 & +3.6337\end{pmatrix}\begin{pmatrix}x\\y\\z\end{pmatrix} = 10^5$	$\begin{pmatrix}+0.7394 & -0.6726 & -0.0302\\ -0.5541 & -0.5823 & -0.5949\\ -0.3826 & -0.4566 & +0.8032\end{pmatrix}$	$\frac{X^2}{148^2}+\frac{Y^2}{140^2}+\frac{Z^2}{188^2}=1$

Table 5: Ellipsoidal fit & rotation into standard form: dilational stress

	MOST PROBABLE ELLIPSOID	ROTATION MATRIX	NORMAL EQUATION
CORE A:	$(x\ y\ z)\begin{pmatrix}+24.3890 & +5.0718 & +9.4410\\ +5.0718 & +26.8860 & +4.4907\\ +9.4410 & +4.4907 & +29.2990\end{pmatrix}\begin{pmatrix}x\\y\\z\end{pmatrix} = 10^5$	$\begin{pmatrix}+0.1437 & -0.8762 & +0.4601\\ +0.8128 & -0.1608 & -0.5599\\ -0.5645 & -0.4544 & -0.6891\end{pmatrix}$	$\frac{X^2}{65^2}+\frac{Y^2}{77^2}+\frac{Z^2}{50^2}=1$
CORE B:	$(x\ y\ z)\begin{pmatrix}+25.8910 & +0.2703 & +6.1703\\ +0.2703 & +26.5880 & +6.9839\\ +6.1703 & +6.9839 & +21.3010\end{pmatrix}\begin{pmatrix}x\\y\\z\end{pmatrix} = 10^5$	$\begin{pmatrix}+0.7596 & -0.6496 & +0.0324\\ +0.5034 & +0.6187 & +0.6031\\ +0.4119 & +0.4418 & -0.7970\end{pmatrix}$	$\frac{X^2}{62^2}+\frac{Y^2}{55^2}+\frac{Z^2}{84^2}=1$
CORE C:	$(x\ y\ z)\begin{pmatrix}+30.2960 & -1.8442 & +1.6255\\ -1.8442 & +25.6830 & +1.2403\\ +1.6255 & +1.2403 & +24.7900\end{pmatrix}\begin{pmatrix}x\\y\\z\end{pmatrix} = 10^5$	$\begin{pmatrix}+0.9430 & -0.2753 & +0.1871\\ -0.0947 & -0.7609 & -0.6420\\ -0.3191 & -0.5876 & +0.7435\end{pmatrix}$	$\frac{X^2}{57^2}+\frac{Y^2}{61^2}+\frac{Z^2}{66^2}=1$
CORE D:	$(x\ y\ z)\begin{pmatrix}+27.6970 & +1.8288 & +5.6967\\ +1.8288 & +22.4310 & +8.0860\\ +5.6967 & +8.0860 & +24.7830\end{pmatrix}\begin{pmatrix}x\\y\\z\end{pmatrix} = 10^5$	$\begin{pmatrix}+0.7884 & -0.5366 & -0.3009\\ +0.2086 & +0.6932 & -0.6899\\ -0.5788 & -0.4811 & -0.6585\end{pmatrix}$	$\frac{X^2}{64^2}+\frac{Y^2}{82^2}+\frac{Z^2}{53^2}=1$
AGGREGATE RESULTS:	$(x\ y\ z)\begin{pmatrix}+26.8410 & +1.5489 & +5.8495\\ +1.5489 & +24.9430 & +5.7087\\ +5.8495 & +5.7087 & +24.2070\end{pmatrix}\begin{pmatrix}x\\y\\z\end{pmatrix} = 10^5$	$\begin{pmatrix}+0.6931 & -0.7124 & -0.1102\\ -0.3955 & -0.5036 & +0.7681\\ +0.6027 & +0.4888 & +0.6308\end{pmatrix}$	$\frac{X^2}{64^2}+\frac{Y^2}{76^2}+\frac{Z^2}{54^2}=1$

Table 6: Ellipsoidal fit & rotation into standard form: yield stress

	MOST PROBABLE ELLIPSOID	ROTATION MATRIX	NORMAL EQUATION
CORE A:	$(x\ y\ z)\begin{pmatrix}+21.6680 & -4.7490 & -1.1748\\ -4.7490 & +24.2610 & -0.9451\\ -1.1748 & -0.9451 & +11.4470\end{pmatrix}\begin{pmatrix}x\\y\\z\end{pmatrix} = 10^5$	$\begin{pmatrix}+0.6066 & -0.7950 & +0.0024\\ -0.7771 & -0.5923 & +0.2127\\ +0.1677 & +0.1309 & +0.9771\end{pmatrix}$	$\frac{X^2}{60^2}+\frac{Y^2}{74^2}+\frac{Z^2}{95^2}=1$
CORE B:	$(x\ y\ z)\begin{pmatrix}+15.8380 & -1.8802 & +6.4337\\ -1.8802 & +13.9990 & +7.3063\\ +6.4337 & +7.3063 & +8.2016\end{pmatrix}\begin{pmatrix}x\\y\\z\end{pmatrix} = 10^5$	$\begin{pmatrix}+0.6806 & -0.7249 & -0.1063\\ -0.6206 & -0.4932 & -0.6096\\ -0.3895 & -0.4808 & +0.7856\end{pmatrix}$	$\frac{X^2}{77^2}+\frac{Y^2}{70^2}+\frac{Z^2}{430^2}=1$
CORE C:	$(x\ y\ z)\begin{pmatrix}+13.0790 & +1.6550 & +2.7818\\ +1.6550 & +17.6720 & +0.0678\\ +2.7818 & +0.0678 & +9.7430\end{pmatrix}\begin{pmatrix}x\\y\\z\end{pmatrix} = 10^5$	$\begin{pmatrix}-0.3577 & -0.9275 & -0.1233\\ -0.7842 & +0.3695 & -0.4986\\ -0.5071 & +0.0816 & +0.8580\end{pmatrix}$	$\frac{X^2}{74^2}+\frac{Y^2}{84^2}+\frac{Z^2}{111^2}=1$
CORE D:	$(x\ y\ z)\begin{pmatrix}+15.3180 & -4.1823 & +7.5275\\ -4.1823 & +18.0590 & -3.1342\\ +7.5275 & -3.1342 & +11.7280\end{pmatrix}\begin{pmatrix}x\\y\\z\end{pmatrix} = 10^5$	$\begin{pmatrix}+0.4588 & +0.8039 & +0.3783\\ +0.6230 & +0.0125 & -0.7821\\ +0.6336 & -0.5946 & +0.4951\end{pmatrix}$	$\frac{X^2}{84^2}+\frac{Y^2}{132^2}+\frac{Z^2}{63^2}=1$
AGGREGATE RESULTS:	$(x\ y\ z)\begin{pmatrix}+15.2450 & -1.4084 & +3.9823\\ -1.4084 & +16.8470 & +1.2242\\ +3.9823 & +1.2242 & +9.9786\end{pmatrix}\begin{pmatrix}x\\y\\z\end{pmatrix} = 10^5$	$\begin{pmatrix}+0.7237 & -0.6376 & +0.2640\\ -0.4995 & -0.7479 & -0.4372\\ -0.4762 & -0.1846 & +0.8597\end{pmatrix}$	$\frac{X^2}{75^2}+\frac{Y^2}{78^2}+\frac{Z^2}{115^2}=1$

Table 7: Ellipsoidal fit & rotation into standard form: 40% tangent modulus

	MOST PROBABLE ELLIPSOID	ROTATION MATRIX	NORMAL EQUATION
CORE A:	$(x\ y\ z)\begin{pmatrix}+33.5150 & +5.7149 & +15.8967\\ +5.7149 & +27.4323 & +15.7201\\ +15.8967 & +15.7201 & +33.5340\end{pmatrix}\begin{pmatrix}x\\y\\z\end{pmatrix} = 10^5$	$\begin{pmatrix}+0.7370 & -0.6560 & -0.1629\\ +0.3715 & +0.5945 & -0.7131\\ -0.5646 & -0.4651 & -0.6819\end{pmatrix}$	$\frac{X^2}{63^2}+\frac{Y^2}{91^2}+\frac{Z^2}{42^2}=1$
CORE B:	$(x\ y\ z)\begin{pmatrix}+42.2647 & +6.1894 & +8.1965\\ +6.1894 & +23.5358 & +10.0408\\ +8.1965 & +10.0408 & +33.4813\end{pmatrix}\begin{pmatrix}x\\y\\z\end{pmatrix} = 10^5$	$\begin{pmatrix}+0.0460 & -0.8596 & +0.5089\\ +0.6600 & -0.3563 & -0.6614\\ -0.7498 & -0.3663 & -0.5510\end{pmatrix}$	$\frac{X^2}{76^2}+\frac{Y^2}{57^2}+\frac{Z^2}{44^2}=1$
CORE C:	$(x\ y\ z)\begin{pmatrix}+49.9291 & -11.0040 & -4.0001\\ -11.0040 & +41.8906 & -3.7761\\ -4.0001 & -3.7761 & +45.0434\end{pmatrix}\begin{pmatrix}x\\y\\z\end{pmatrix} = 10^5$	$\begin{pmatrix}+0.8281 & -0.5521 & -0.0967\\ -0.1386 & -0.3689 & +0.9191\\ +0.5431 & +0.7477 & +0.3821\end{pmatrix}$	$\frac{X^2}{42^2}+\frac{Y^2}{46^2}+\frac{Z^2}{56^2}=1$
CORE D:	$(x\ y\ z)\begin{pmatrix}+40.5265 & +4.1222 & +11.4282\\ +4.1222 & +32.6082 & +10.4512\\ +11.4282 & +10.4512 & +36.0291\end{pmatrix}\begin{pmatrix}x\\y\\z\end{pmatrix} = 10^5$	$\begin{pmatrix}+0.6961 & -0.6703 & -0.2571\\ +0.3178 & +0.6088 & -0.7269\\ -0.6438 & -0.4243 & -0.6368\end{pmatrix}$	$\frac{X^2}{56^2}+\frac{Y^2}{67^2}+\frac{Z^2}{43^2}=1$
AGGREGATE RESULTS:	$(x\ y\ z)\begin{pmatrix}+39.6942 & +3.9583 & +9.4109\\ +3.9583 & +28.2623 & +10.4983\\ +9.4109 & +10.4983 & +35.5573\end{pmatrix}\begin{pmatrix}x\\y\\z\end{pmatrix} = 10^5$	$\begin{pmatrix}+0.7466 & -0.5013 & -0.4373\\ +0.1483 & +0.7662 & -0.6253\\ -0.6485 & -0.4020 & -0.6464\end{pmatrix}$	$\frac{X^2}{56^2}+\frac{Y^2}{70^2}+\frac{Z^2}{44^2}=1$

Table 8: Ellipsoidal fit & rotation into standard form: 50% tangent modulus

	MOST PROBABLE ELLIPSOID	ROTATION MATRIX	NORMAL EQUATION
CORE A:	$(x\ y\ z)\begin{pmatrix}+29.5780 & +4.5710 & +14.8839\\ +4.5710 & +25.7330 & +12.6529\\ +14.8839 & +12.6529 & +30.5258\end{pmatrix}\begin{pmatrix}x\\y\\z\end{pmatrix} = 10^5$	$\begin{pmatrix}+0.6676 & -0.7409 & -0.0734\\ +0.4773 & +0.5016 & -0.7215\\ -0.5714 & -0.4466 & -0.6885\end{pmatrix}$	$\frac{X^2}{66^2}+\frac{Y^2}{92^2}+\frac{Z^2}{44^2}=1$
CORE B:	$(x\ y\ z)\begin{pmatrix}+36.0660 & +6.9754 & +7.0236\\ +6.9754 & +21.4735 & +7.8675\\ +7.0236 & +7.8675 & +30.7409\end{pmatrix}\begin{pmatrix}x\\y\\z\end{pmatrix} = 10^5$	$\begin{pmatrix}-0.1721 & +0.8954 & -0.4106\\ +0.6671 & -0.2008 & -0.7174\\ +0.7249 & +0.3973 & +0.5628\end{pmatrix}$	$\frac{X^2}{78^2}+\frac{Y^2}{62^2}+\frac{Z^2}{47^2}=1$
CORE C:	$(x\ y\ z)\begin{pmatrix}+43.6180 & -9.3051 & -2.4055\\ -9.3051 & +38.2721 & -4.7087\\ -2.4055 & -4.7087 & +40.1079\end{pmatrix}\begin{pmatrix}x\\y\\z\end{pmatrix} = 10^5$	$\begin{pmatrix}+0.7788 & -0.6195 & +0.0984\\ -0.3331 & -0.2755 & +0.9018\\ +0.5316 & +0.7350 & +0.4209\end{pmatrix}$	$\frac{X^2}{44^2}+\frac{Y^2}{49^2}+\frac{Z^2}{59^2}=1$
CORE D:	$(x\ y\ z)\begin{pmatrix}+34.3204 & +4.2599 & +10.2990\\ +4.2599 & +31.1394 & +8.4528\\ +10.2990 & +8.4528 & +31.9687\end{pmatrix}\begin{pmatrix}x\\y\\z\end{pmatrix} = 10^5$	$\begin{pmatrix}+0.6474 & -0.7592 & -0.0672\\ +0.4502 & +0.4521 & -0.7700\\ -0.6150 & -0.4682 & -0.6345\end{pmatrix}$	$\frac{X^2}{59^2}+\frac{Y^2}{69^2}+\frac{Z^2}{46^2}=1$
AGGREGATE RESULTS:	$(x\ y\ z)\begin{pmatrix}+34.4429 & +3.9925 & +8.7016\\ +3.9925 & +26.1781 & +8.1455\\ +8.7016 & +8.1455 & +32.1620\end{pmatrix}\begin{pmatrix}x\\y\\z\end{pmatrix} = 10^5$	$\begin{pmatrix}+0.7444 & -0.5287 & -0.4078\\ +0.1807 & +0.7475 & -0.6392\\ -0.6428 & -0.4021 & -0.6520\end{pmatrix}$	$\frac{X^2}{61^2}+\frac{Y^2}{70^2}+\frac{Z^2}{47^2}=1$

Table 9: Ellipsoidal fit & rotation into standard form: 25 MPa tangent modulus

	MOST PROBABLE ELLIPSOID	ROTATION MATRIX	NORMAL EQUATION
CORE A:	$(x\ y\ z)\begin{pmatrix} +74.6706 & +3.5736 & +19.7912 \\ +3.5736 & +57.8620 & +8.6109 \\ +19.7912 & +8.6109 & +86.2936 \end{pmatrix}\begin{pmatrix} x \\ y \\ z \end{pmatrix} = 10^5$	$\begin{pmatrix} +0.2330 & +0.8899 & -0.3923 \\ +0.7813 & -0.4115 & -0.4694 \\ +0.5791 & +0.1971 & +0.7911 \end{pmatrix}$	$\frac{X^2}{43^2}+\frac{Y^2}{41^2}+\frac{Z^2}{31^2}=1$
CORE B:	$(x\ y\ z)\begin{pmatrix} +100.8986 & +4.2454 & +0.0682 \\ +4.2454 & +46.0644 & +10.3378 \\ +0.0682 & +10.3378 & +87.0140 \end{pmatrix}\begin{pmatrix} x \\ y \\ z \end{pmatrix} = 10^5$	$\begin{pmatrix} +0.9936 & +0.0894 & +0.0695 \\ +0.0880 & -0.2231 & -0.9708 \\ +0.0713 & -0.9707 & +0.2295 \end{pmatrix}$	$\frac{X^2}{31^2}+\frac{Y^2}{33^2}+\frac{Z^2}{48^2}=1$
CORE C:	$(x\ y\ z)\begin{pmatrix} +108.4837 & -19.4175 & -21.4524 \\ -19.4175 & +67.7841 & -9.9806 \\ -21.4524 & -9.9806 & +109.1249 \end{pmatrix}\begin{pmatrix} x \\ y \\ z \end{pmatrix} = 10^5$	$\begin{pmatrix} -0.7366 & +0.1211 & +0.6654 \\ +0.5233 & -0.5212 & +0.6741 \\ -0.4285 & -0.8448 & -0.3206 \end{pmatrix}$	$\frac{X^2}{28^2}+\frac{Y^2}{32^2}+\frac{Z^2}{43^2}=1$
CORE D:	$(x\ y\ z)\begin{pmatrix} +88.7664 & +9.1381 & +4.2434 \\ +9.1381 & +50.9475 & +11.6984 \\ +4.2434 & +11.6984 & +90.7838 \end{pmatrix}\begin{pmatrix} x \\ y \\ z \end{pmatrix} = 10^5$	$\begin{pmatrix} -0.7861 & +0.0014 & +0.6181 \\ +0.5906 & +0.2966 & +0.7505 \\ +0.1823 & -0.9550 & 0.2340 \end{pmatrix}$	$\frac{X^2}{34^2}+\frac{Y^2}{32^2}+\frac{Z^2}{46^2}=1$
AGGREGATE RESULTS:	$(x\ y\ z)\begin{pmatrix} +90.2094 & +0.1862 & +3.3788 \\ +0.1862 & +54.8844 & +6.4858 \\ +3.3788 & +6.4858 & +91.4607 \end{pmatrix}\begin{pmatrix} x \\ y \\ z \end{pmatrix} = 10^5$	$\begin{pmatrix} -0.8159 & +0.1072 & +0.5681 \\ +0.5781 & +0.1330 & +0.8051 \\ -0.0108 & -0.9853 & +0.1705 \end{pmatrix}$	$\frac{X^2}{34^2}+\frac{Y^2}{32^2}+\frac{Z^2}{43^2}=1$

Table 10: Ellipsoidal fit & rotation into standard form: 40% Poisson's ratio

	MOST PROBABLE ELLIPSOID	ROTATION MATRIX	NORMAL EQUATION
CORE A:	$(x\ y\ z)\begin{pmatrix}+3.3448 & -0.7742 & +0.0584\\ -0.7742 & +3.3769 & -0.9943\\ +0.0584 & -0.9943 & +7.5731\end{pmatrix}\begin{pmatrix}x\\y\\z\end{pmatrix}=1$	$\begin{pmatrix}+0.6625 & +0.7365 & +0.1366\\ +0.7473 & -0.6371 & -0.1890\\ +0.0521 & -0.2273 & +0.9724\end{pmatrix}$	$\frac{X^2}{0.63^2}+\frac{Y^2}{0.50^2}+\frac{Z^2}{0.36^2}=1$
CORE B:	$(x\ y\ z)\begin{pmatrix}+4.5165 & +1.2443 & -2.4775\\ +1.2443 & +4.1643 & -2.2231\\ -2.4775 & -2.2231 & +7.7888\end{pmatrix}\begin{pmatrix}x\\y\\z\end{pmatrix}=1$	$\begin{pmatrix}+0.4709 & -0.8673 & -0.1615\\ -0.7655 & -0.3107 & -0.5635\\ -0.4385 & -0.3890 & +0.8102\end{pmatrix}$	$\frac{X^2}{0.57^2}+\frac{Y^2}{0.56^2}+\frac{Z^2}{0.31^2}=1$
CORE C:	$(x\ y\ z)\begin{pmatrix}+8.3136 & -1.6264 & -1.6010\\ -1.6264 & +3.2964 & +1.5290\\ -1.6010 & 1.5290 & +4.1585\end{pmatrix}\begin{pmatrix}x\\y\\z\end{pmatrix}=1$	$\begin{pmatrix}-0.0715 & -0.8247 & +0.5611\\ +0.4676 & +0.4692 & +0.7491\\ +0.8810 & -0.3159 & -0.3521\end{pmatrix}$	$\frac{X^2}{0.69^2}+\frac{Y^2}{0.49^2}+\frac{Z^2}{0.32^2}=1$
CORE D:	$(x\ y\ z)\begin{pmatrix}+7.0599 & +0.0572 & -1.8941\\ +0.0572 & +4.1669 & +2.5802\\ -1.8941 & +2.5802 & +5.1458\end{pmatrix}\begin{pmatrix}x\\y\\z\end{pmatrix}=1$	$\begin{pmatrix}+0.6689 & +0.6188 & +0.4119\\ +0.7024 & -0.3447 & -0.6227\\ +0.2433 & -0.7059 & +0.6653\end{pmatrix}$	$\frac{X^2}{0.41^2}+\frac{Y^2}{0.34^2}+\frac{Z^2}{0.76^2}=1$
AGGREGATE RESULTS:	$(x\ y\ z)\begin{pmatrix}+4.3918 & -0.3528 & -0.8783\\ -0.3528 & +3.3752 & +0.0656\\ -0.8783 & +0.0656 & +5.7137\end{pmatrix}\begin{pmatrix}x\\y\\z\end{pmatrix}=1$	$\begin{pmatrix}+0.3647 & +0.9252 & +0.1051\\ +0.8129 & -0.3714 & +0.4487\\ -0.4541 & +0.0782 & +0.8875\end{pmatrix}$	$\frac{X^2}{0.56^2}+\frac{Y^2}{0.50^2}+\frac{Z^2}{0.40^2}=1$

Table 11: Ellipsoidal fit & rotation into standard form: 50% Poisson's ratio

	MOST PROBABLE ELLIPSOID	ROTATION MATRIX	NORMAL EQUATION
CORE A:	$(x\ y\ z)\begin{pmatrix}+5.2612 & -0.2714 & +1.8519\\ -0.2714 & +5.5985 & -1.4117\\ +1.8519 & -1.4117 & +11.3235\end{pmatrix}\begin{pmatrix}x\\y\\z\end{pmatrix}=1$	$\begin{pmatrix}+0.2523 & +0.9565 & +0.1468\\ +0.9317 & -0.1991 & -0.3037\\ +0.2612 & -0.2134 & +0.9414\end{pmatrix}$	$\frac{X^2}{0.43^2}+\frac{Y^2}{0.46^2}+\frac{Z^2}{0.29^2}=1$
CORE B:	$(x\ y\ z)\begin{pmatrix}+8.0749 & +0.9602 & -2.5473\\ +0.9602 & +9.1739 & -5.0595\\ -2.5473 & -5.0595 & +10.7397\end{pmatrix}\begin{pmatrix}x\\y\\z\end{pmatrix}=1$	$\begin{pmatrix}+0.9002 & -0.4345 & +0.0295\\ -0.3030 & -0.6735 & -0.6742\\ -0.3128 & -0.5980 & +0.7379\end{pmatrix}$	$\frac{X^2}{0.36^2}+\frac{Y^2}{0.47^2}+\frac{Z^2}{0.25^2}=1$
CORE C:	$(x\ y\ z)\begin{pmatrix}+13.4534 & -3.2750 & -2.4735\\ -3.2750 & +5.9139 & +1.7246\\ -2.4735 & +1.7246 & +7.5798\end{pmatrix}\begin{pmatrix}x\\y\\z\end{pmatrix}=1$	$\begin{pmatrix}+0.2490 & +0.9180 & +0.3086\\ -0.4196 & -0.1849 & -0.8887\\ +0.8729 & -0.3508 & -0.3391\end{pmatrix}$	$\frac{X^2}{0.47^2}+\frac{Y^2}{0.38^2}+\frac{Z^2}{0.25^2}=1$
CORE D:	$(x\ y\ z)\begin{pmatrix}+12.1302 & -0.9790 & -2.7956\\ -0.9790 & +7.5528 & +4.2955\\ -2.7956 & +4.2955 & +8.4063\end{pmatrix}\begin{pmatrix}x\\y\\z\end{pmatrix}=1$	$\begin{pmatrix}+0.6969 & +0.5730 & +0.4313\\ +0.7021 & -0.4227 & -0.5730\\ +0.1460 & -0.7021 & +0.6969\end{pmatrix}$	$\frac{X^2}{0.32^2}+\frac{Y^2}{0.26^2}+\frac{Z^2}{0.54^2}=1$
AGGREGATE RESULTS:	$(x\ y\ z)\begin{pmatrix}+7.3675 & -0.2504 & -0.1785\\ -0.2504 & +5.8919 & +0.1031\\ -0.1785 & +0.1031 & +8.6205\end{pmatrix}\begin{pmatrix}x\\y\\z\end{pmatrix}=1$	$\begin{pmatrix}+0.1596 & +0.9868 & -0.0264\\ +0.9762 & -0.1537 & +0.1531\\ -0.1471 & +0.0502 & +0.9878\end{pmatrix}$	$\frac{X^2}{0.41^2}+\frac{Y^2}{0.37^2}+\frac{Z^2}{0.34^2}=1$

Table 12: Mean maximum anisotropies of uniaxial mechanical properties

Core Section	Compressive Strength (MPa)			Tangent Modulus of Elasticity (GPa)			Poisson's Ratio	
	Uniaxial	Dilational	Yield	50%	40%	@ 25 MPa	50%	40%
A	1.56	1.54	1.58	2.07	2.17	1.37	1.77	1.61
B	1.52	1.53	6.14	1.66	1.72	1.53	1.82	1.87
C	1.14	1.16	1.50	1.33	1.34	1.56	2.12	1.88
D	1.53	1.55	2.10	1.52	1.56	1.46	2.25	2.07
Mean	1.44	1.44	2.83	1.64	1.70	1.48	1.99	1.86
Std. Dev.	0.20	0.19	2.22	0.32	0.35	0.08	0.23	0.19
Aggregate Results	1.34	1.41	1.53	1.51	1.59	1.33	1.38	1.22

Appendix A

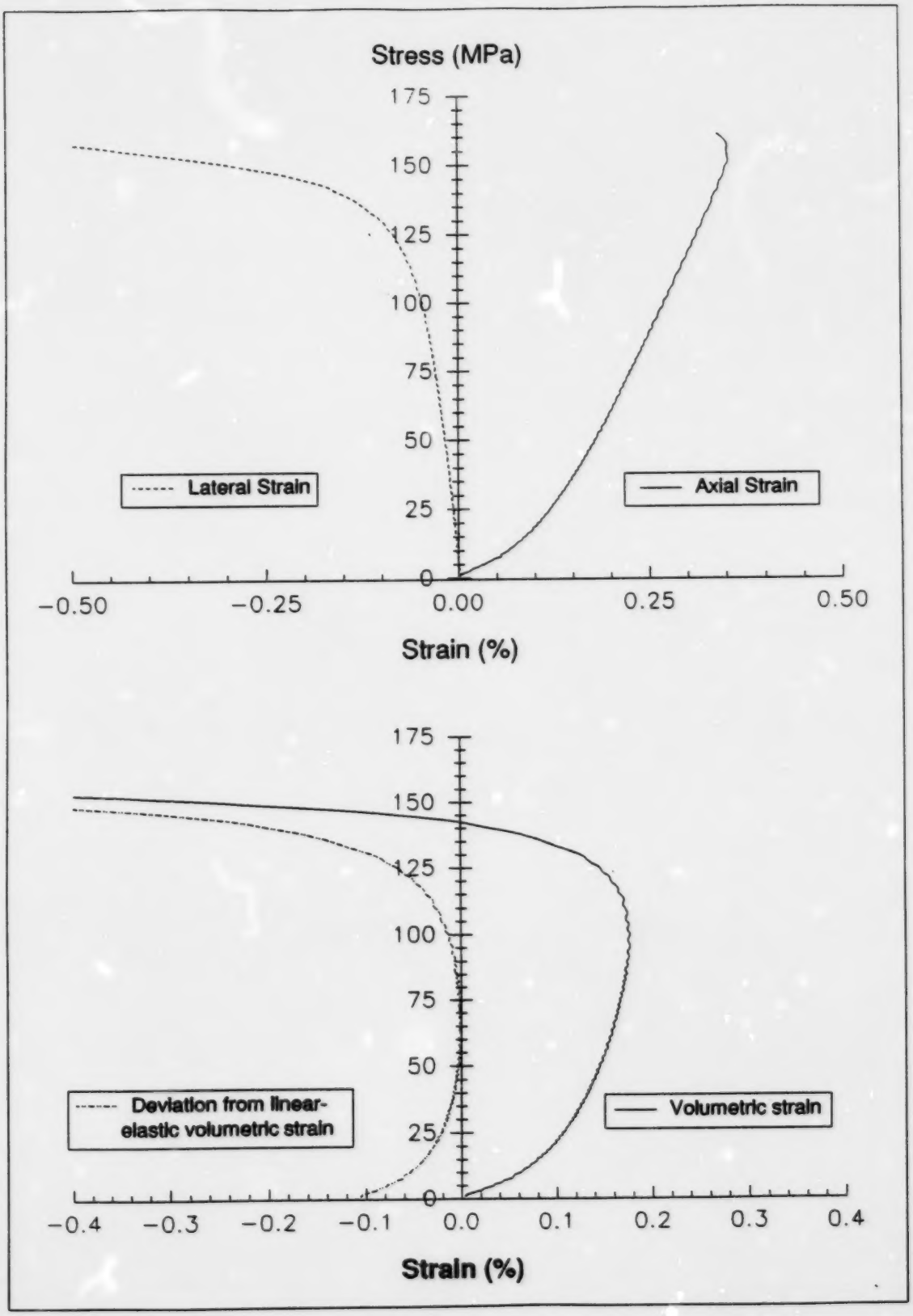

Figure A1 - Stress/strain curves for sample no. 1.304

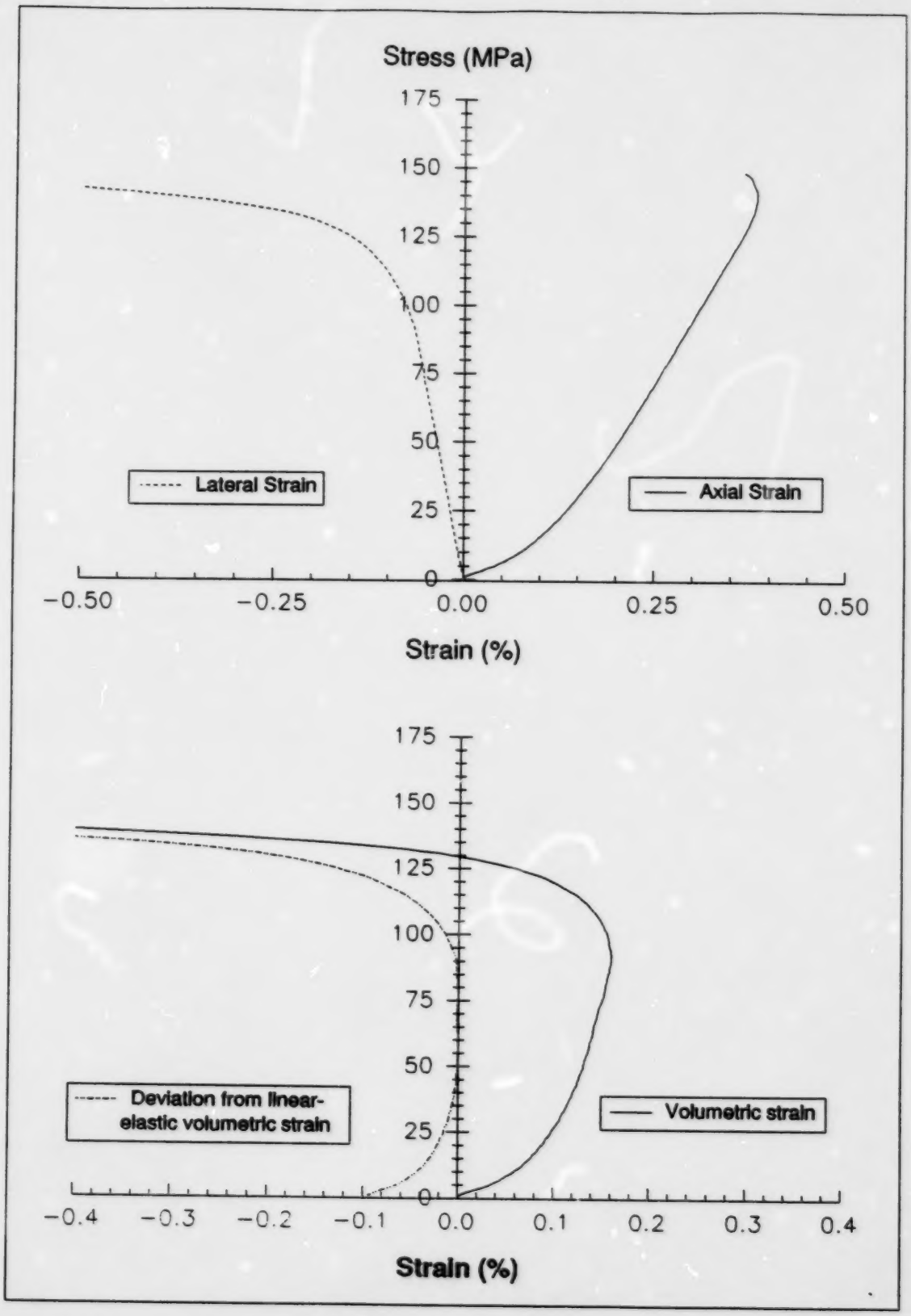

Figure A2 - Stress/strain curves for sample no. 1.912

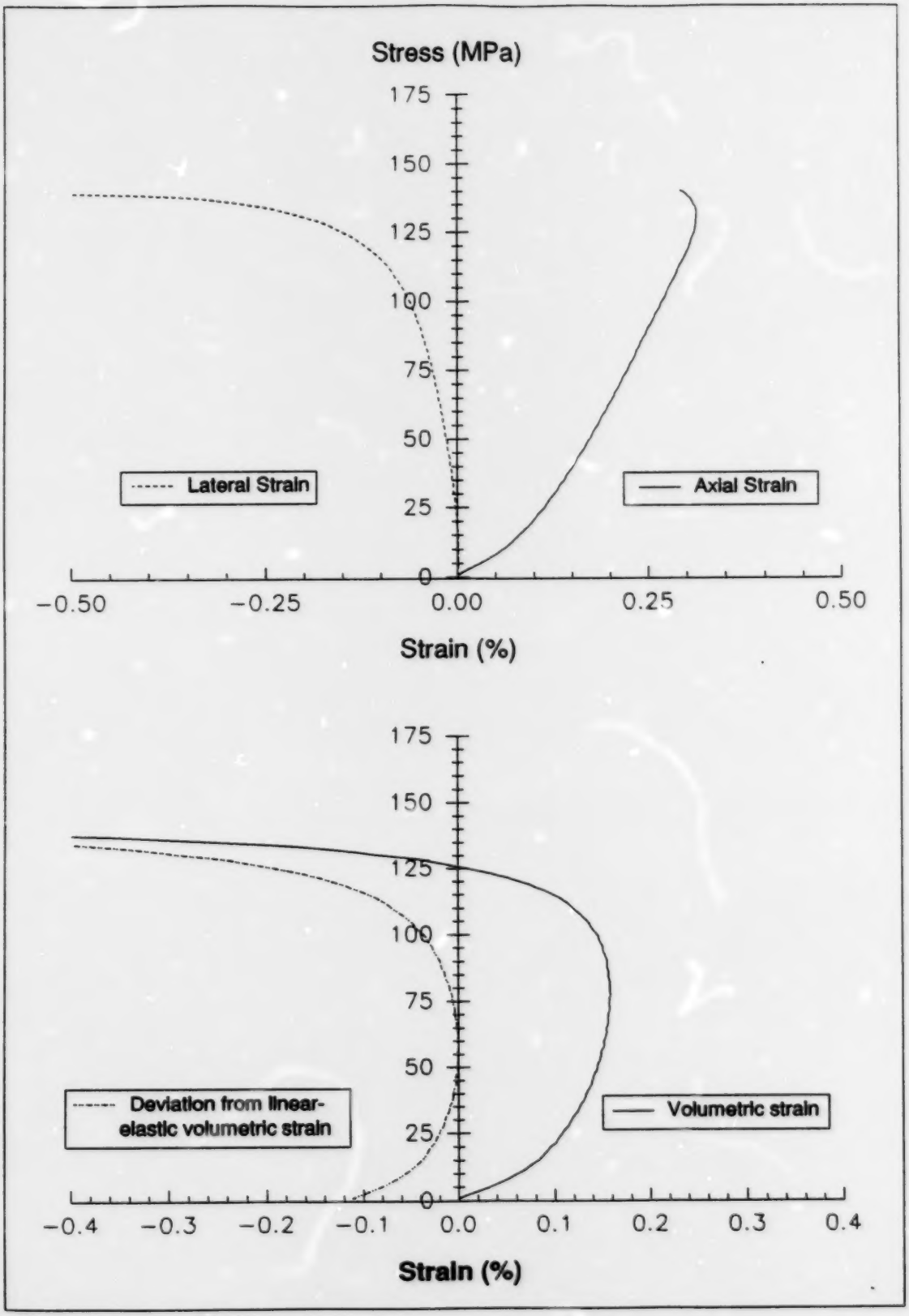

Figure A3 - Stress/strain curves for sample no. 1.774

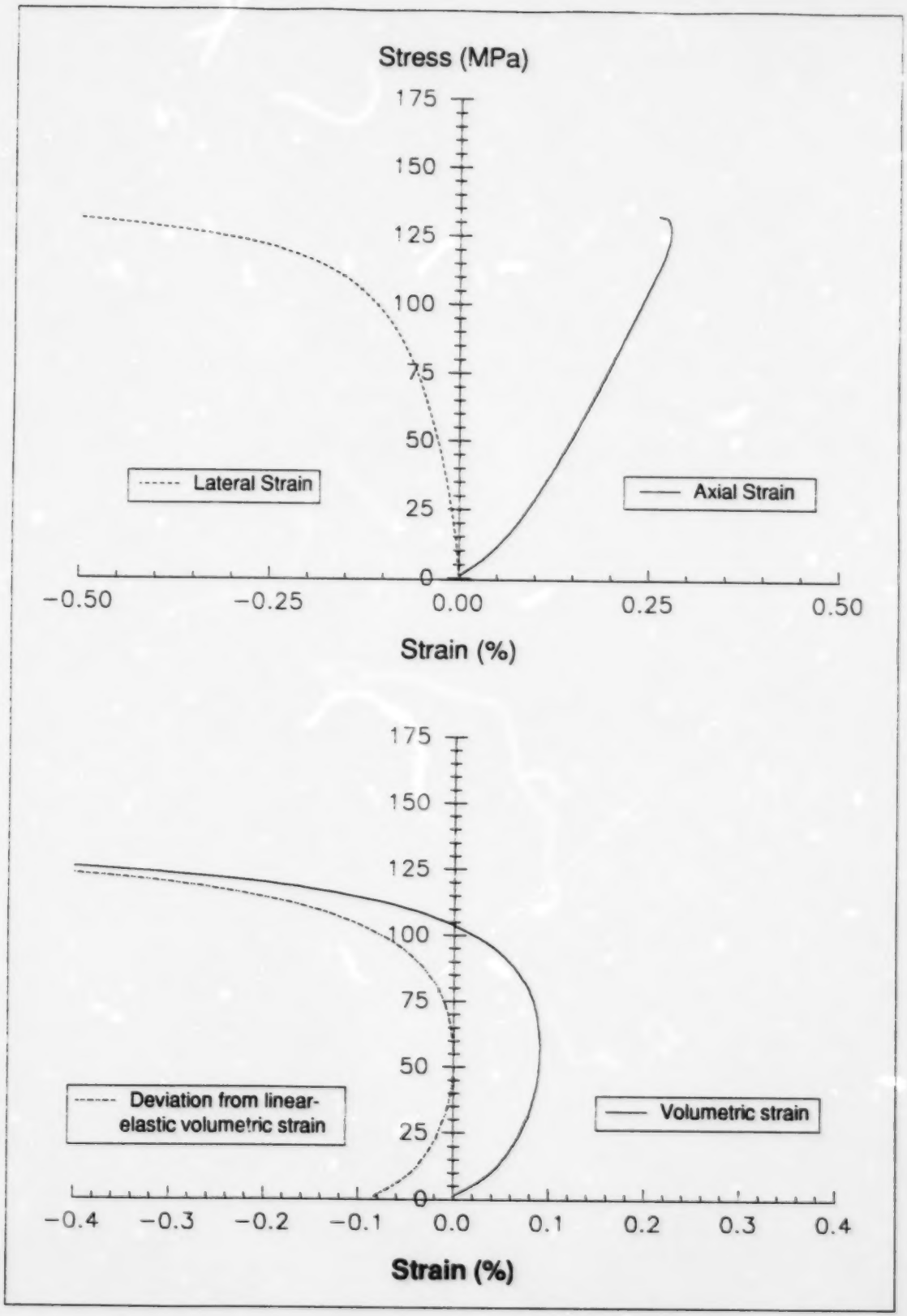

Figure A4 - Stress/strain curves for sample no. 1.681

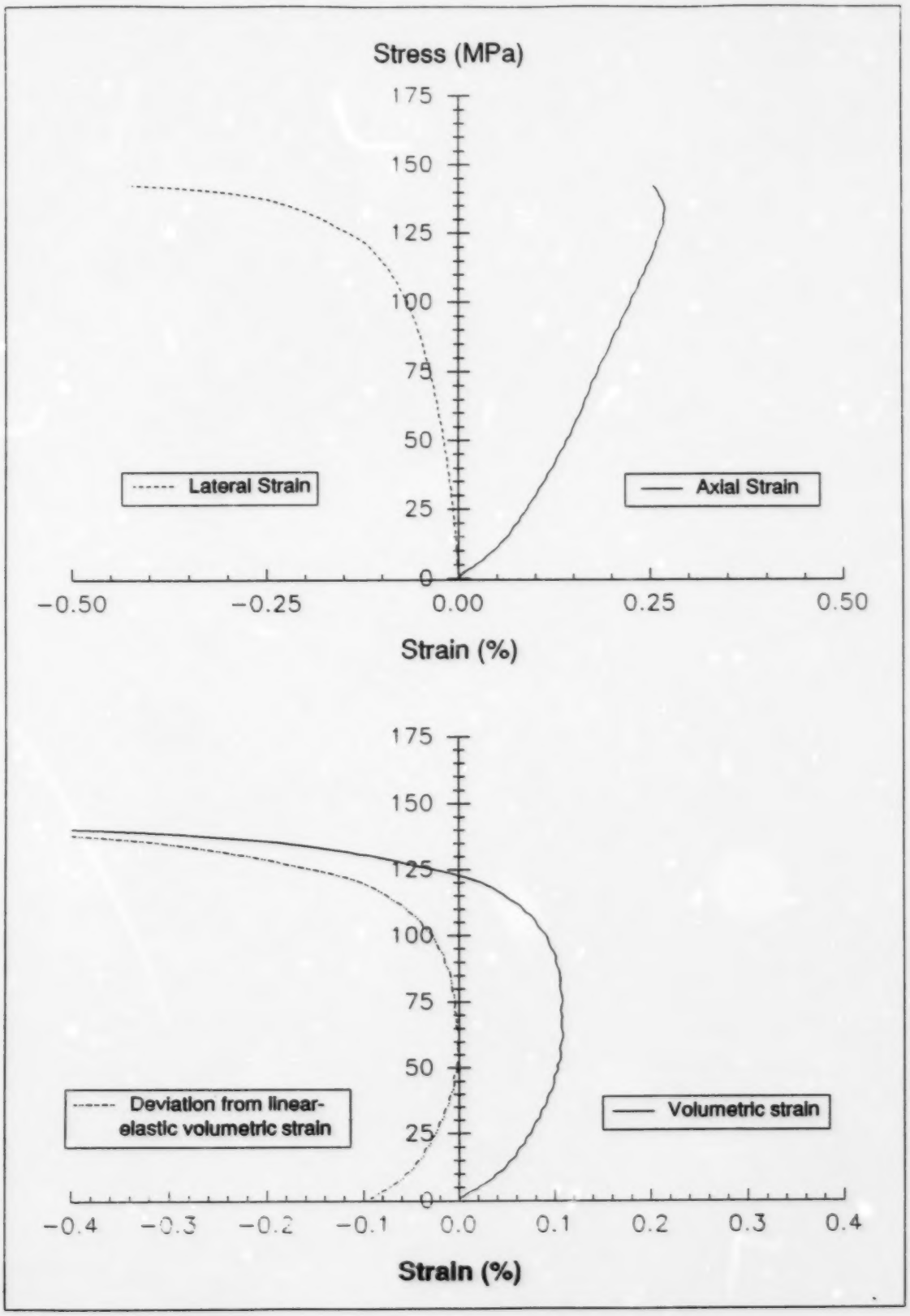

Figure A5 - Stress/strain curves for sample no. 1.599

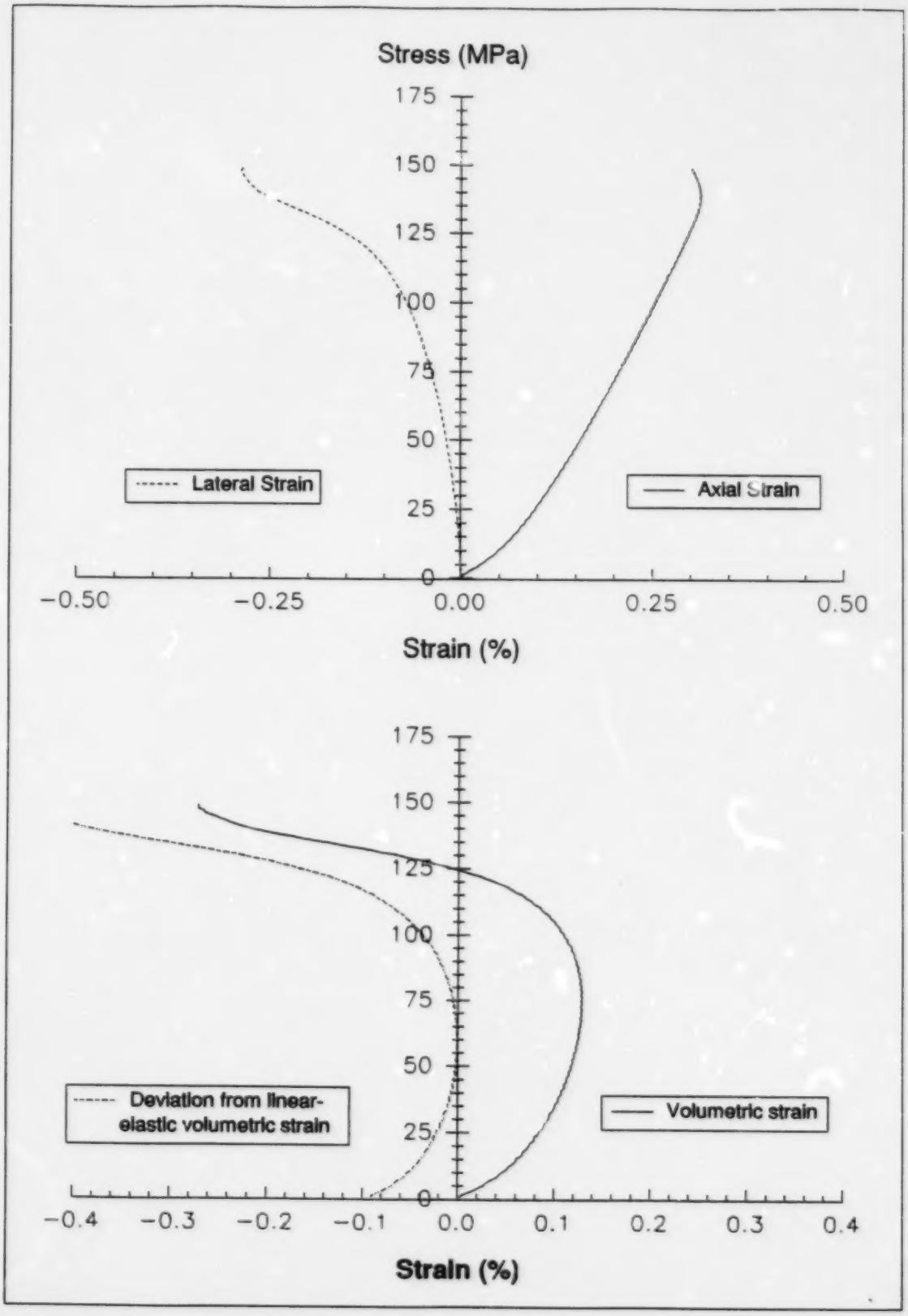

Figure A6 - Stress/strain curves for sample no. 1.394

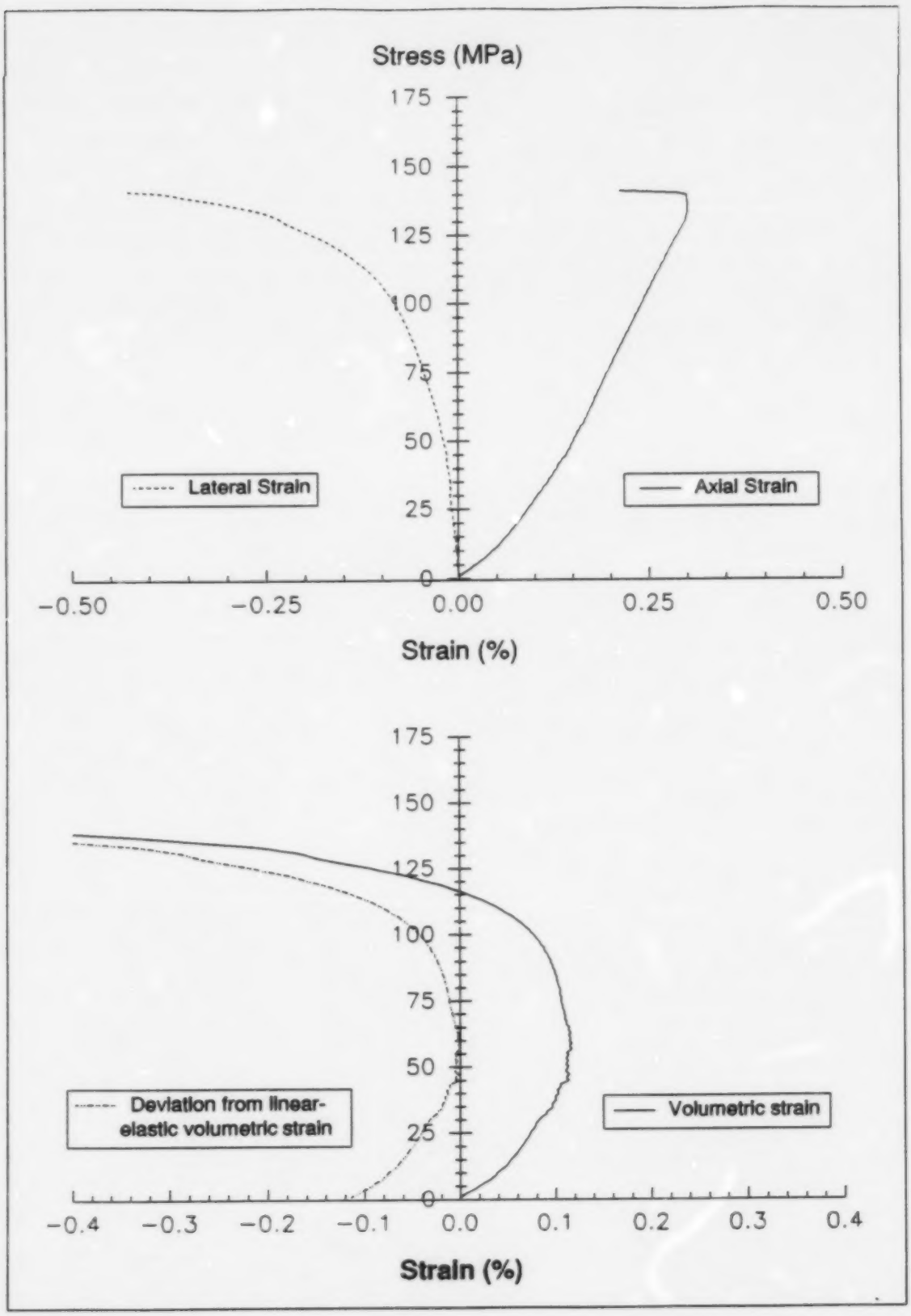

Figure A7 - Stress/strain curves for sample no. 1.442

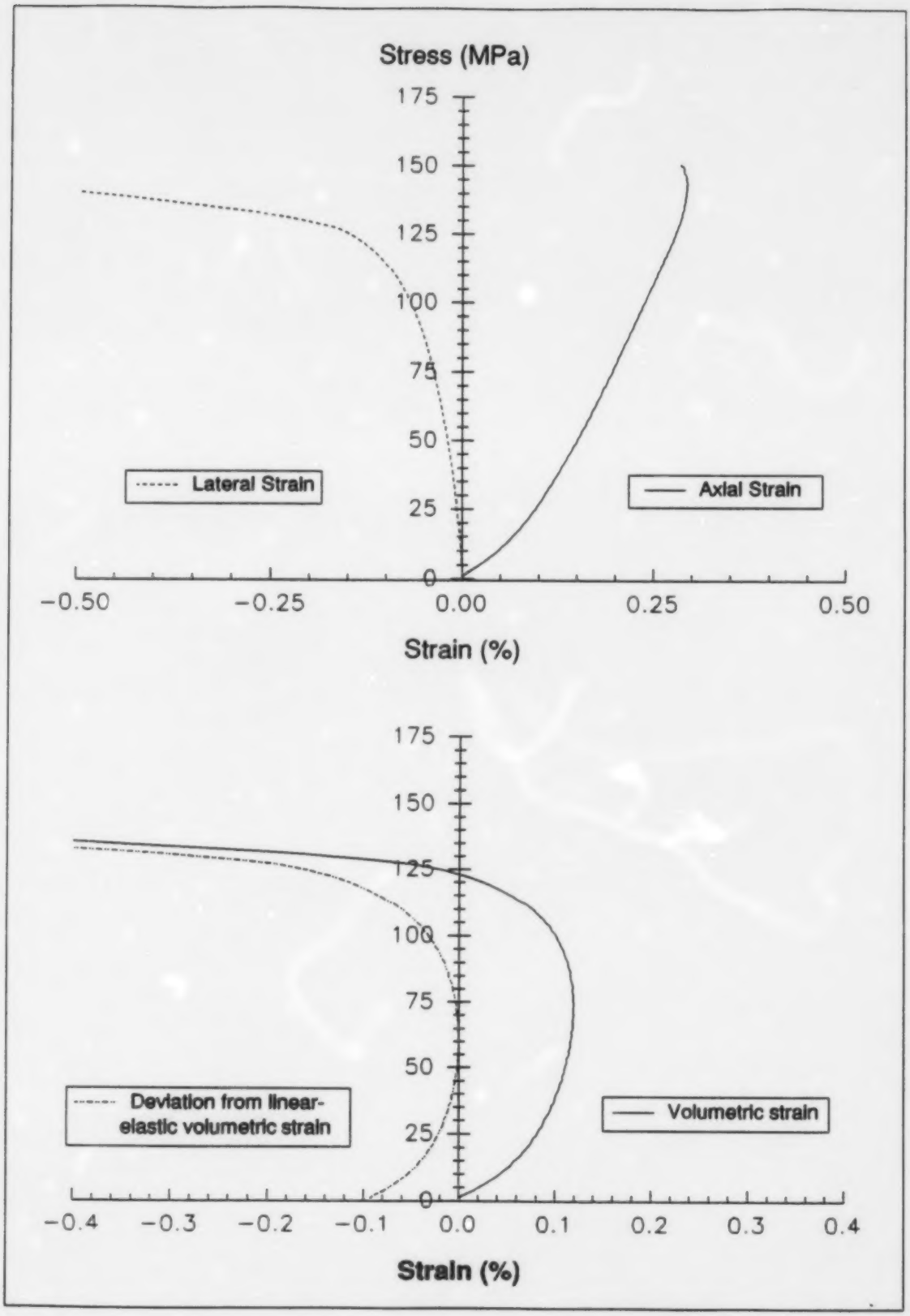

Figure A8 - Stress/strain curves for sample no. 1.485

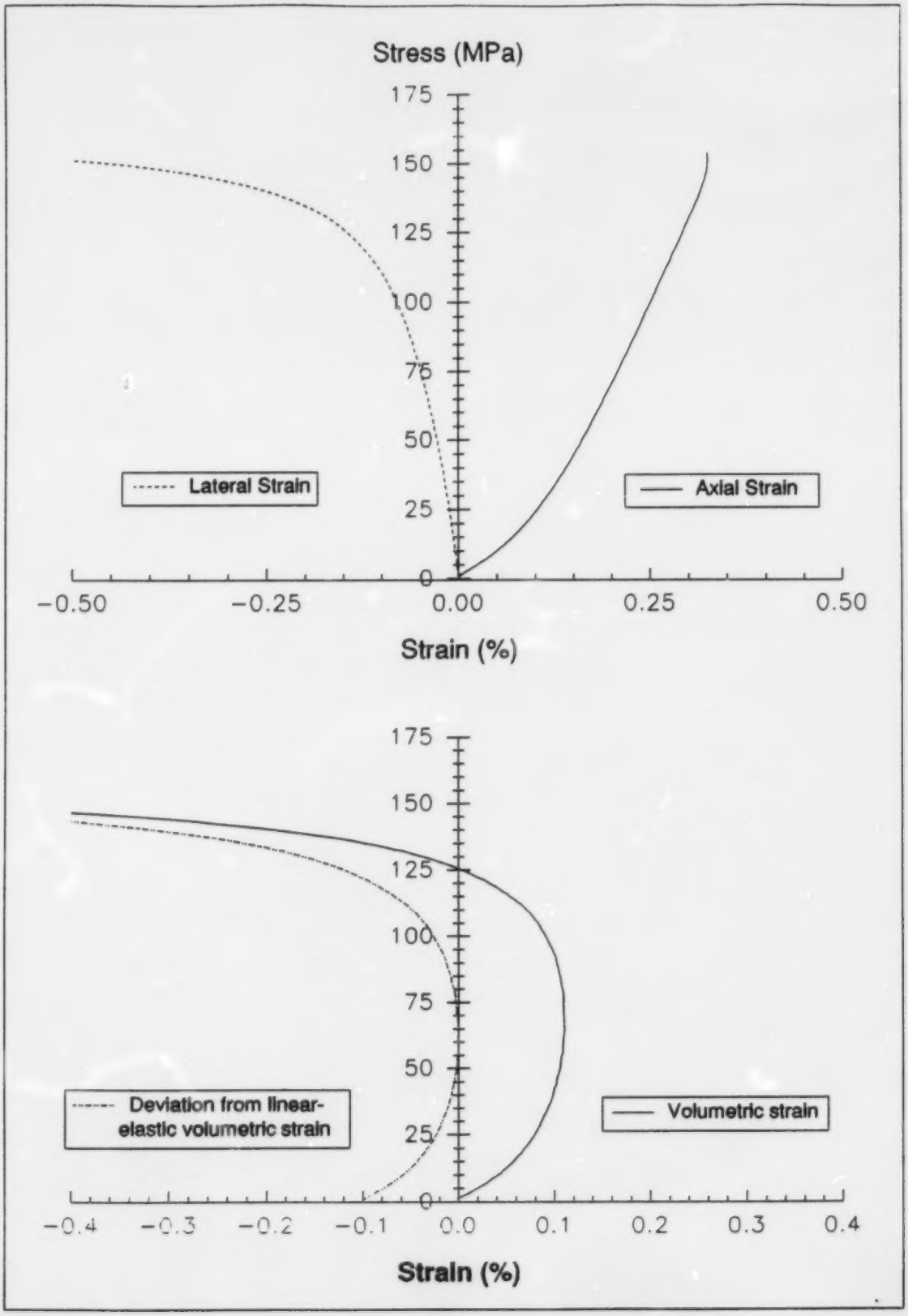

Figure A9 - Stress/strain curves for sample no. 1.537

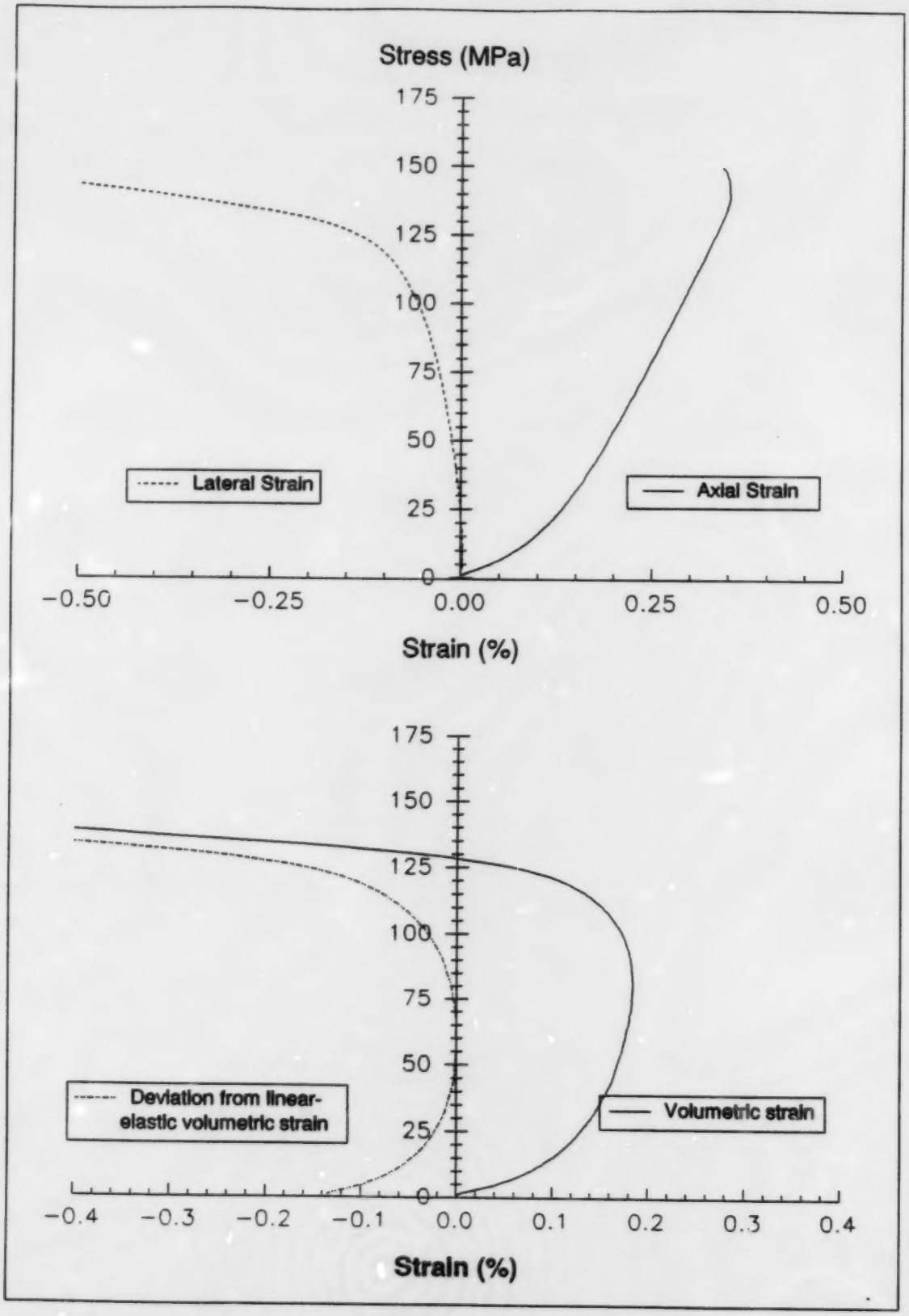

Figure A10 - Stress/strain curves for sample no. 1.882

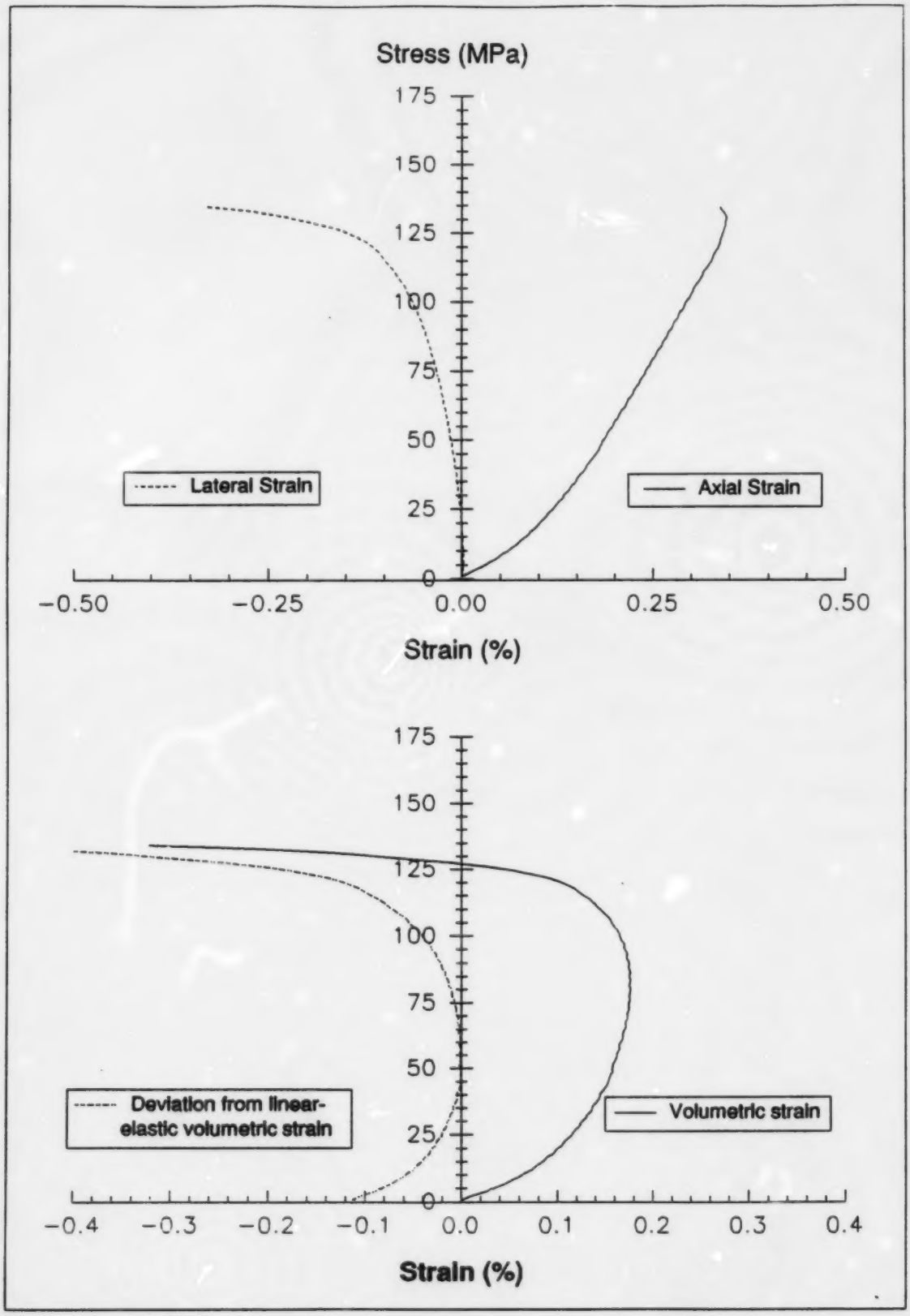

Figure A11 - Stress/strain curves for sample no. 2.105

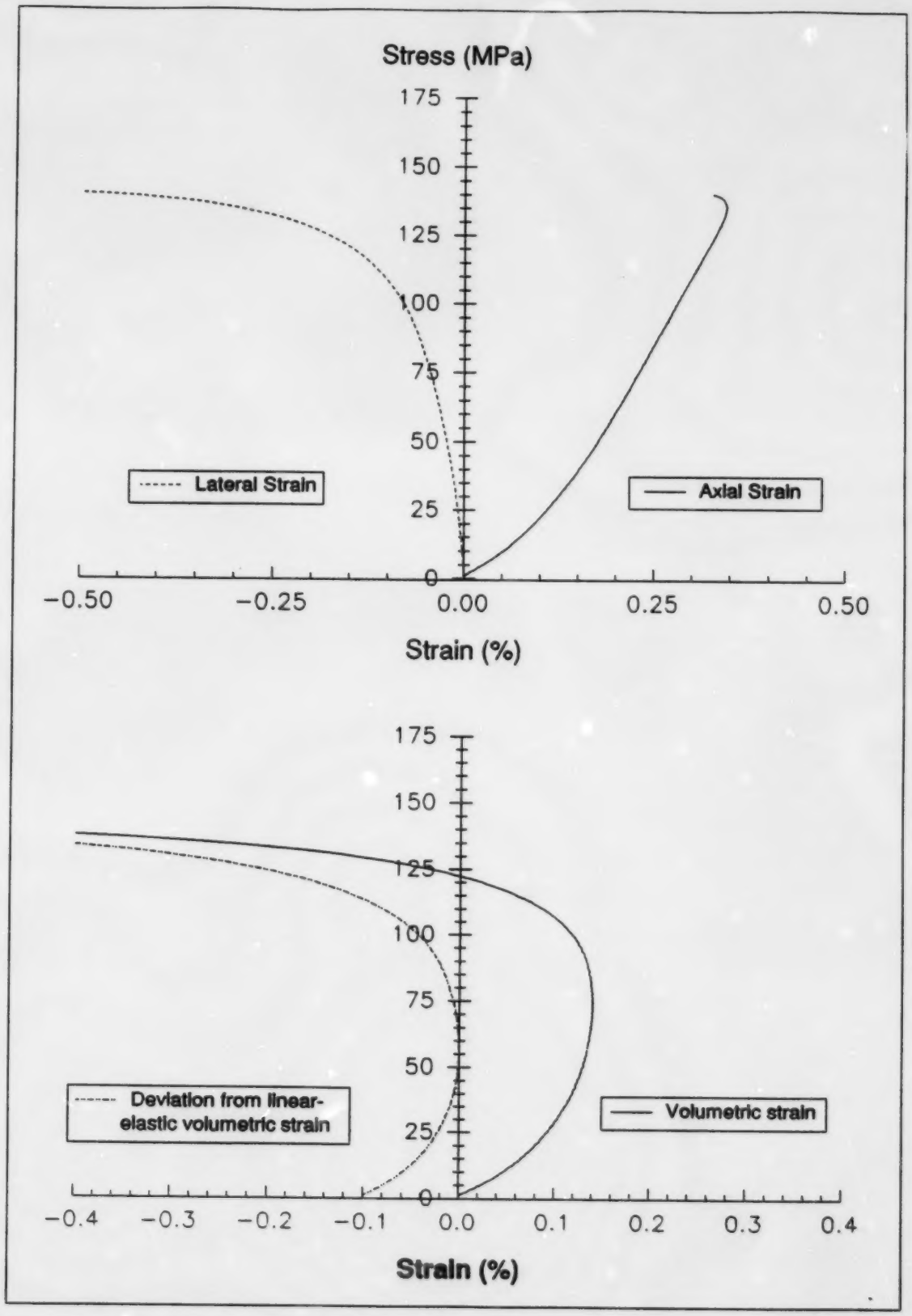

Figure A12 - Stress/strain curves for sample no. 2.164

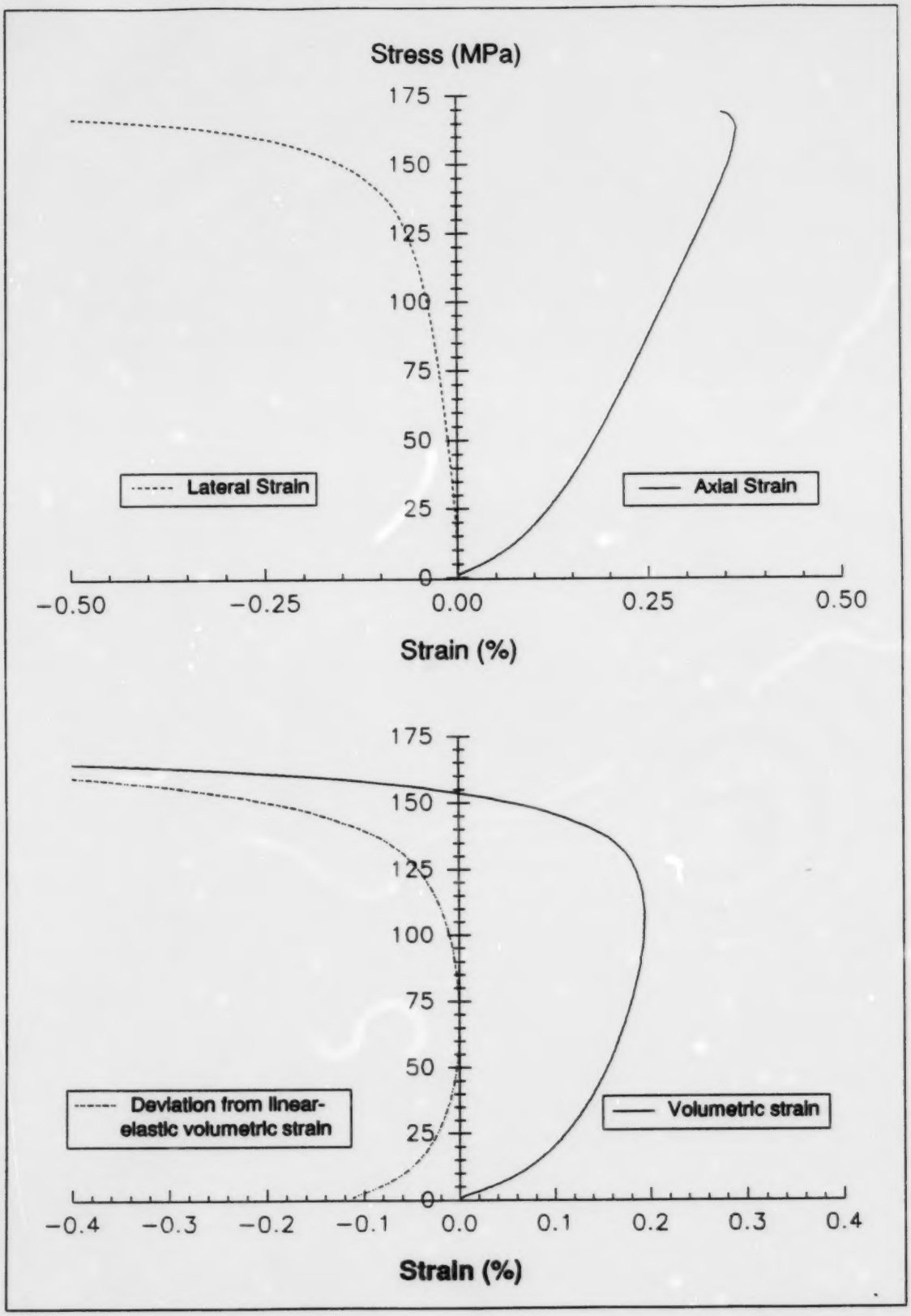

Figure A13 - Stress/strain curves for sample no. 2.314

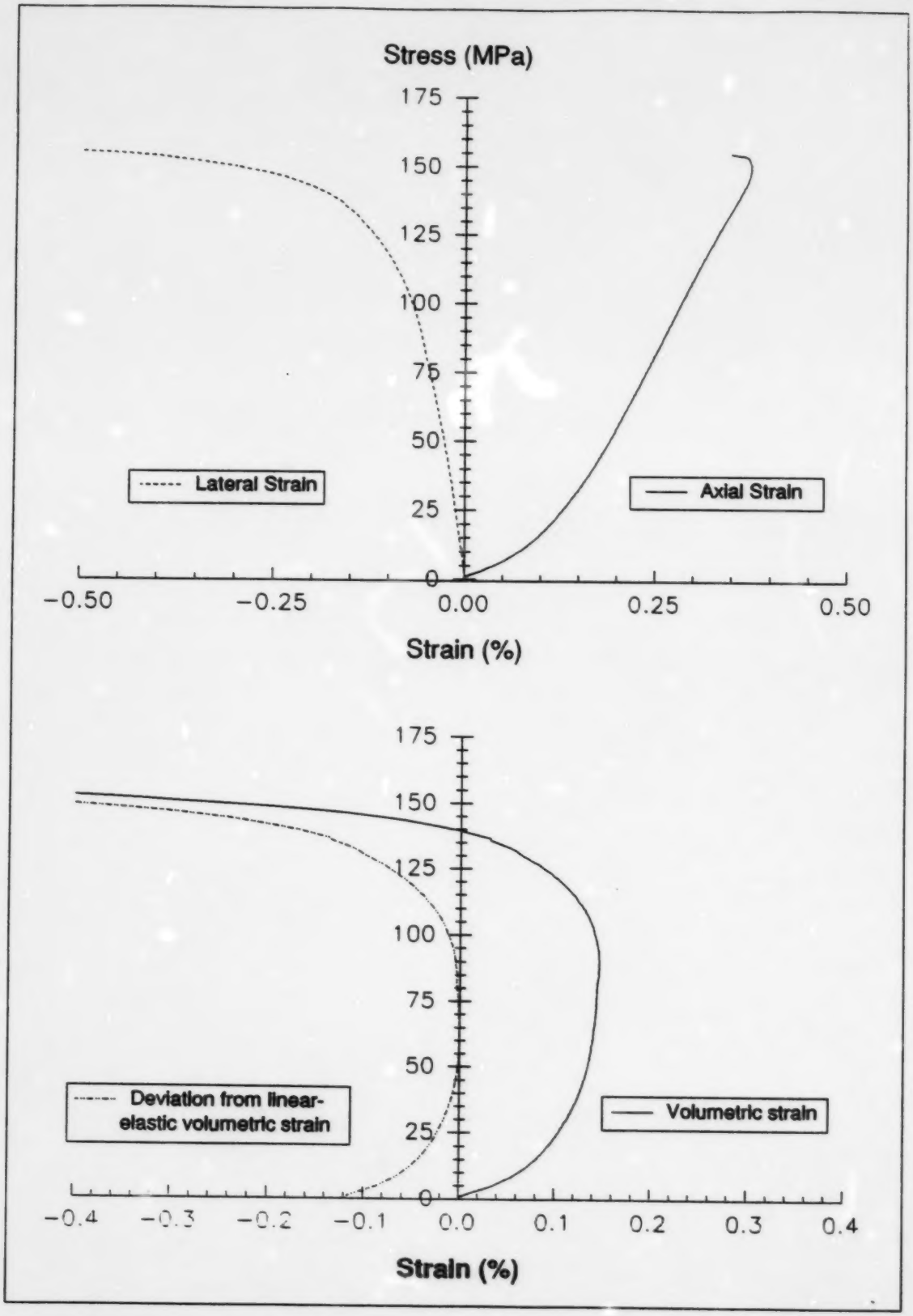

Figure A14 - Stress/strain curves for sample no. 2.908

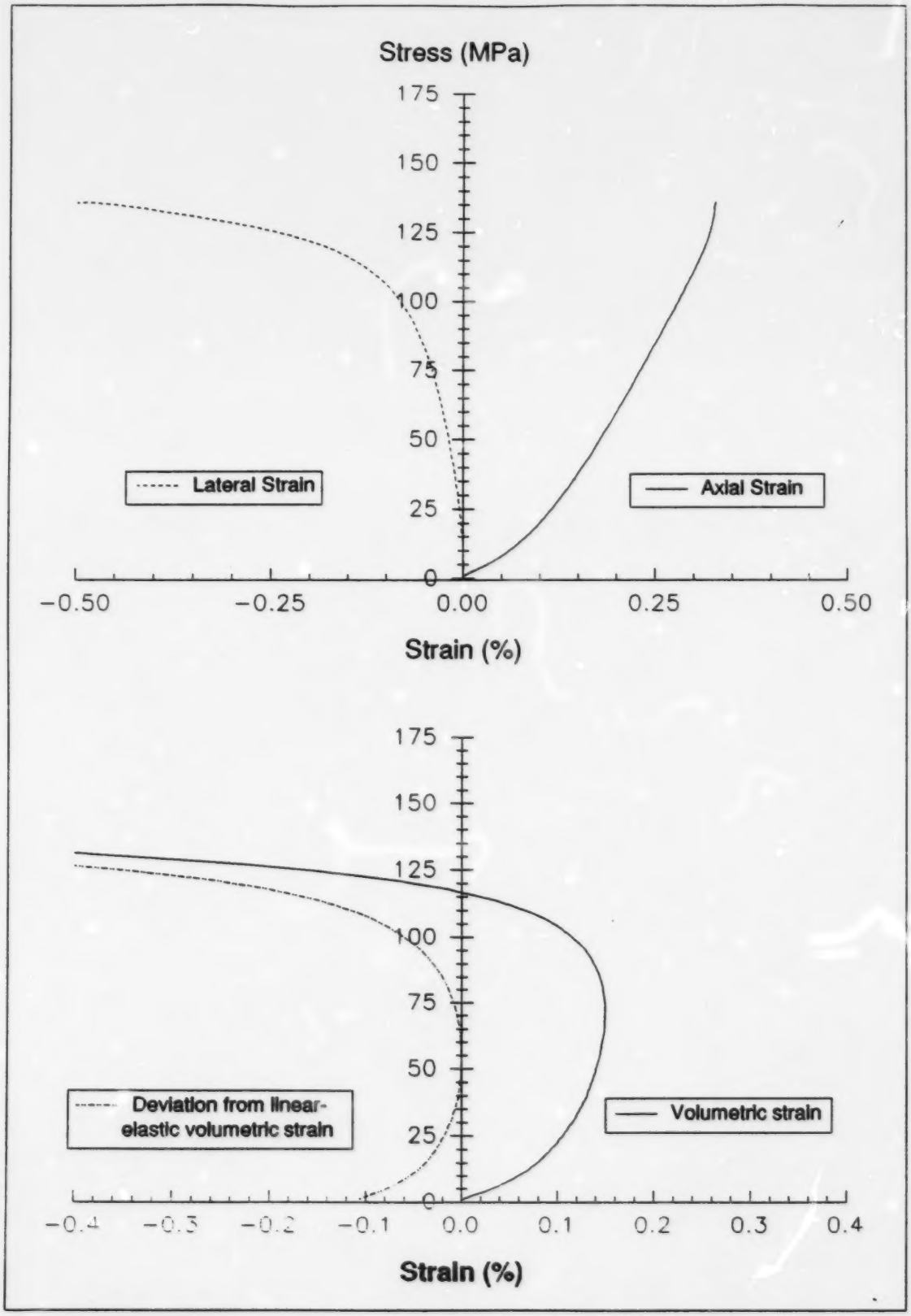

Figure A15 - Stress/strain curves for sample no. 2.784

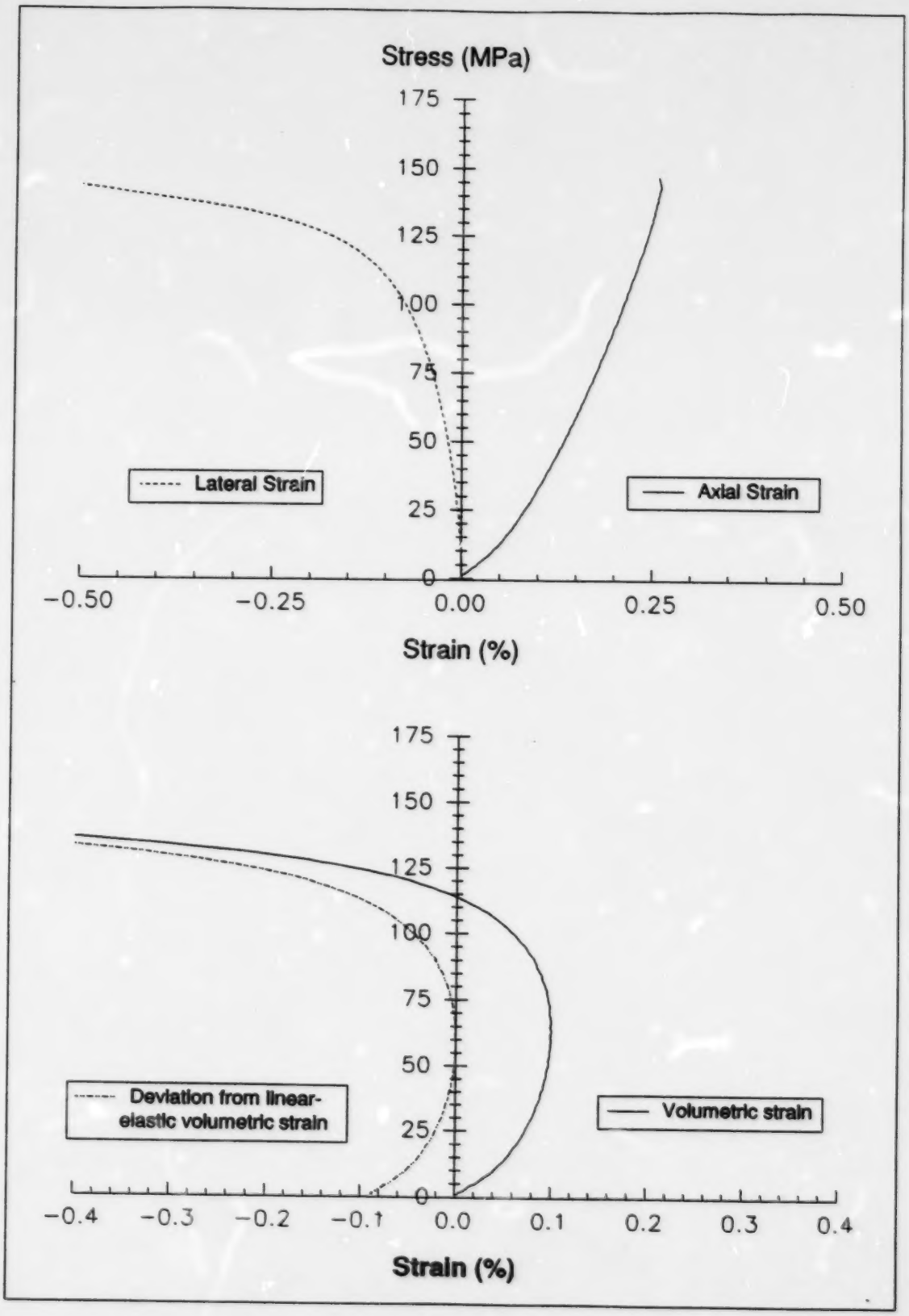

Figure A16 - Stress/strain curves for sample no. 2.709

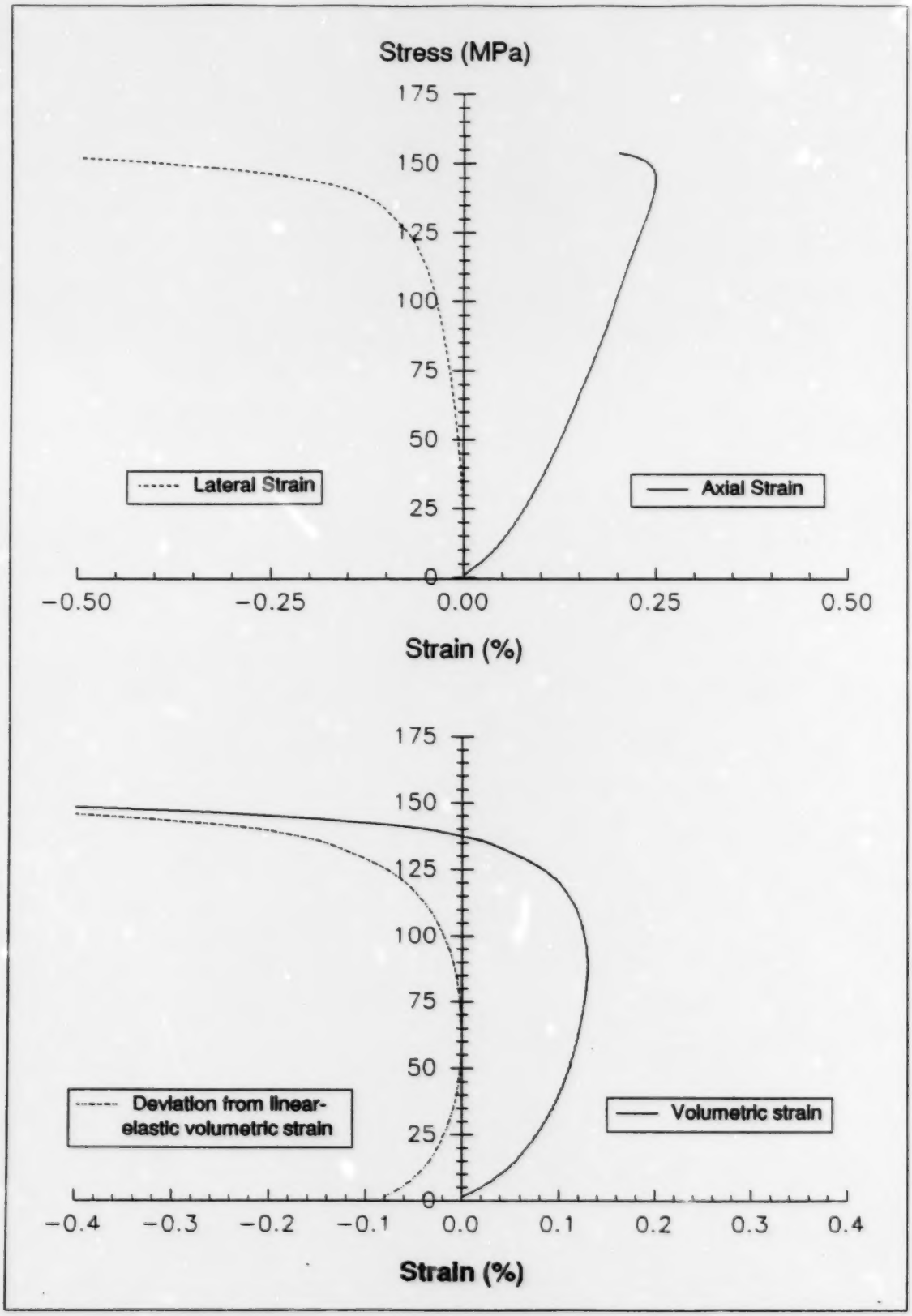

Figure A17 - Stress/strain curves for sample no. 2.358

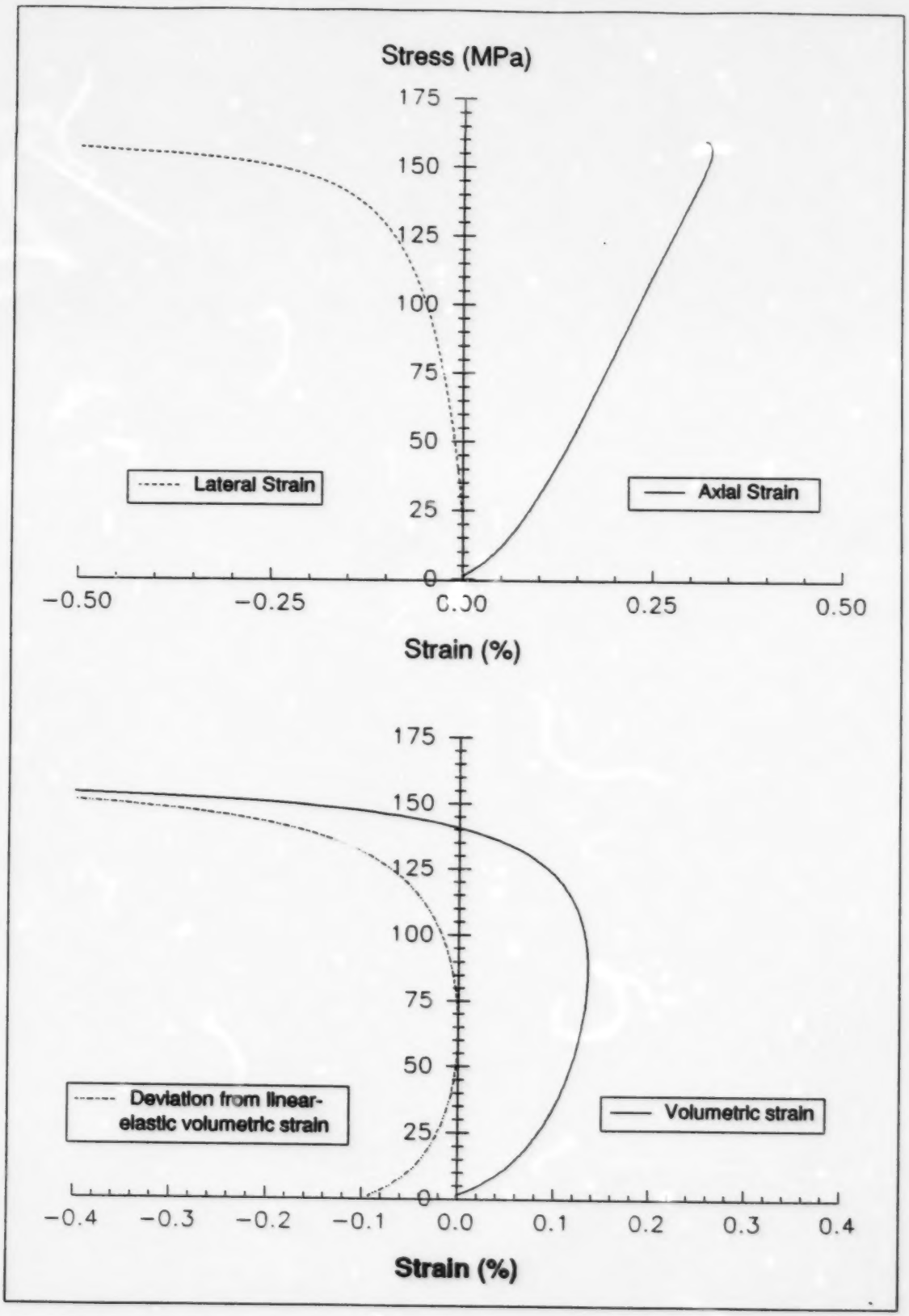

Figure A18 - Stress/strain curves for sample no. 2.408

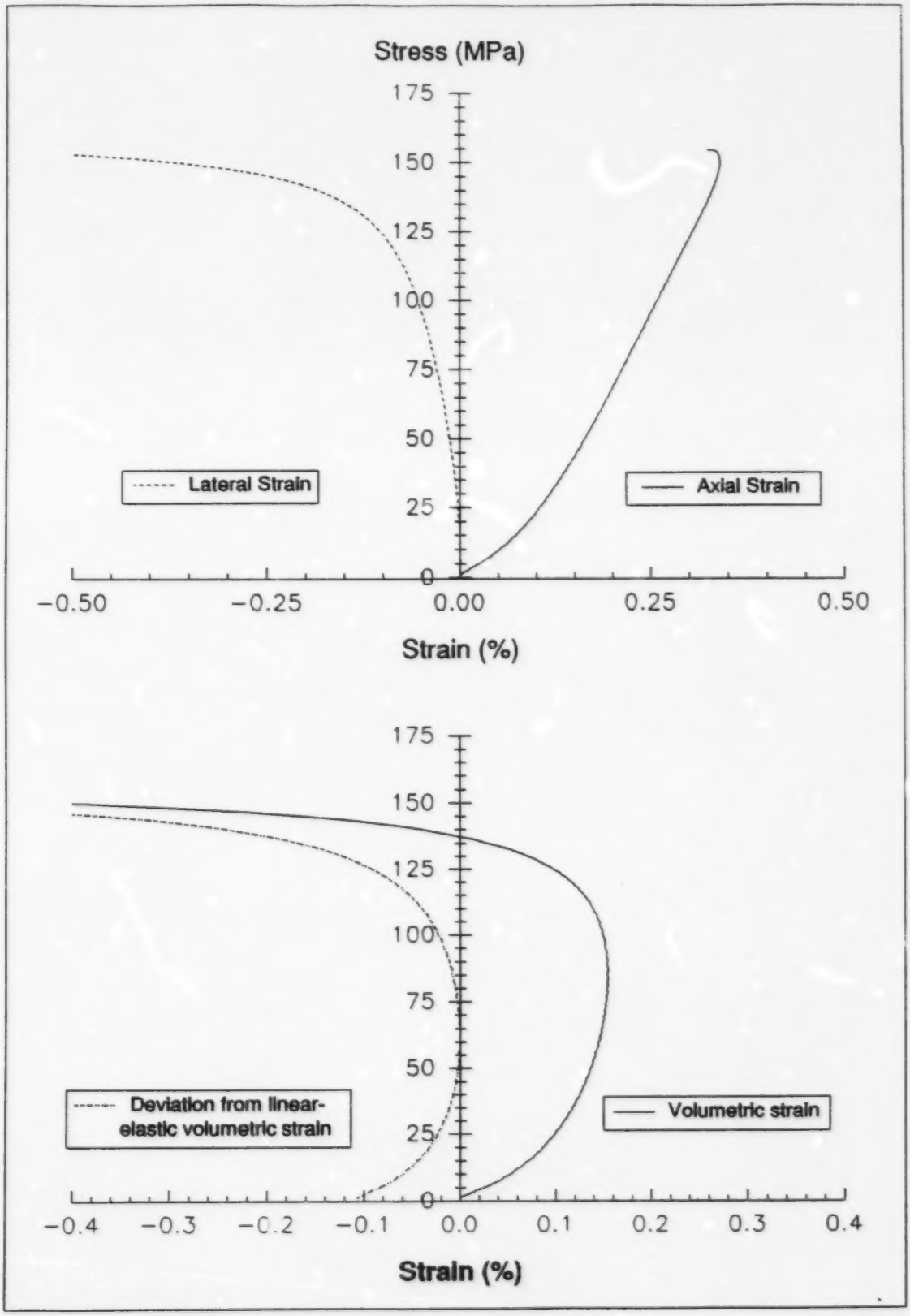

Figure A19 - Stress/strain curves for sample no. 2.462

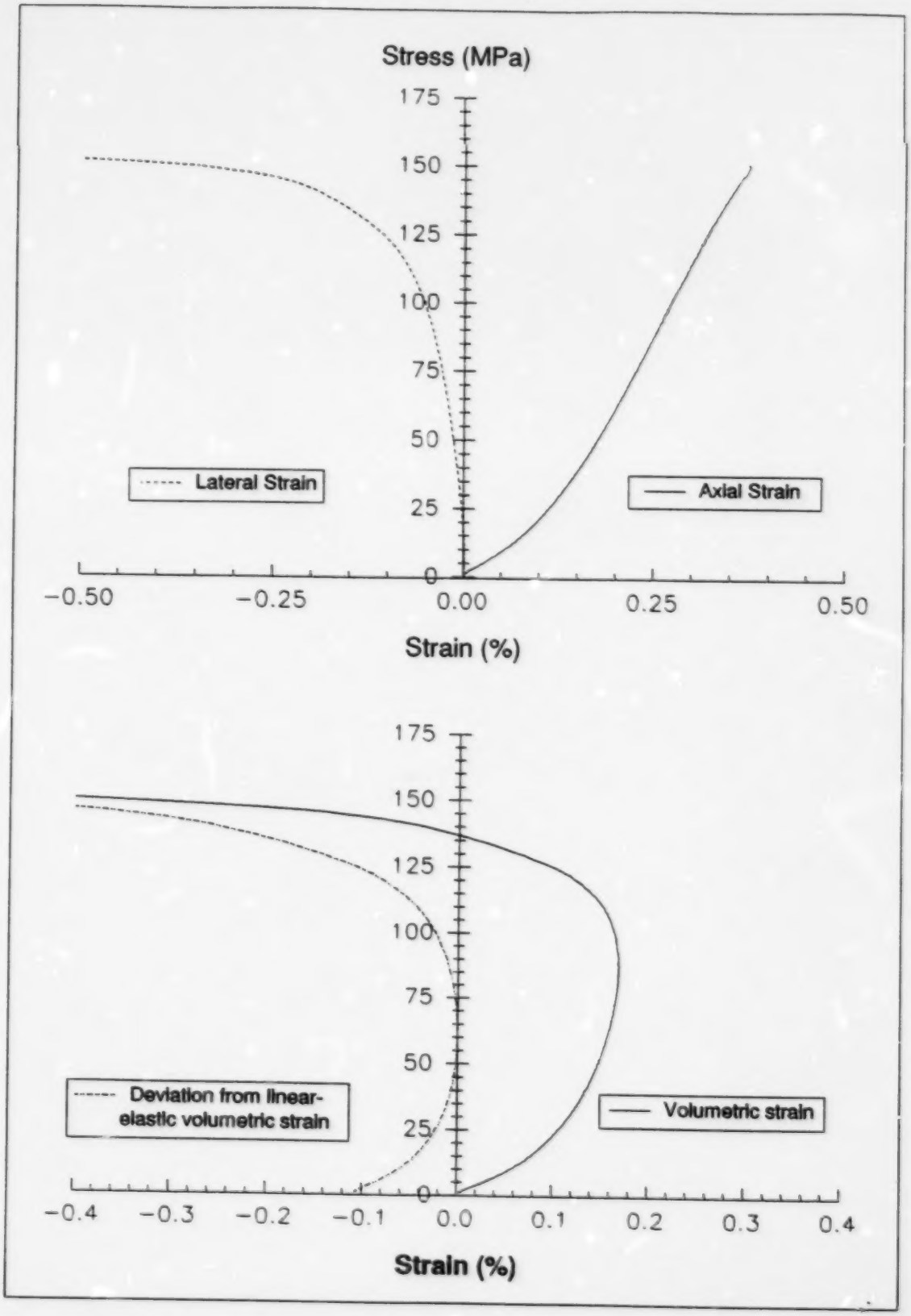

Figure A20 - Stress/strain curves for sample no. 2.627

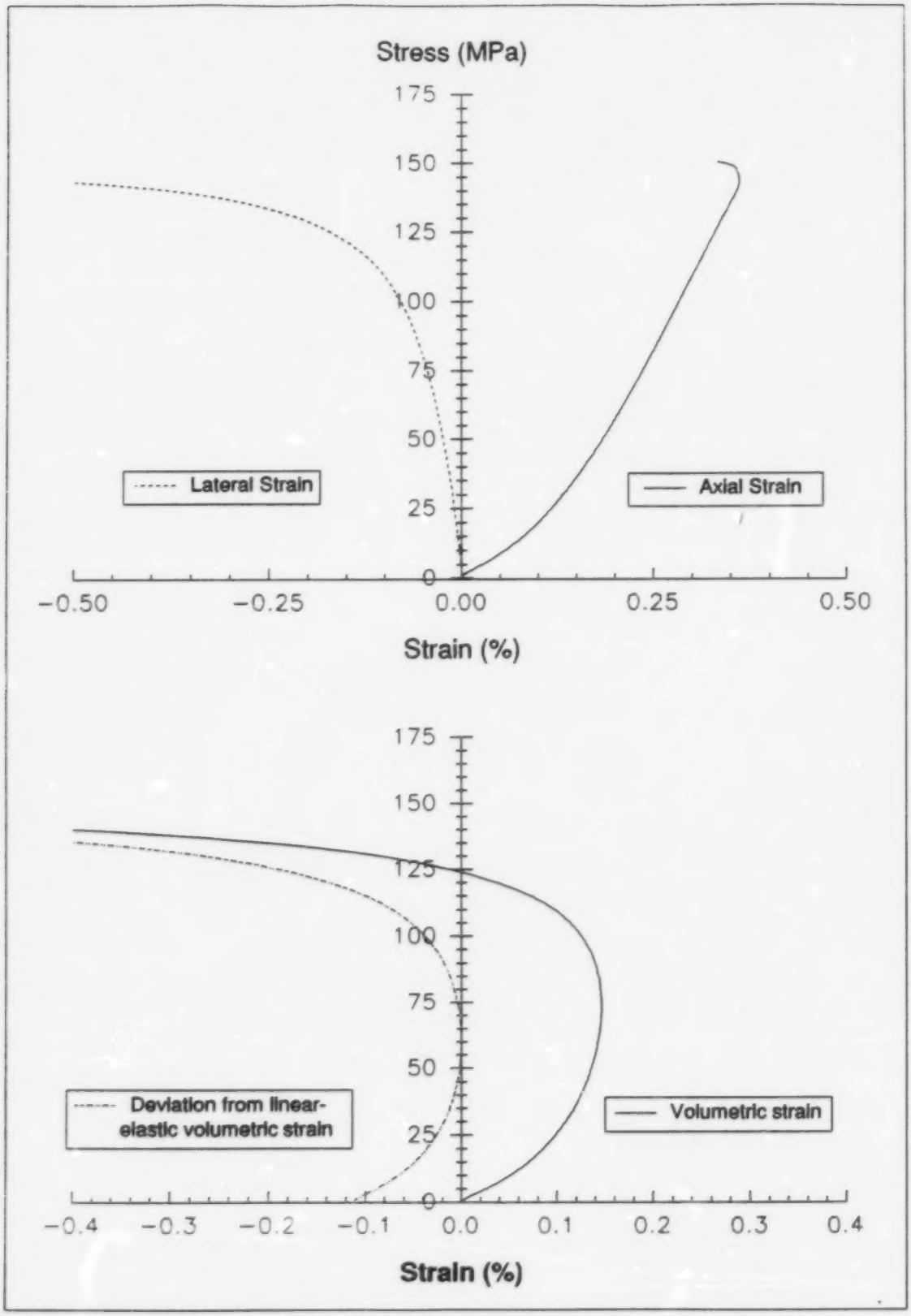

Figure A21 - Stress/strain curves for sample no. 2.566

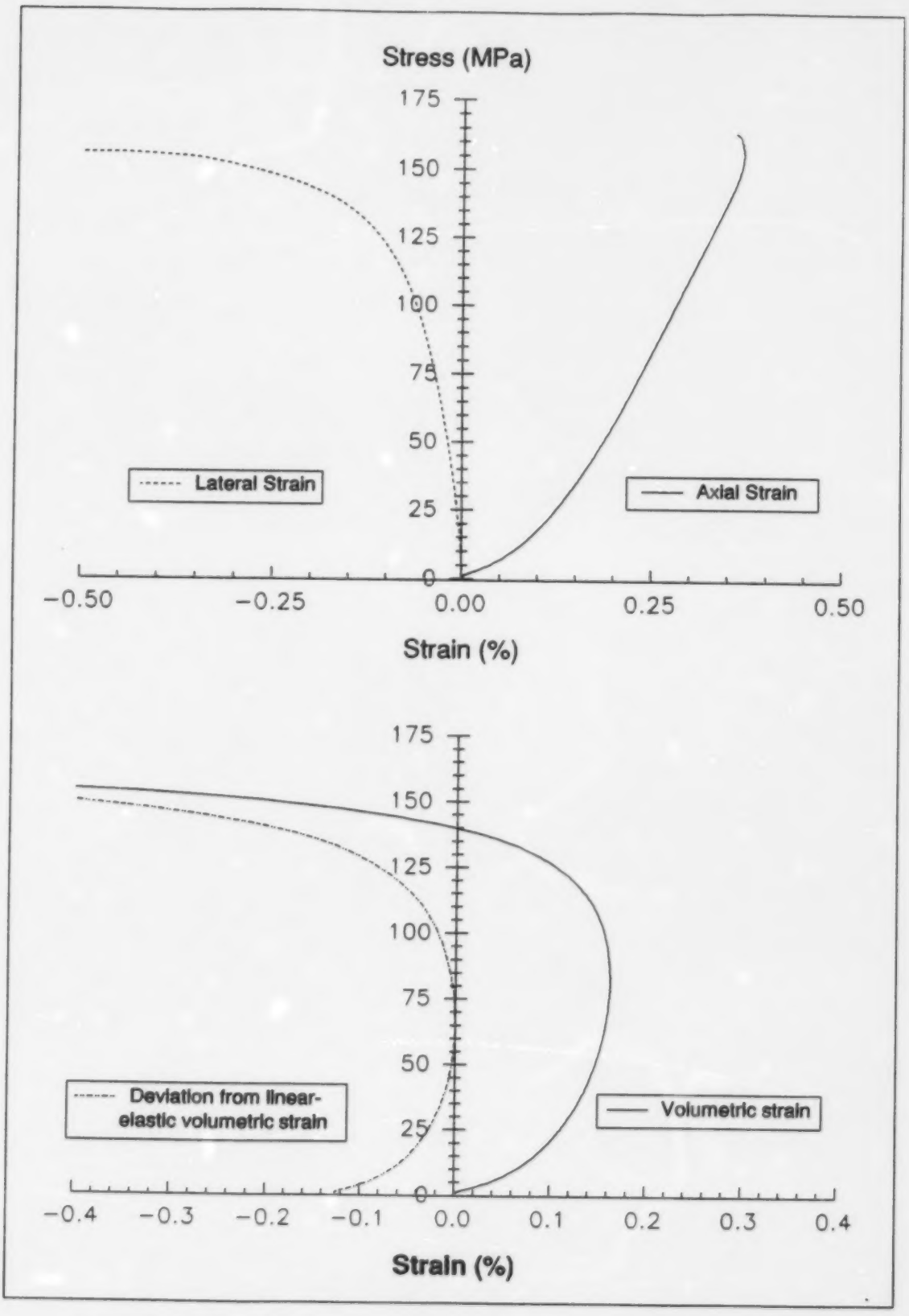

Figure A22 - Stress/strain curves for sample no. 2.861

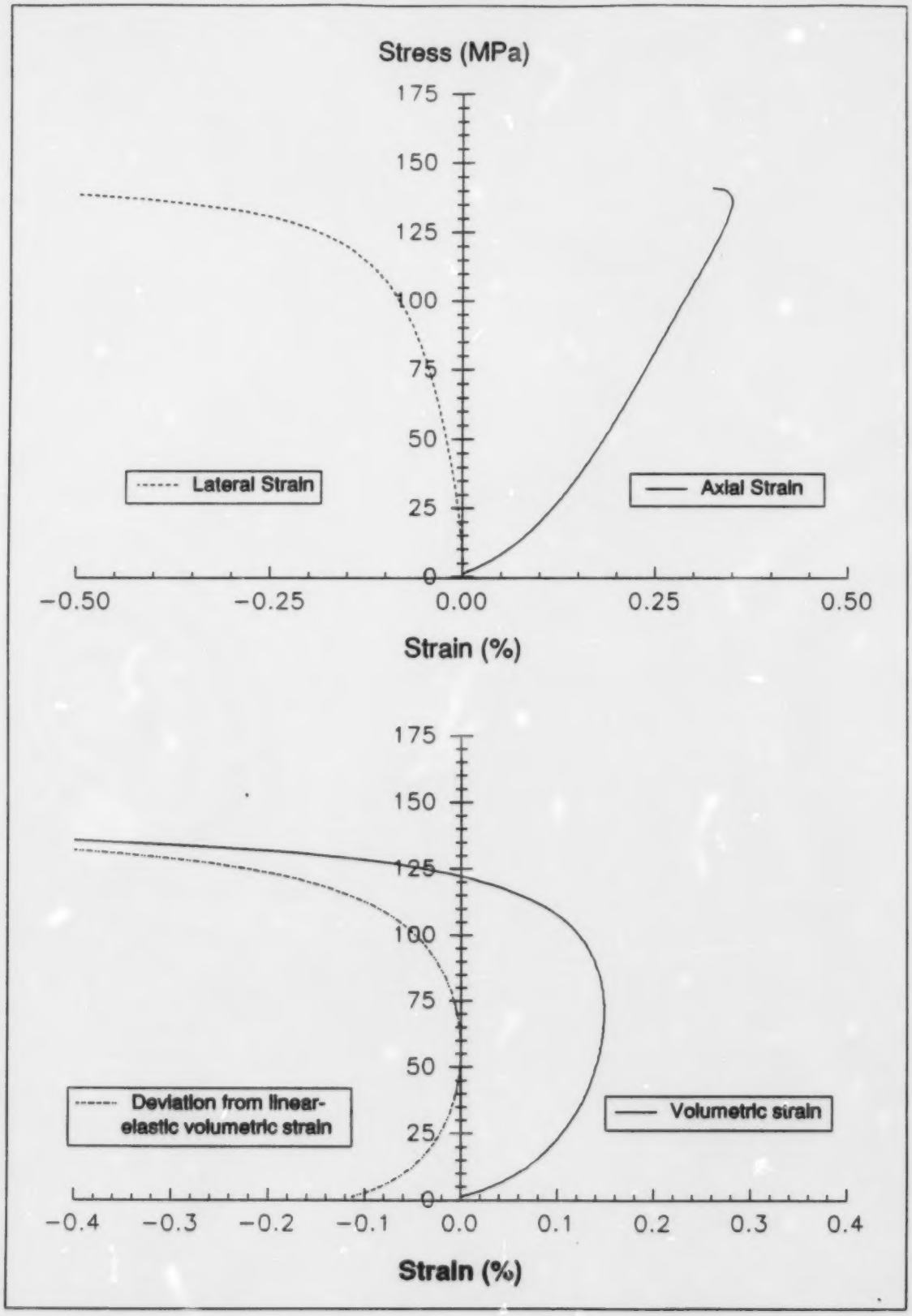

Figure A23 - Stress/strain curves for sample no. 3.110

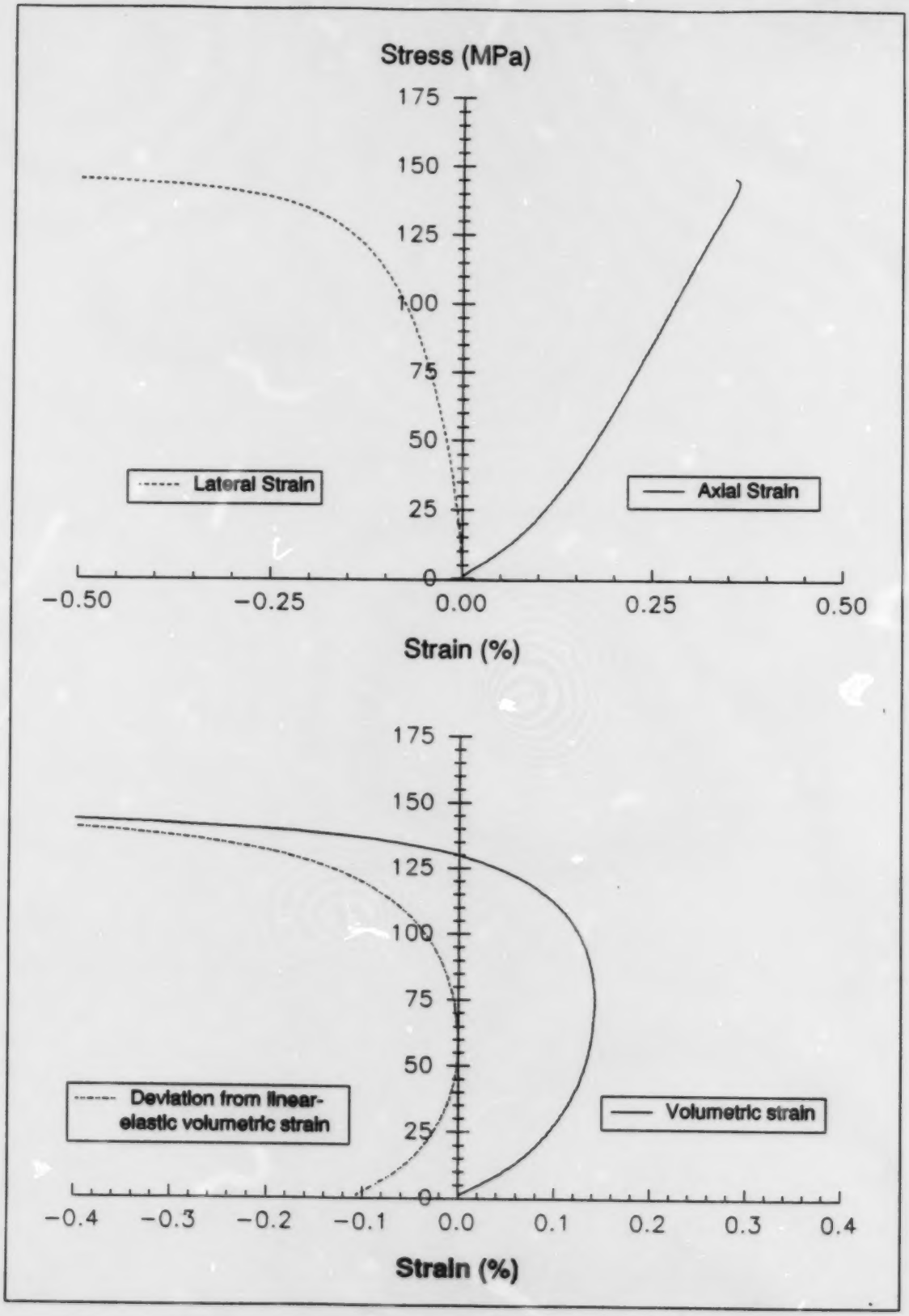

Figure A24 - Stress/strain curves for sample no. 3.170

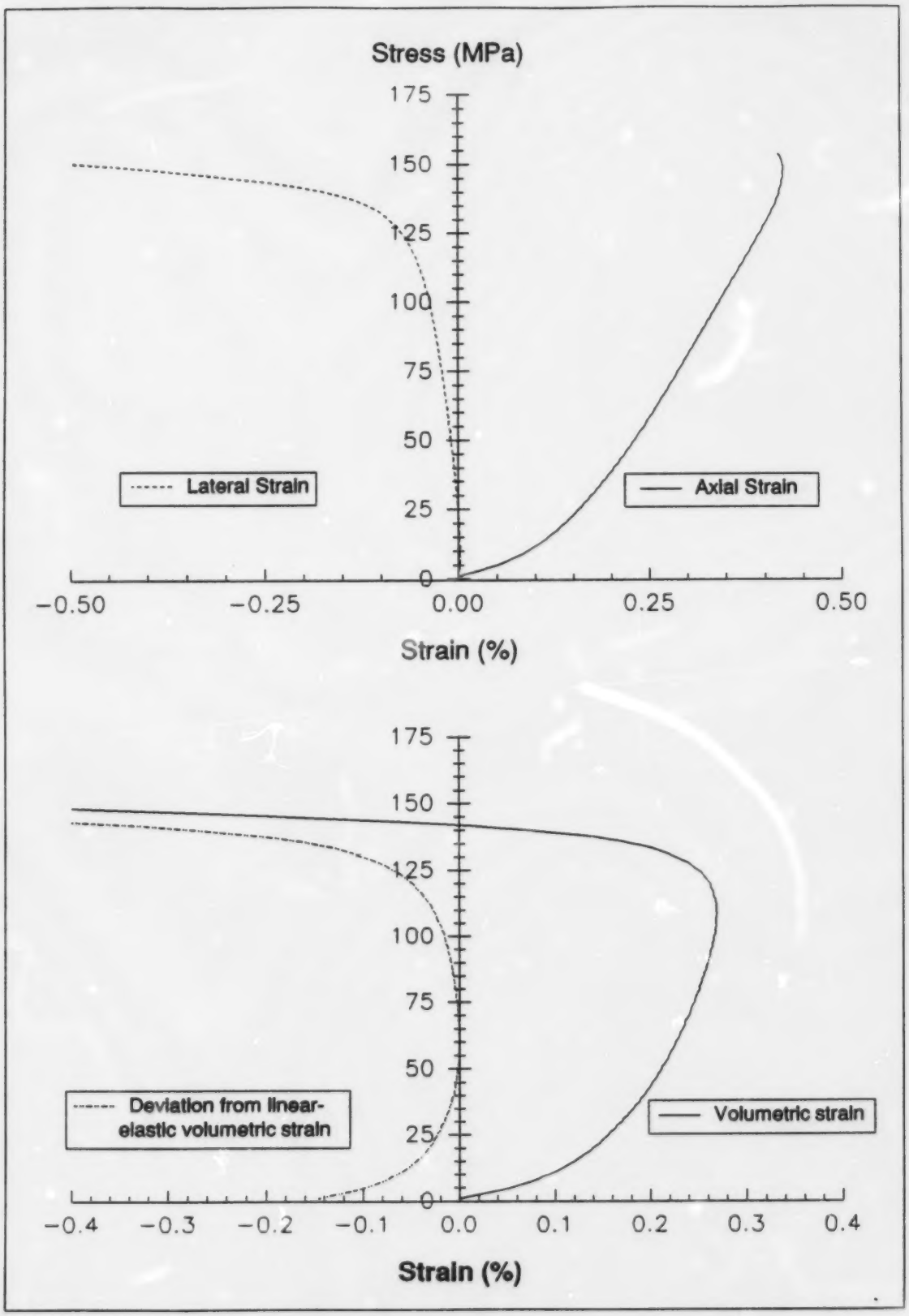

Figure A25 - Stress/strain curves for sample no. 5.066

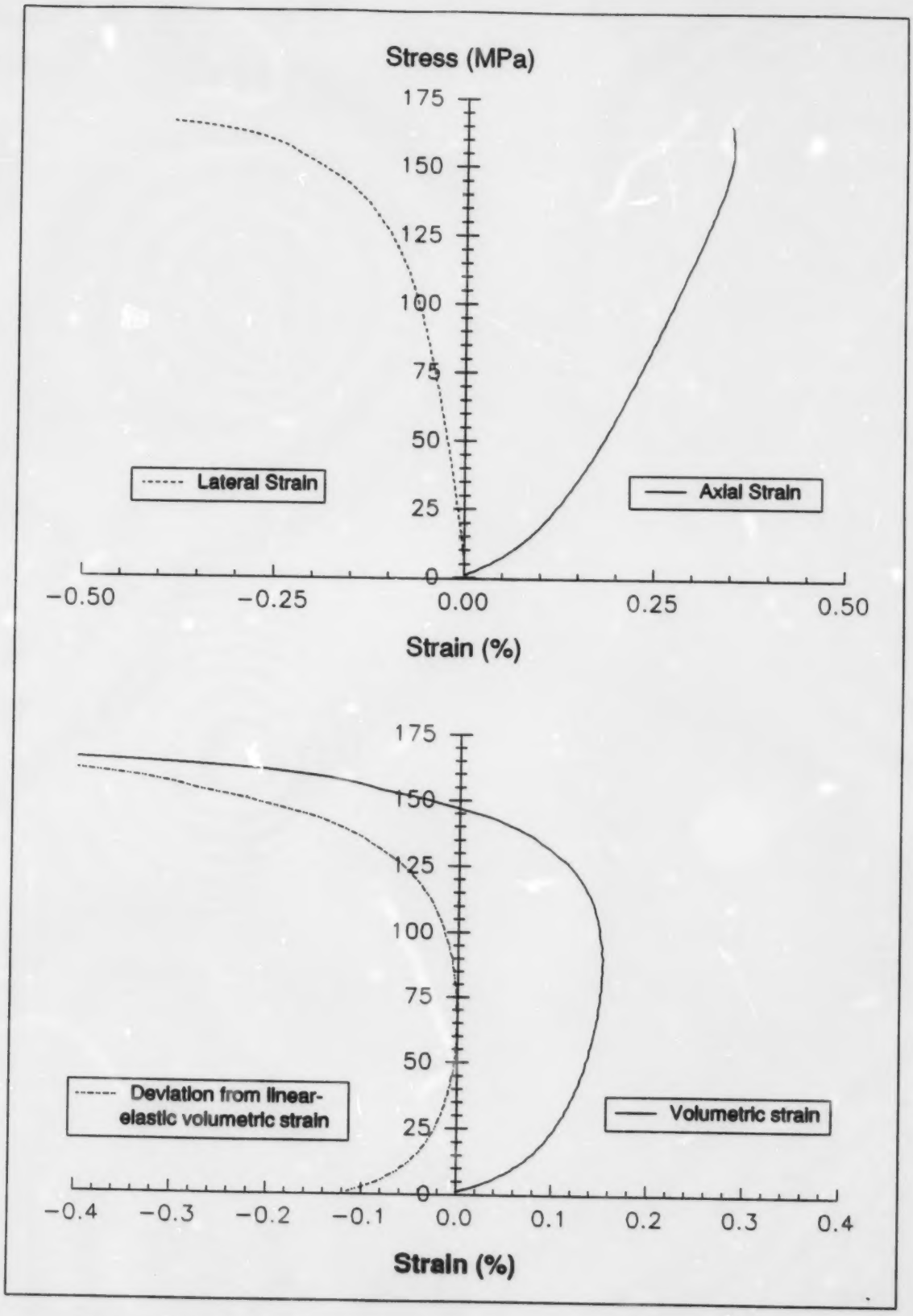

Figure A26 - Stress/strain curves for sample no. 5.682

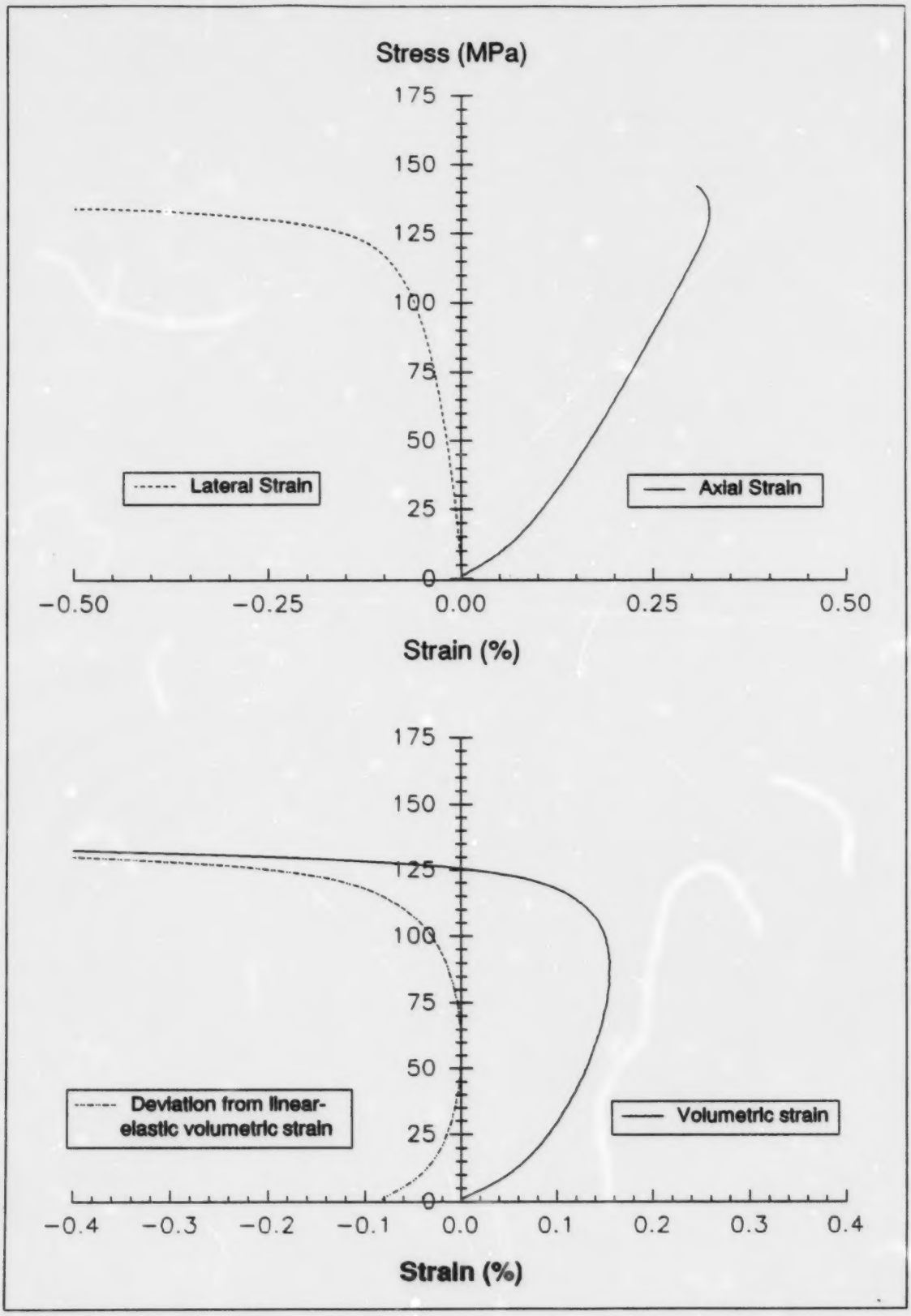

Figure A27 - Stress/strain curves for sample no. 5.516

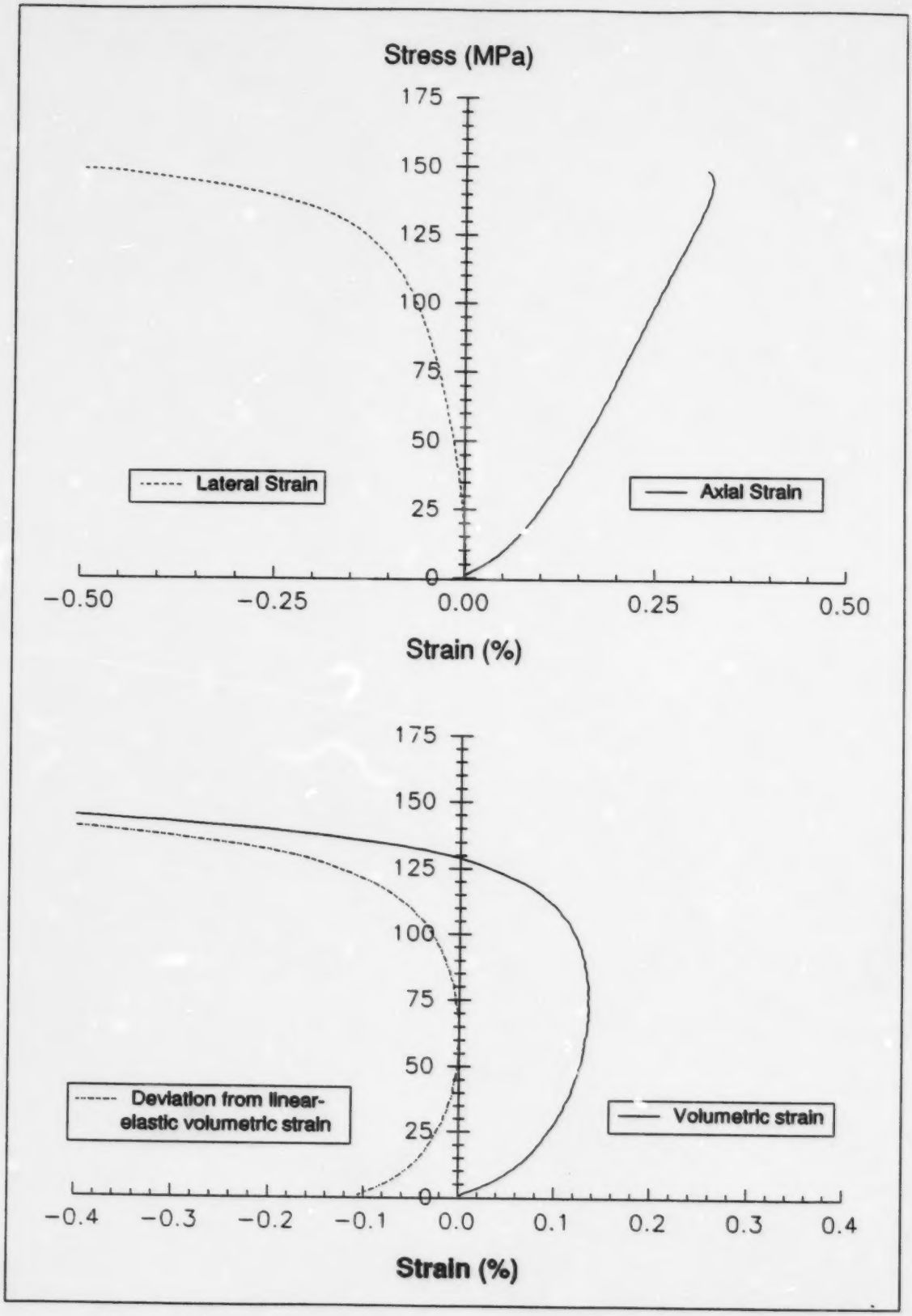

Figure A28 - Stress/strain curves for sample no. 5.436

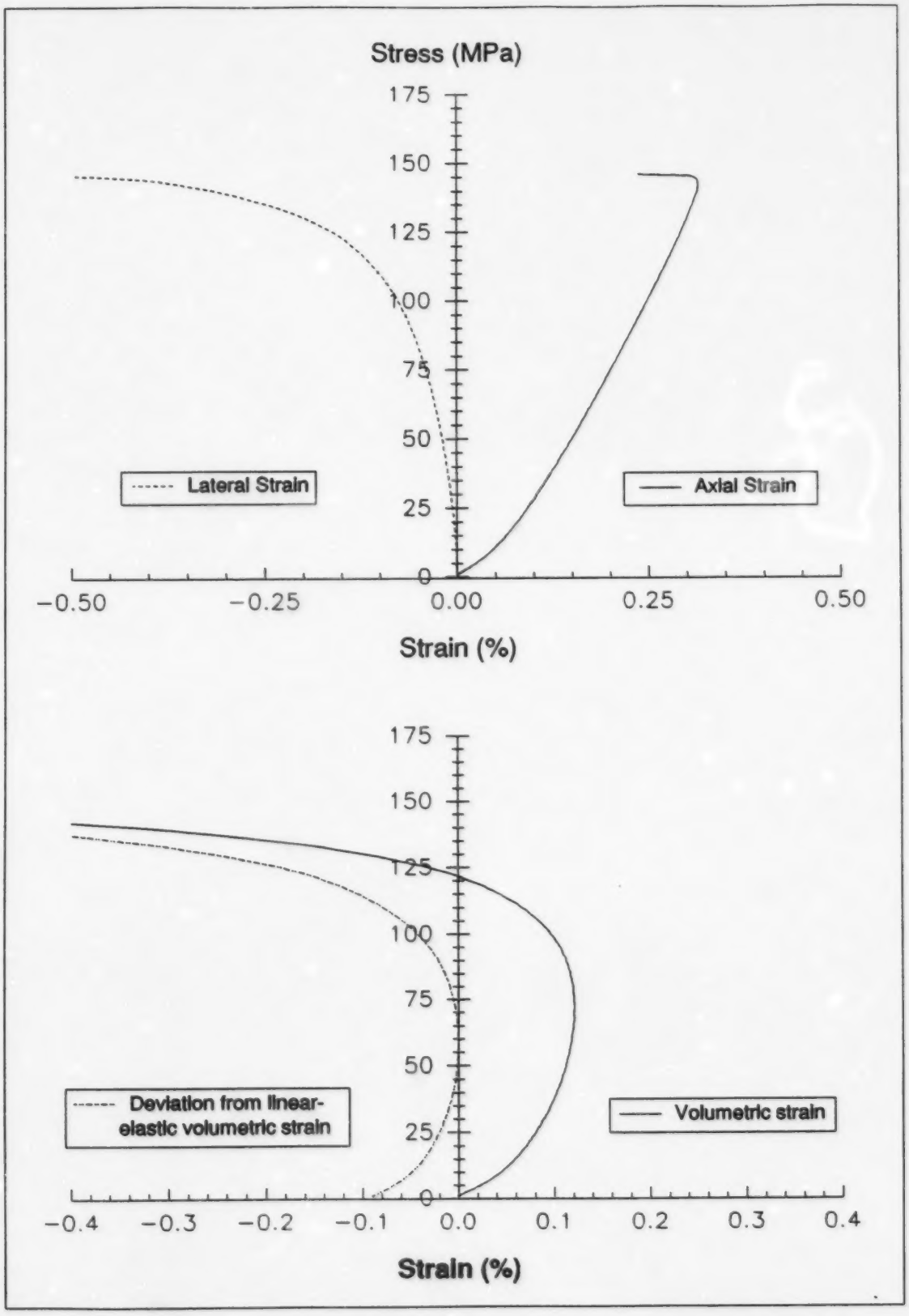

Figure A29 - Stress/strain curves for sample no. 5.109

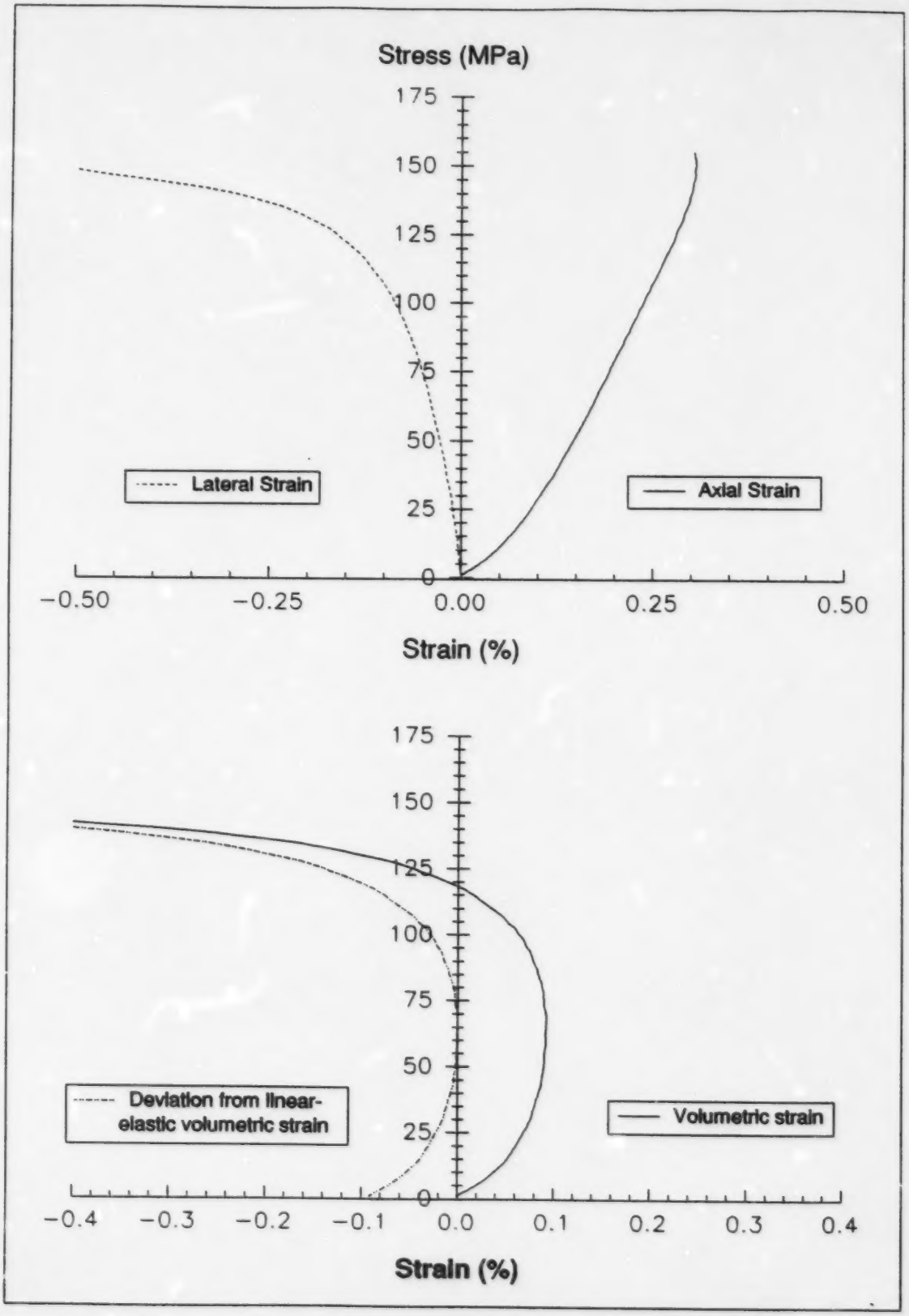

Figure A30 - Stress/strain curves for sample no. 5.165

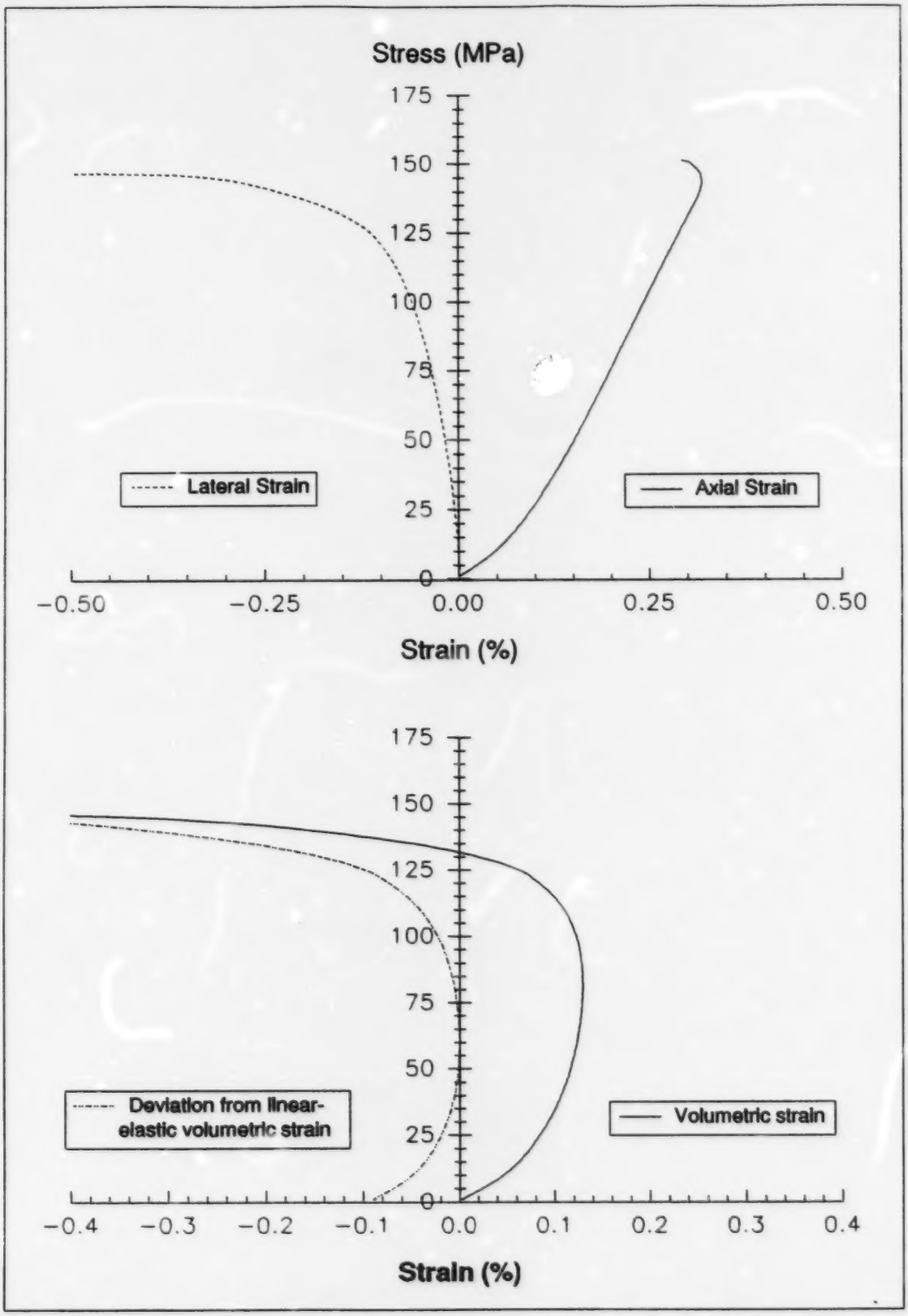

Figure A31 - Stress/strain curves for sample no. 5.361

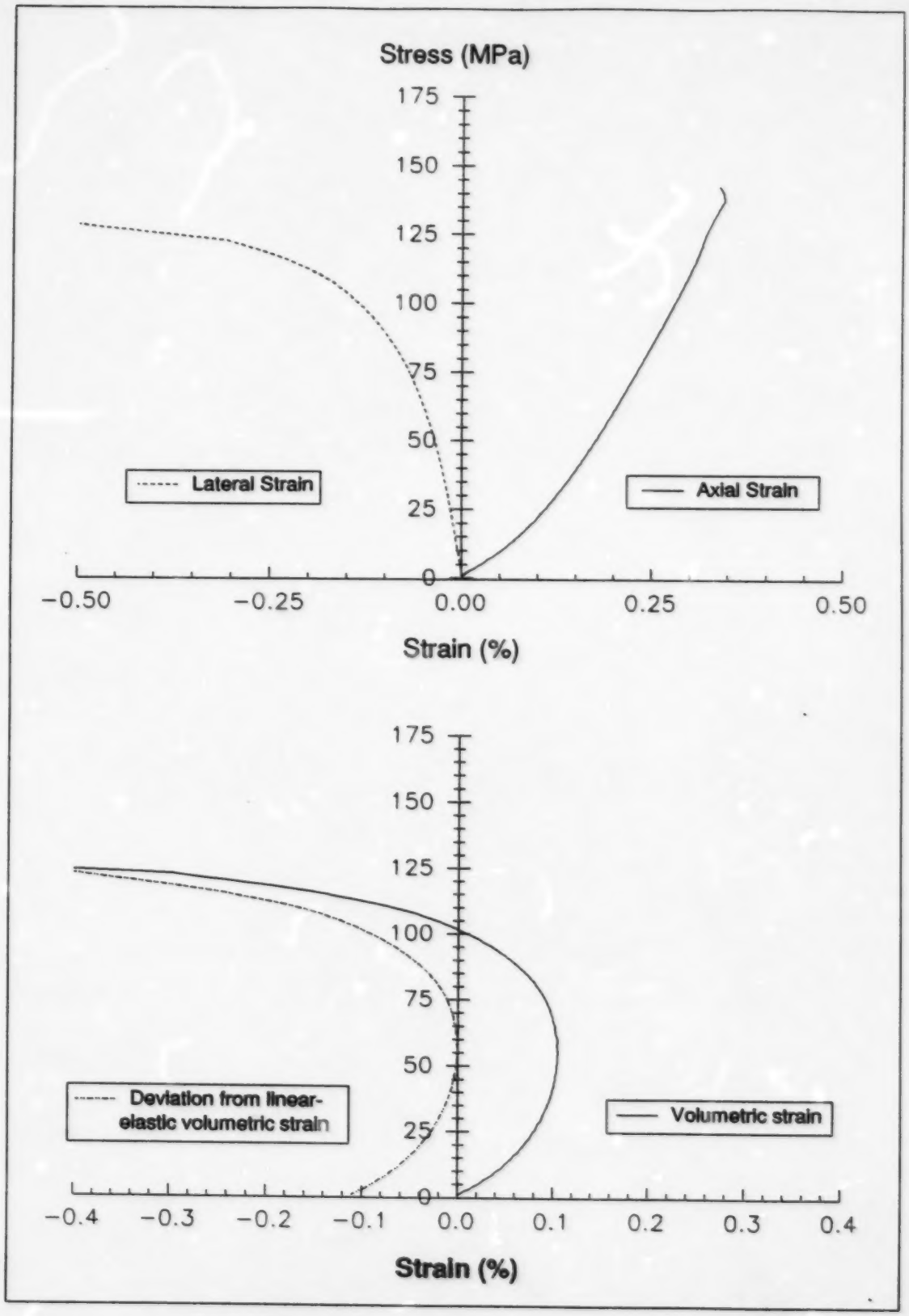

Figure A32 - Stress/strain curves for sample no. 5.260

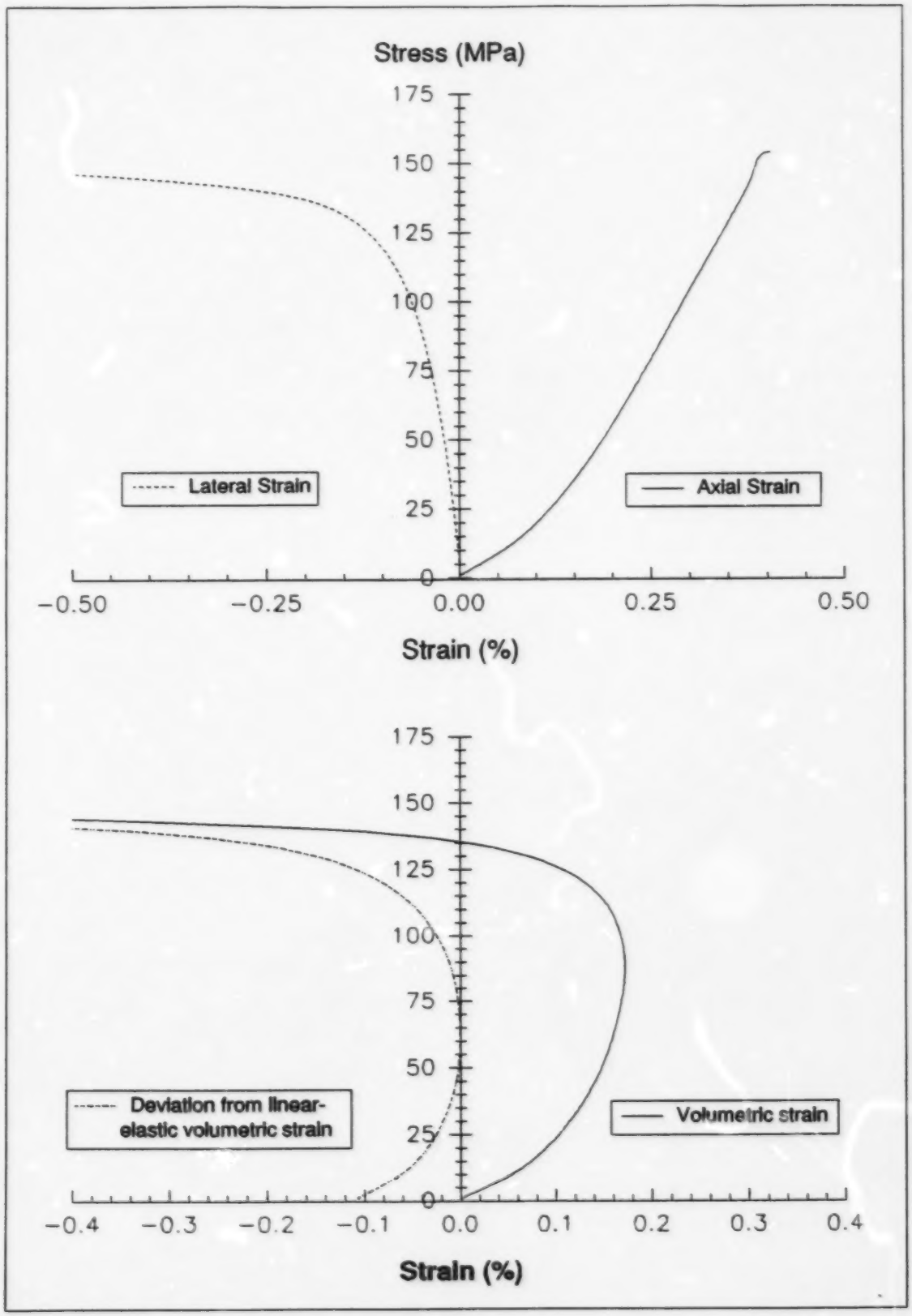

Figure A33 - Stress/strain curves for sample no. 5.298

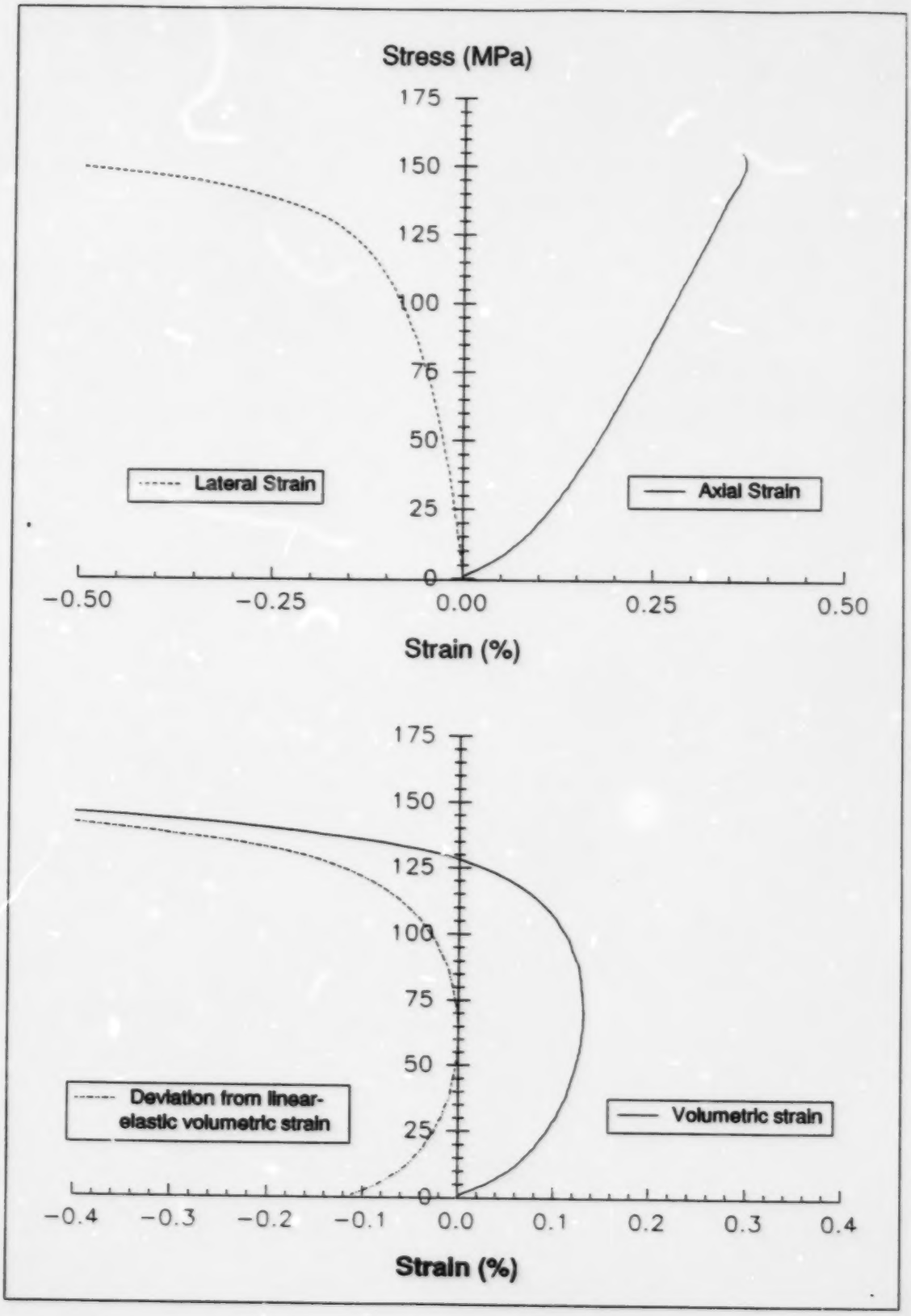

Figure A34 - Stress/strain curves for sample no. 5.651

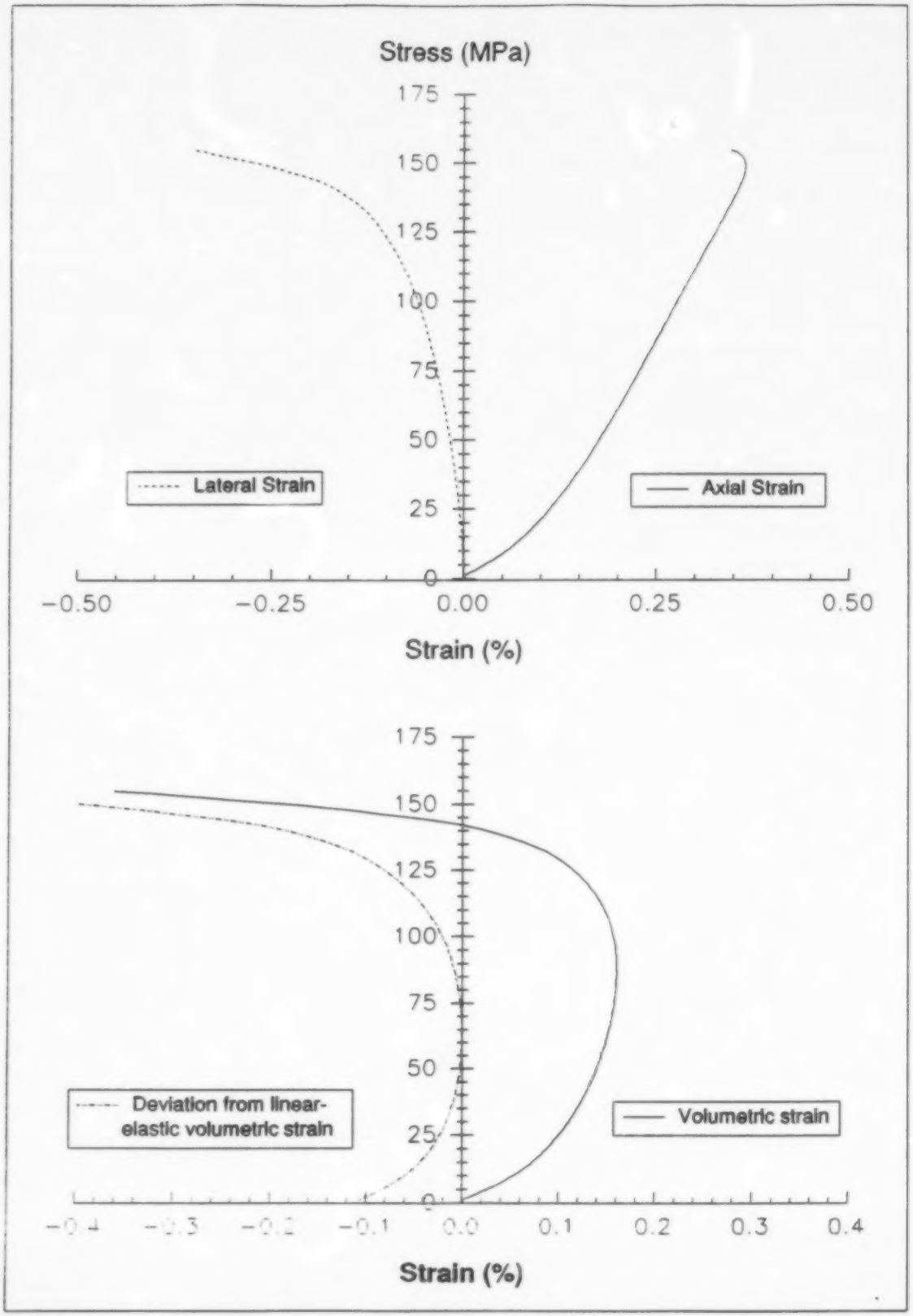

Figure A35 - Stress/strain curves for sample no. 5.882

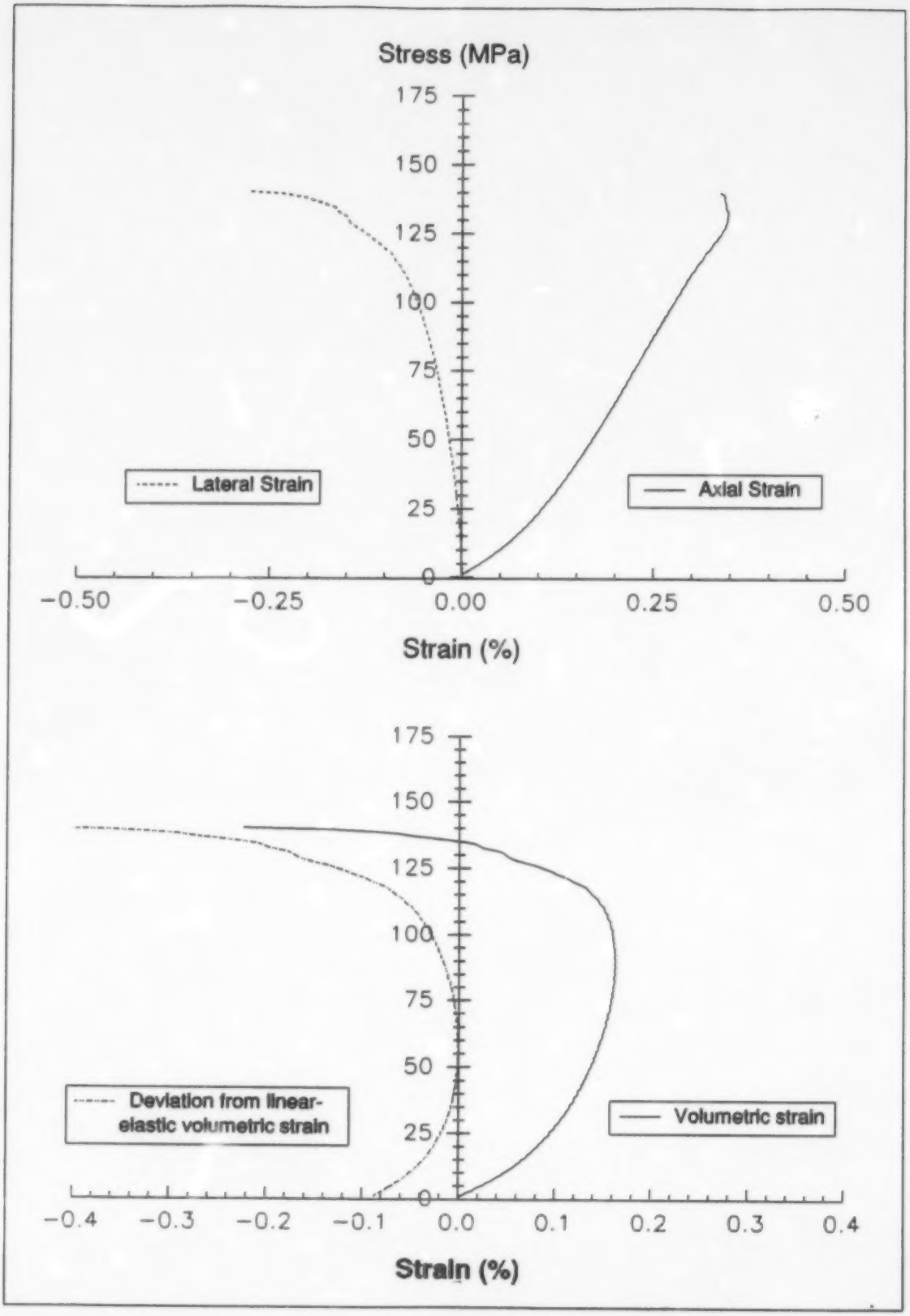

Figure A36 - Stress/strain curves for sample no. 5.927

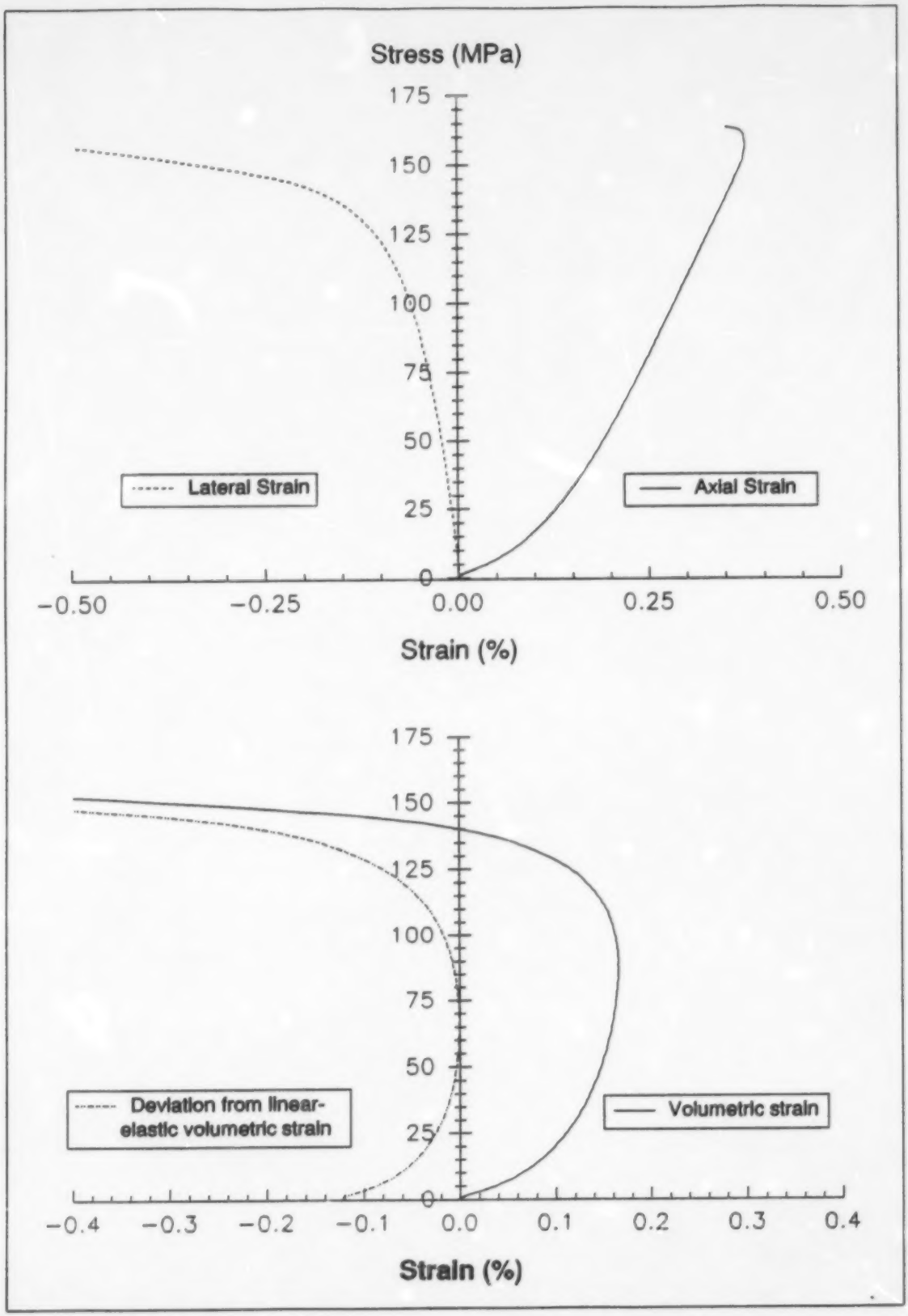

Figure A37 - Stress/strain curves for sample no. 6.080

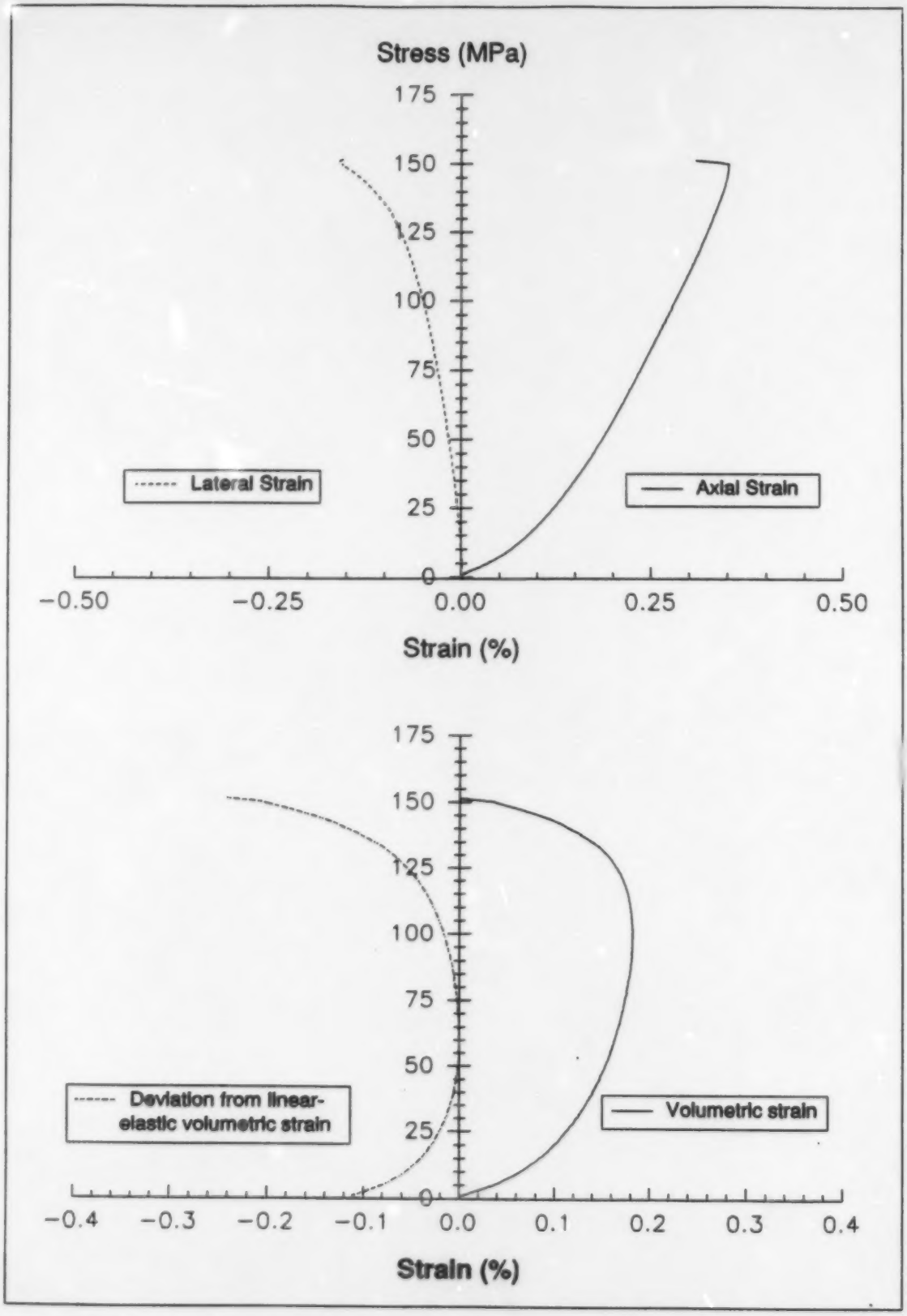

Figure A38 - Stress/strain curves for sample no. 6.700

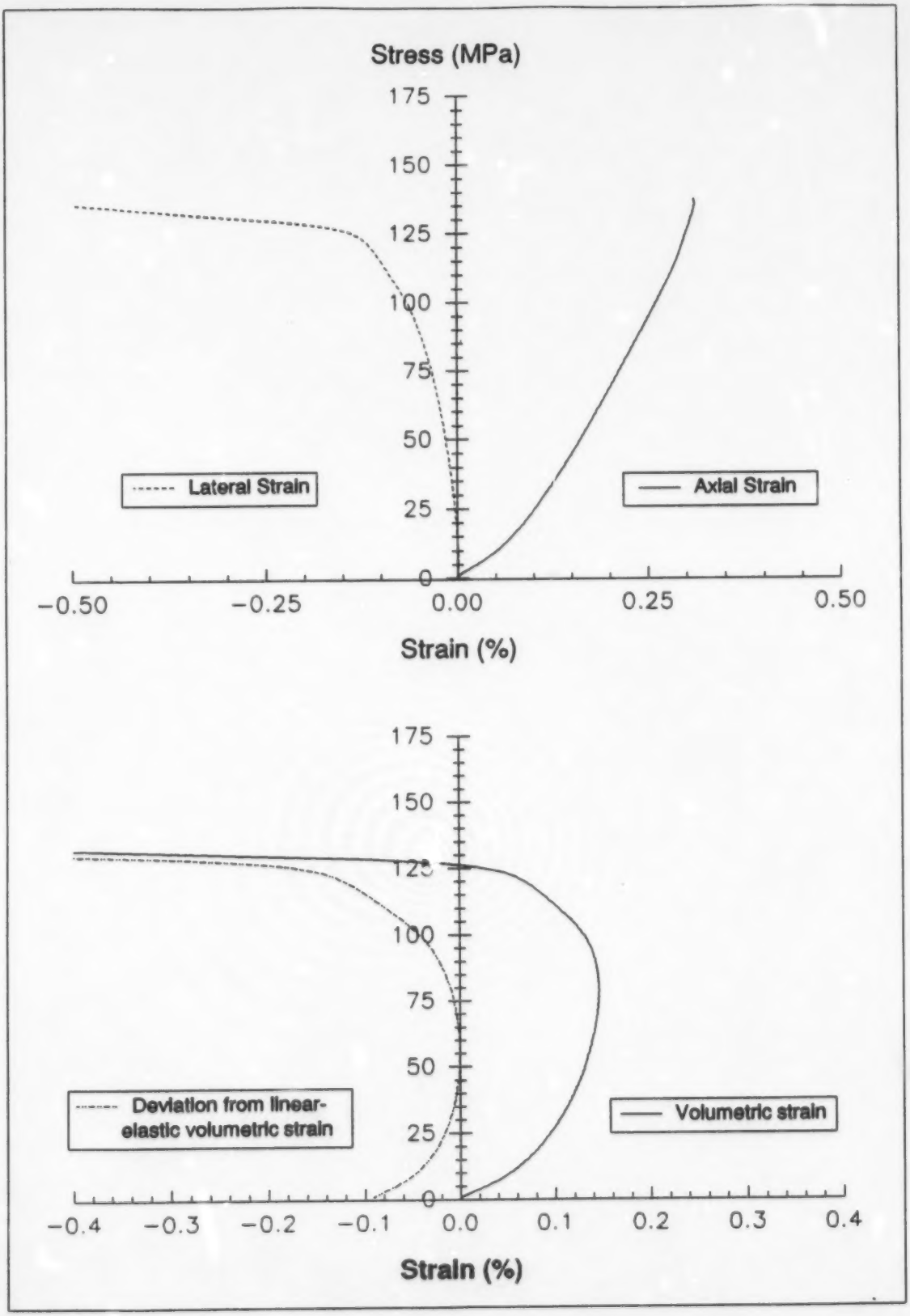

Figure A39 - Stress/strain curves for sample no. 6.572

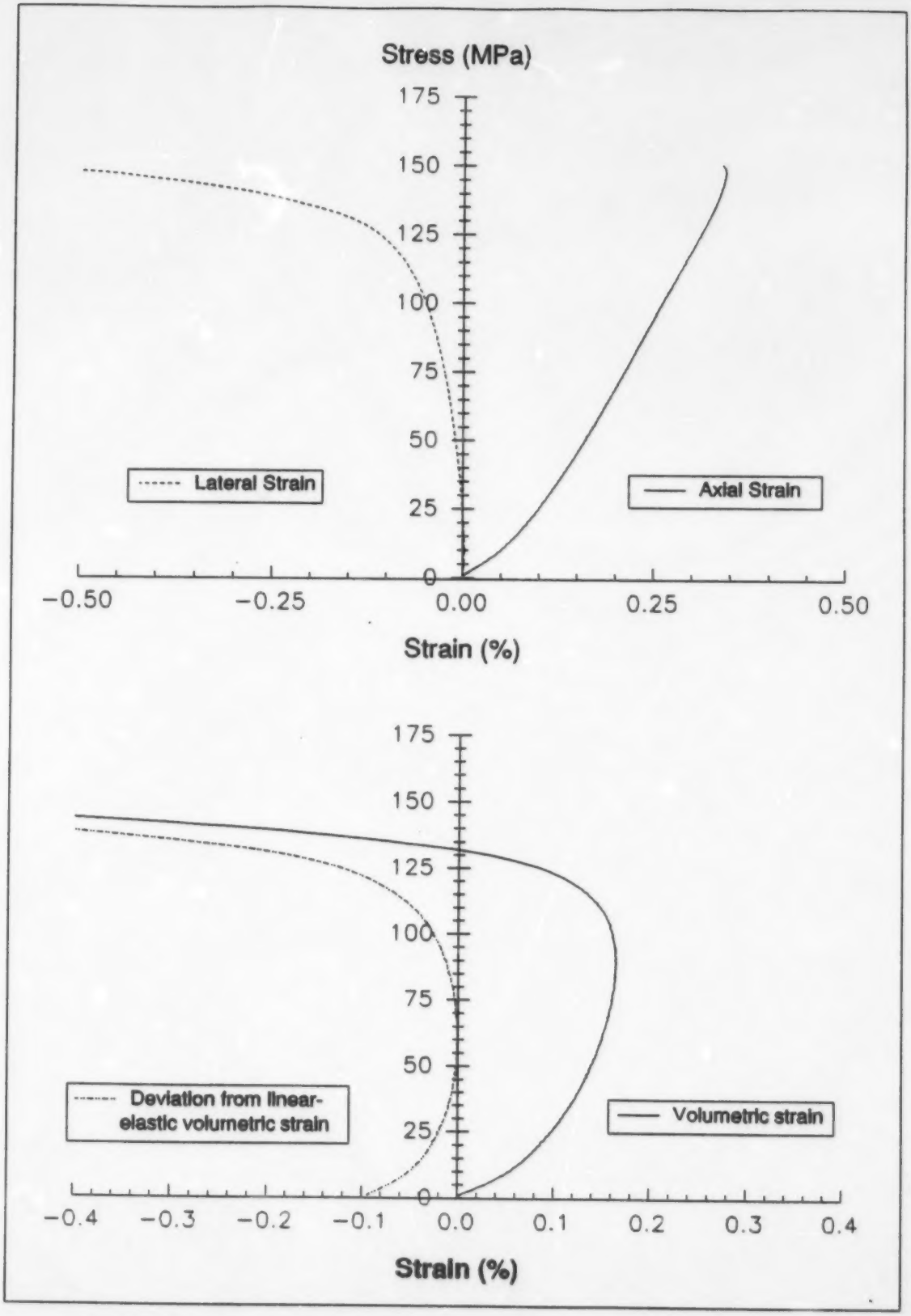

Figure A40 - Stress/strain curves for sample no. 6.477

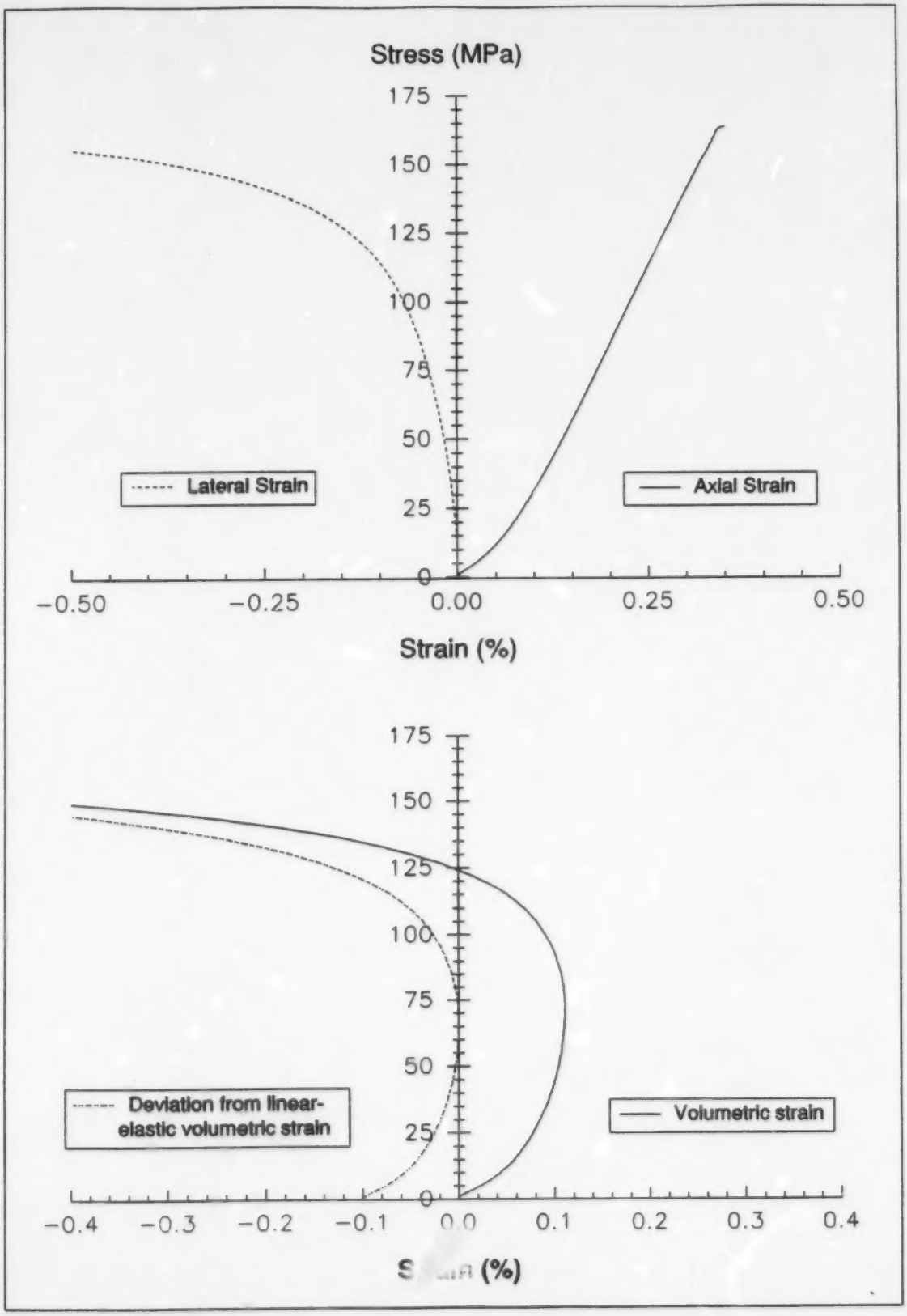

Figure A41 - Stress/strain curves for sample no. 6.125

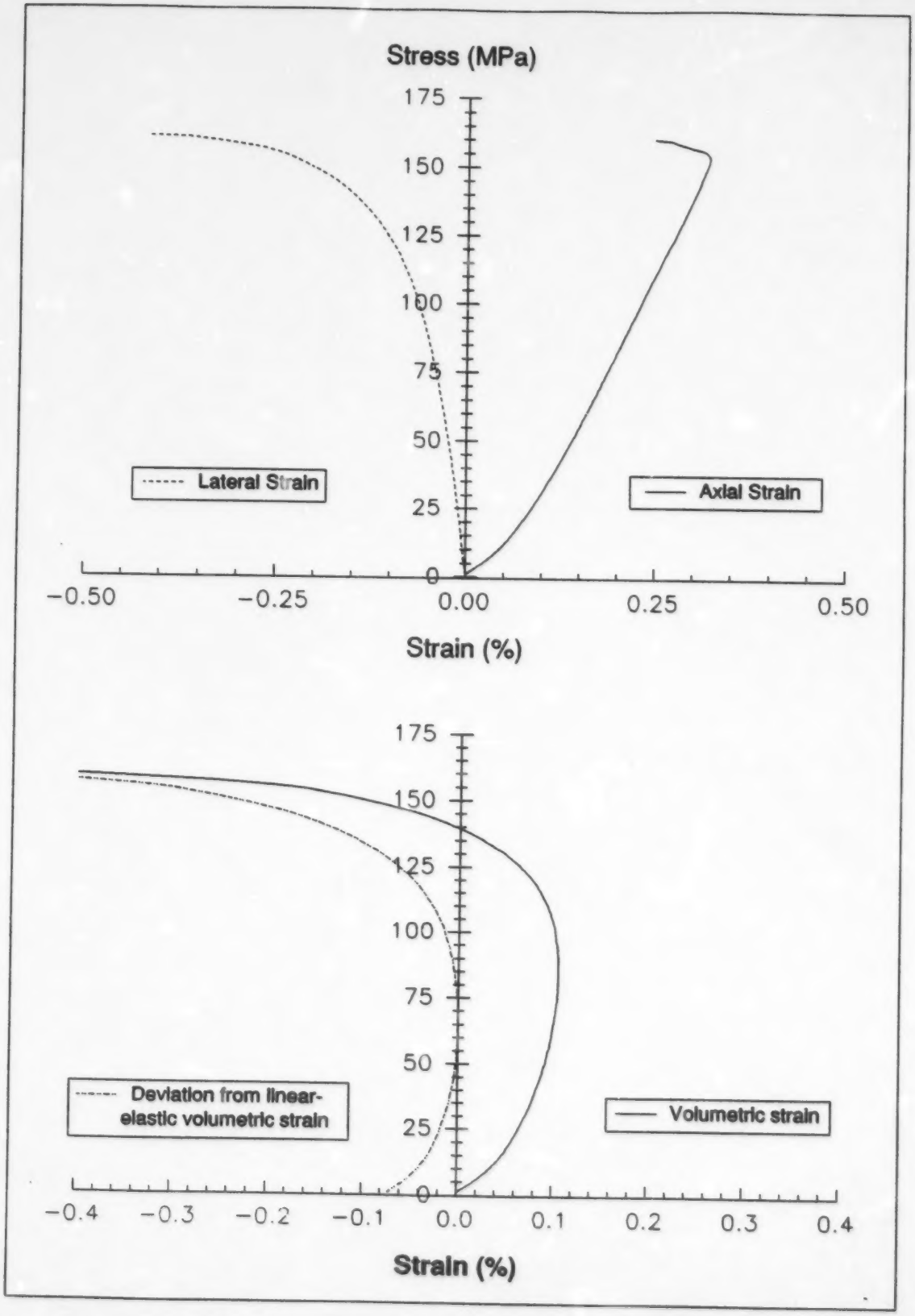

Figure A42 - Stress/strain curves for sample no. 6.174

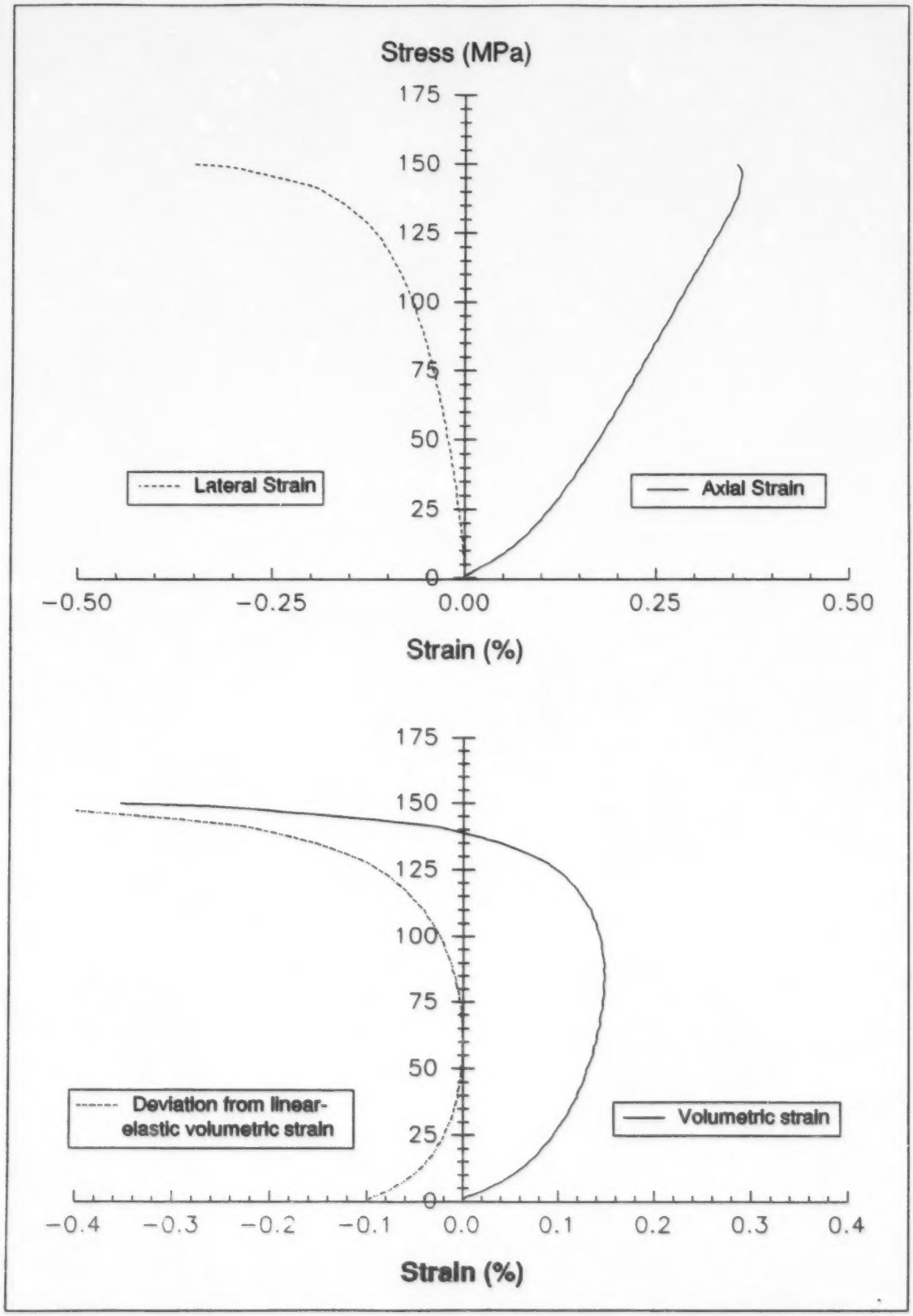

Figure A43 - Stress/strain curves for sample no. 6.221

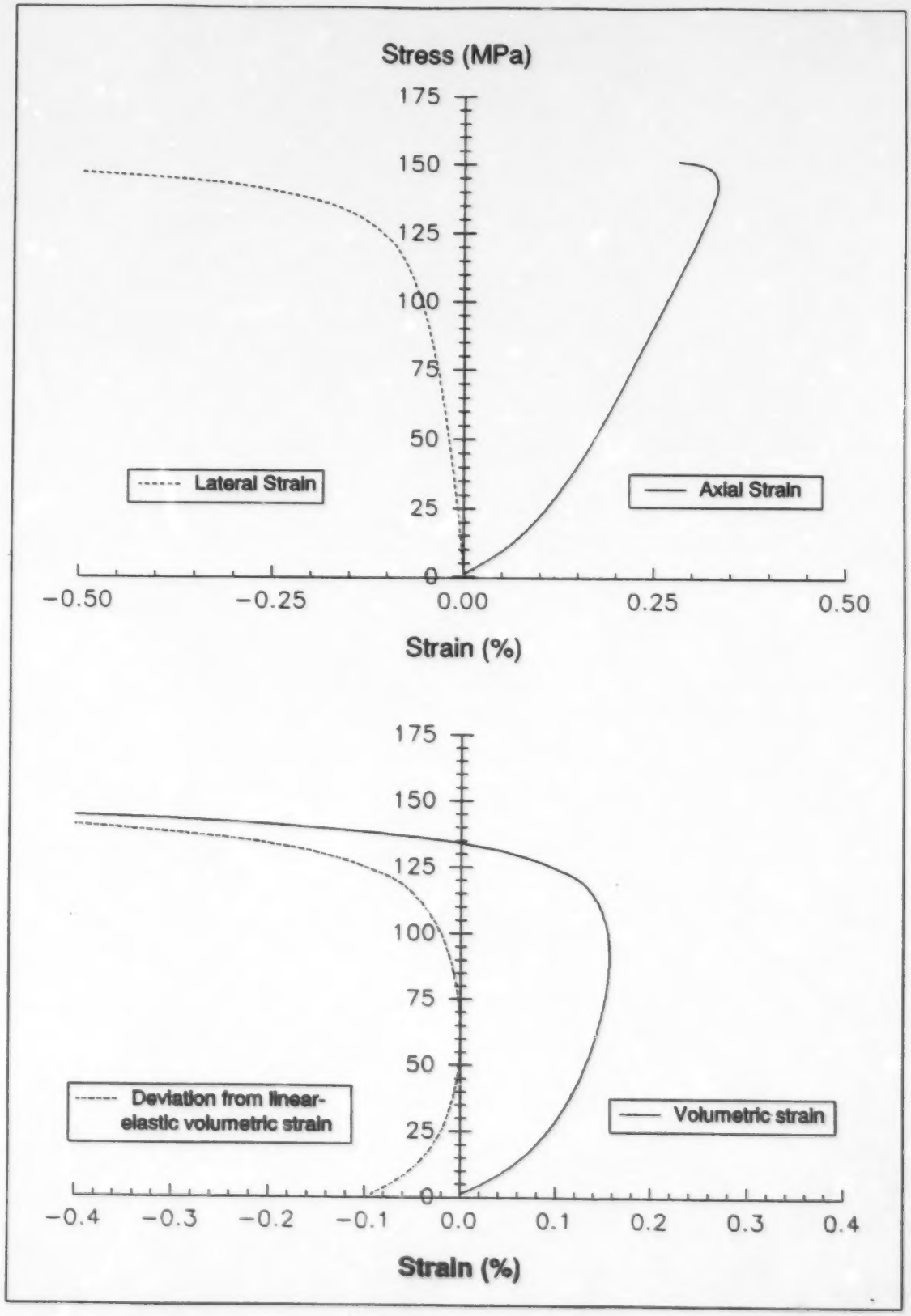

Figure A44 - Stress/strain curves for sample no. 6.380

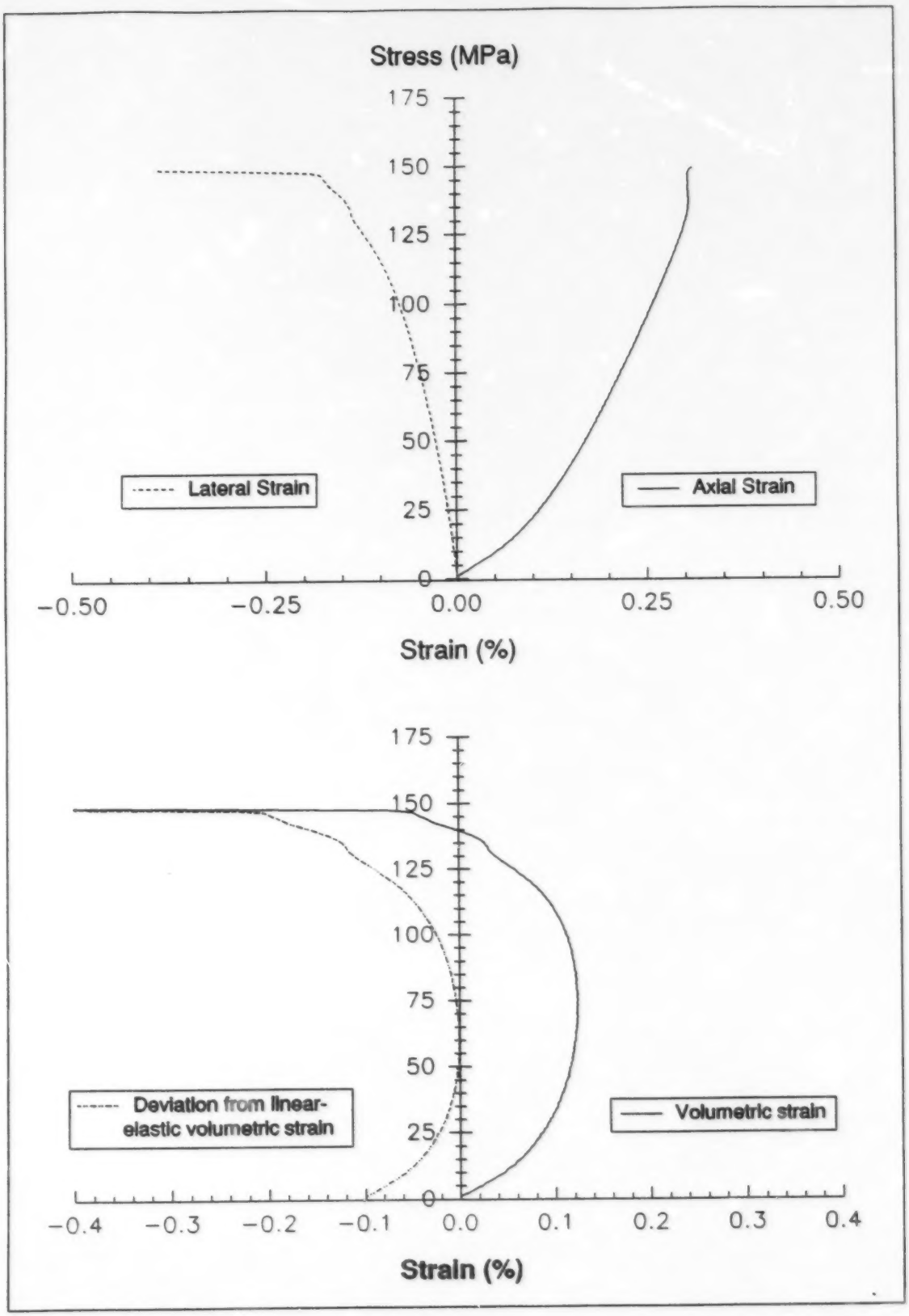

Figure A45 - Stress/strain curves for sample no. 6.320

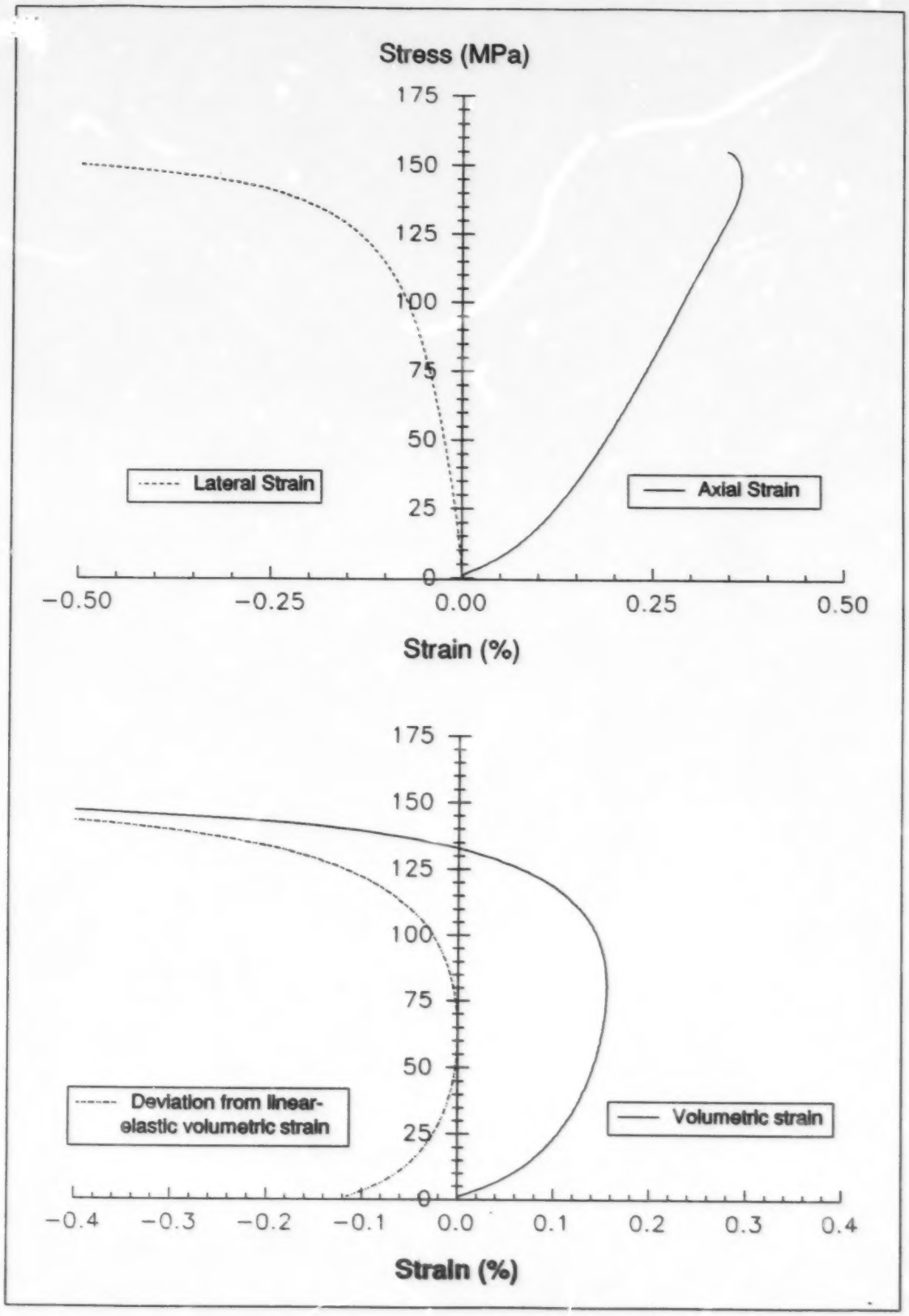

Figure A46 - Stress/strain curves for sample no. 6.659

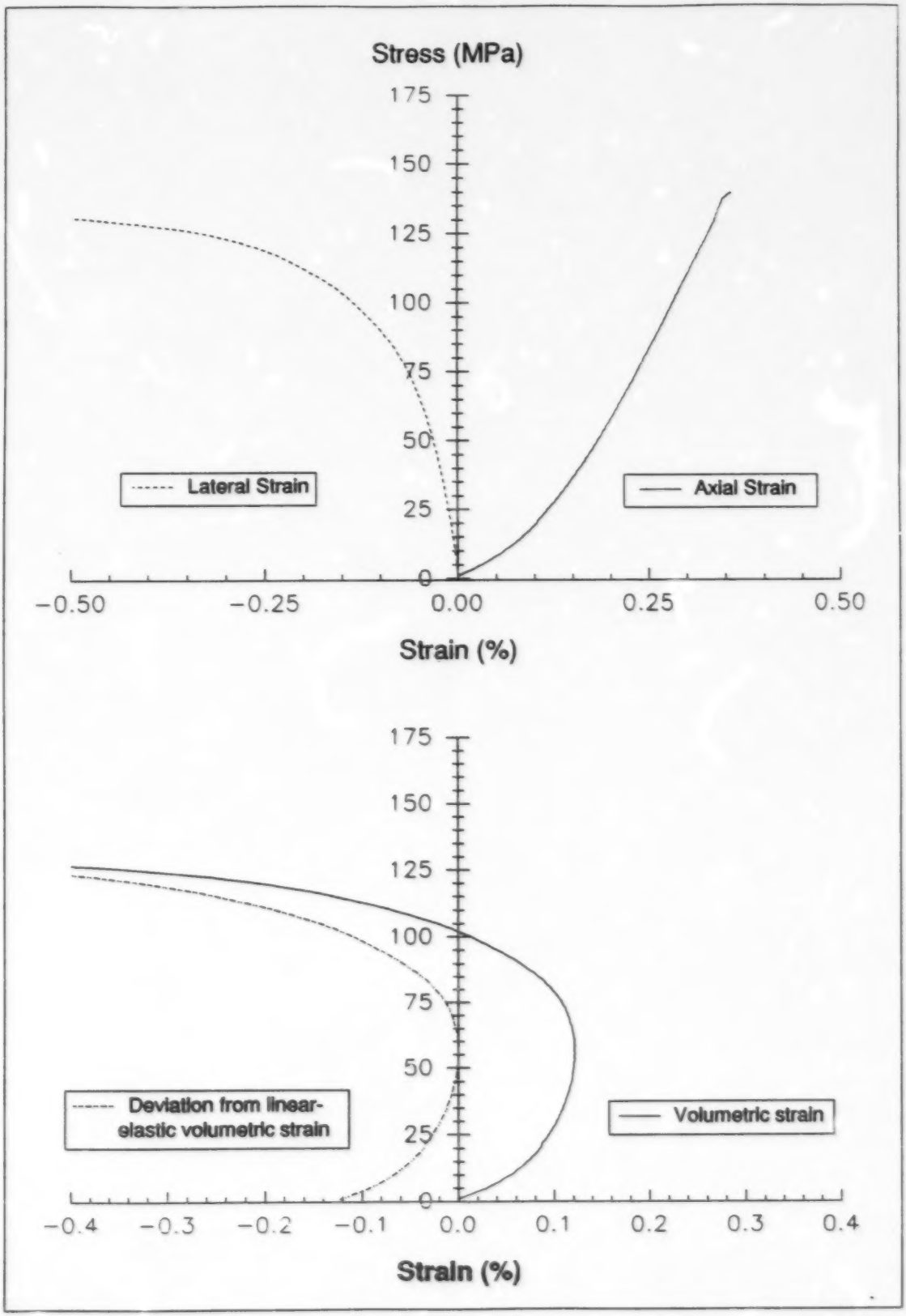

Figure A47 - Stress/strain curves for sample no. 6.895

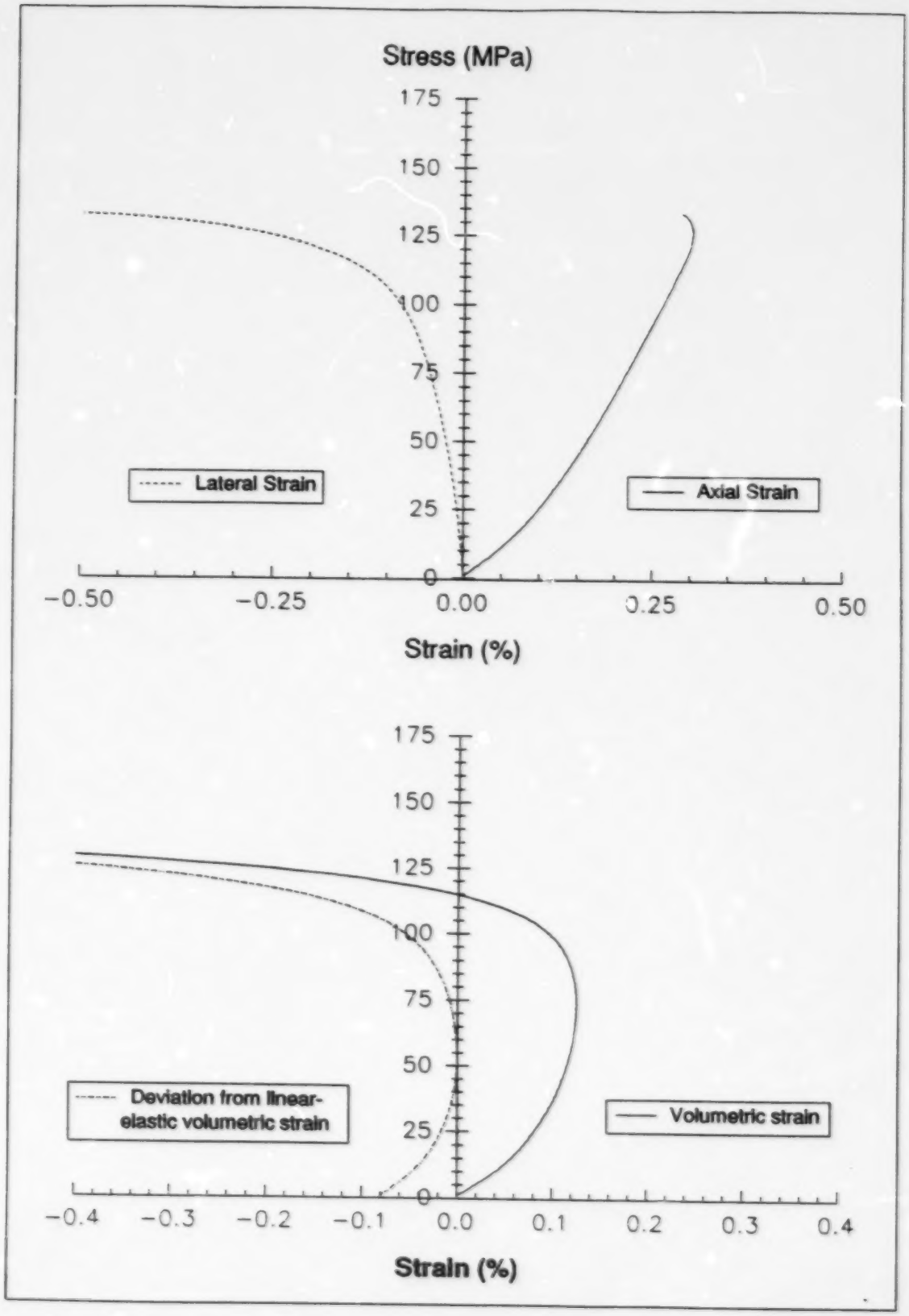

Figure A48 - Stress/strain curves for sample no. 7.020